MEDICAL UNIVERSITY OF VIENNA

Cytotoxic T cell responses against SARS-CoV-2 mutants

Doctoral thesis at the Medical University of Vienna
for obtaining the academic degree
Doctor of Philosophy

Submitted by

Benedikt Agerer, MSc

Supervisor:
Dr. Andreas Bergthaler

CeMM, Research Center for Molecular Medicine
of the Austrian Academy of Sciences
Lazarettgasse 14, AKH BT 25.3,1090 Vienna, Austria

Vienna, 07/2021

Declaration

This thesis is written in a cumulative format and includes a first author publication published in Science Immunology on March 4th 2021. The study is the result of a collaborative effort which I managed and helped conceptualize. I designed and performed experiments, analyzed and interpreted data and wrote the manuscript with input from Maximilian Koblischke, Venugopal Gudipati, (both shared first authors), Johannes B. Huppa, Judith Aberle and Andreas Bergthaler.

My individual contributions to the manuscript:

- Preparation of samples for next-generation sequencing: Figures 1A to 1E and S1A to S1H
- Bioinformatic analysis and interpretation of next-generation sequencing data Figures 1A to 1E and S1A to S1H
- Selection of peptides for further analysis performed in Figures 2 to 4
- Experimental design and data interpretation together with collaborators: Figure 2A to 2F, 3A to 3L, 4A to 4H, S2A to S2L, S3A to S3E, S4A to S4K and S5A to S5H.
- Assembly of figures and presentation of data: Figures 1 to 4 and S1 to S5

Maximilian Koblischke, Venugopal Gudipati, David M. Florian, Vanessa Mühlgrabner, Marianne Graninger, Anna-Maria Hus, Lisa Ellen Shaw, Alexander Lercher, Pia Gattinger, Doris Trapin, Thomas Penz, Ingrid Fae, Sabine Wenda, Marianna Traugott, Winfried F. Pickl, Rudolf Valenta, Wolfgang Paster, René Geyeregger, Matthias Farlik, Johannes B. Huppa and Judith H. Aberle performed experiments and/or generated reagents and/or provided experimental advise.

Luis Fernando Montaño-Gutierrez, Mark Smyth, Alexandra Popa, Jakob-Wendelin Genger, Lukas Endler, Ricard Torralba-Gombau, Daniele Barreca and Florian Halbritter performed initial bioinformatic analysis of virus derived sequences or scRNA-seq data.

Stephan W. Aberle, Gernot Walder, Volker Thiel, Franz Allerberger, Hannes Stockinger, Elisabeth Puchhammer-Stöckl, Wolfgang Weninger, Gottfried Fischer, Wolfgang Hoepler, Erich Pawelka, Alexander Zoufaly, Christoph Bock provided reagents and/or patient samples and/or critically reviewed the manuscript.

As shared first author, Maximilian Koblischke and Venugopal Gudipati designed and performed experiments (Figure 2 and Figure 3) and will not use any of the content of this thesis for the purpose of dissertation.

Table of Contents

List of Figures

Introduction

Manuscript

Abstract

The COVID-19 pandemic caused by SARS-CoV-2 rapidly spread around the globe and affected multiple aspects of life. In unparalleled speed novel vaccines to protect against SARS-CoV-2 have been developed. Vaccine-induced and natural immunity after infection is characterized by neutralizing antibody responses against the viral Spike protein. Additionally, a broad range of virus specific T cell responses are triggered. Viral mutations have accumulated that reduce the neutralization by vaccine and infection-induced antibodies. However, if and how mutations in SARS-CoV-2 T cell epitopes affect T cell responses has not been described. Here, we analyzed mutations occurring in the SARS-CoV-2 genome sampled from 747 individuals. We investigated the effect of these mutations on T cell responses using a combination of bioinformatic approaches and cell free *in vitro* and *ex vivo* assays. With this approach we identified several mutations that led to decreased peptide presentation on MHC-I and subsequently reduced T cell responses against the mutant peptide. The ability of single amino-acid mutations to subvert T cell responses further highlights the importance of global surveying mechanisms for mutation tracking and functional analysis of potential immune escape variants.

Zusammenfassung

Die durch SARS-CoV-2 verursachte COVID-19 Pandemie hat sich rapide auf der ganzen Welt ausgebreitet und hatte große Auswirkungen auf verschiedenste Lebensbereiche. In unvergleichlicher Geschwindigkeit wurden neue Impfstoffe für den Schutz vor SARS-CoV-2 Infektionen entwickelt. Impfinduzierte und natürliche Immunität nach einer Infektion kennzeichnen sich durch neutralisierende Antikörper gegen das virale Spike Protein. Zusätzlich wird eine breite T-Zell Antwort induziert. Es haben sich Mutationen angehäuft, die die Effektivität von neutralisierenden Antikörpern beeinträchtigt. Ob und wie Mutationen in SARS-CoV-2 T-Zell Antworten beeinflusst war bisher nicht beschrieben. In dieser Studie haben wir Mutationen im SARS-CoV-2 Genom, das aus 747 Individuen isoliert wurde, analysiert. Wir haben den Effekt dieser Mutationen auf T-Zell Antworten mithilfe von bioinformatischen Analysen und *in vitro* und *ex vivo* Experimenten untersucht. Durch diesen Ansatz konnten wir mehrere Mutationen identifizieren, welche zu einer verringerten Peptid Präsentation durch MHC-I und daher verringerten T-Zell Antworten gegen das mutierte Peptid führen. Die Fähigkeit, einzelner Aminosäure Mutationen die T-Zell Antwort zu umgehen, unterstreicht die Wichtigkeit von weltweiten Überwachungsmechanismen für die Mutationsverfolgung und weitere funktionelle Analysen von potenziellen „Fluchtvarianten“.

Publication arising from this Thesis

Benedikt Agerer[†], Maximilian Koblischke[†], Venugopal Gudipati[†], Luis Fernando Montaño-Gutierrez, Mark Smyth, Alexandra Popa, Jakob-Wendelin Genger, Lukas Endler, David M. Florian, Vanessa Mühlgrabner, Marianne Graninger, Stephan W. Aberle, Anna-Maria Hus, Lisa Ellen Shaw, Alexander Lercher, Pia Gattinger, Ricard Torralba-Gombau, Doris Trapin, Thomas Penz, Daniele Barreca, Ingrid Fae, Sabine Wenda, Marianna Traugott, Gernot Walder, Winfried F. Pickl, Volker Thiel, Franz Allerberger, Hannes Stockinger, Elisabeth Puchhammer-Stöckl, Wolfgang Weninger, Gottfried Fischer, Wolfgang Hoepler, Erich Pawelka, Alexander Zoufaly, Rudolf Valenta, Christoph Bock, Wolfgang Paster, René Geyeregger, Matthias Farlik, Florian Halbritter, Johannes B. Huppa[††], Judith H. Aberle[††] and Andreas Bergthaler[††]. **SARS-CoV-2 mutations in MHC-I-restricted epitopes evade CD8+ T cell responses.** Science Immunology. March 04, 2021. doi.org/10.1126/sciimmunol.abg6461

[†, ††] equal contributions

Abbreviations

ACE2	Angiotensin converting enzyme 2
ADCC	Antibody-dependent cellular cytotoxicity
AIM2	Absent in melanoma 2
APC	Antigen presenting cell
ARDS	Acute respiratory distress syndrome
CD	Cluster of differentiation
CDC	Center for Disease Control and Prevention
cGAS	Cyclic GMP-AMP synthase
CMV	Cytomegalovirus
COVID-19	Coronavirus disease 2019
cSMAC	Central supramolecular activation cluster (cSMAC)
CTL	Cytotoxic T lymphocyte
DAG	Diacylglycerol
DC	Dendritic cells
DMVs	Double membrane vesicles
E	Envelope
EMA	European Medicines Agency
ER	Endoplasmic reticulum
GZMK	Granzyme K
HCV	Hepatitis-C virus
HIV-1	Human Immunodeficiency Virus-1
HLA	Human leukocyte antigen
IBV	Infectious bronchitis virus
IFN-I	Type-1 interferon
IKK-i	Inducible I kappa-B kinase
IL	Interleukin
IP3	Inositol-1,4,5-trisphosphate
IRAK	Interleukin-1 receptor-associated kinase
IRF3	Interferon regulatory factor 3
ISG	Interferon stimulated gene
ISGF3	Interferon stimulated gene factor 3
ISRE	Interferon stimulated response elements
LCMV	Lymphocytic choriomeningitis virus
LTB	Lymphotoxin-beta
M	Membrane
MDA5	Melanoma differentiation-associated protein 5
MHC	Major histocompatibility complex

MIS-C	Multisystem inflammatory syndrome in children
Mpro	Main protease
MyD88	Myeloid differentiation primary response 88
N	Nucleocapsid
NF-kB	Nuclear factor kappa-light-chain-enhancer of activated B cells
nsp	Non-structural protein
ORF	Open reading frame
PAMP	Pathogen associated molecular patterns
PIP2	Phosphatidylinositol 4,5-bisphosphate
PKC	Protein kinase C
PLC	Peptide loading complex
PLCG1	1-phosphatidylinositol 4,5-bisphosphate phosphodiesterase gamma-1
PLpro	Papain-like protease
PRR	Pattern recognition receptors
RBD	Receptor binding domain
RdRP	RNA-dependent RNA polymerase
RIG-1	Retinoic acid inducible gene I
RIP1	Receptor-interacting serine/threonine-protein kinase 1
RTC	Replication and transcription complex
S	Spike
scRNA-seq	Single-cell RNA sequencing
sgRNAs	Sub-genomic RNAs
STAT	sSignal transducer and activator of transcription
STING	Stimulator of Interferon Genes
TAP	Transporter associated with antigen processing
TBK1	TANK-binding kinase 1
TCR	T-cell receptor
TH	T-helper
TIR	Toll/IL-1R homology
TLR	Toll-like receptor
TRAF6	TNF receptor associated factor 6
TRIF	TIR-domain-containing adapter-inducing interferon-β

Acknowledgements

First of all, I would like to thank Andreas Bergthaler for the great opportunity to do my PhD in his lab. Thank you for all the discussions and giving me the possibility to work on so many diverse and exciting projects. You really enabled me to work independently, develop my own ideas and thus, grow a lot professionally, but also personally. Thank you for putting your trust in me to establish our sequencing workflow for SARS-CoV-2 in times where most people could not enter the lab and continue their work. I think we made the most out of these challenging times.

Next, I would like to thank the whole Bergthaler lab. All of you helped me to grow throughout the years and I could learn a lot from every one of you. During the last few years, I have seen many people come and go and every single one would deserve his or her own paragraph. Thanks to Linds, Theresa, Michi, Mark and Alex for welcoming me on the 6th floor lab space. Your presence made the difficult times a lot more bearable. Thanks to Bojan and Subhash for joining me on the Phf11 project, even though it was only for a brief time. Special thanks to Alexandra for help with bioinformatics, you helped me a lot to develop my computational skills. Thanks to Csilla for taking over many important tasks in the lab, including being the good soul in the lab and having an open ear for any issues I was facing. Jakob, thank you for your friendship and the discussions about our crazy ideas, I hope we can make some of them reality.

Further, a big thank you goes out to all the people from the Loizou and Winter lab, for your support and for making the 6th floor a very pleasant work environment. Sophie, Alex and Anna for your friendship and all the conversations we had. Thanks to Martin, the best lab rotation supervisor I could imagine.

Thanks to all people at CeMM for making this such a wonderful place to work at, it is really a one-time experience to be a CeMMie. Of course, special thanks go out to all our collaborators throughout the years. Many projects would have never been possible without you.

Thanks to all my friends and family for being there for me and their support. Special thanks to my parents for their limitless support, without you this would have never been possible. Antonia, thank you for being by my side and for bearing with my grumpiness during tough times. You made me realize what really matters to me – thank you so much for that. I am looking forward to our new adventures. Fabio, you were the best friend and flat mate I could have asked for. Thank you for everything and may you rest in peace, this one is for you.

1. Introduction

In December 2019 several cases of pneumonia of unknown etiology were reported in the Hubei province in China (Wu et al., 2020). The novel coronavirus SARS-CoV-2 was identified as the causative agent (Hu et al., 2020). Shortly thereafter the WHO declared the outbreak of SARS-CoV-2 related disease – termed coronavirus disease 2019 (COVID-19) – an epidemic of public health emergency of international concern (Hu et al., 2020). Due to high transmissibility SARS-CoV-2 quickly spread all over the world, which led to the declaration of a world-wide pandemic by the WHO on March 11th 2020 (World Health Organization, 2020). This was connected to unprecedented worldwide countermeasures to contain the spread of this novel coronavirus. Despite widespread actions, over 191 Million cases and 4.1 Million associated deaths were reported, as of 19th July 2021, according to the COVID-19 dashboard of the Johns Hopkins University (Dong et al., 2020).

SARS-CoV-2 is a coronavirus belonging to the family of Sarbecoviruses and is closely related to SARS-CoV, which caused a relatively small pandemic of virus associated pneumonia from 2002 to 2003 with a total of more than 8000 cases and 770 deaths (Peiris et al., 2004). In an unparalleled fashion, massive research efforts were focused on understanding the virology, epidemiology and pathogenesis of SARS-CoV-2 as well as the immune responses against it. This is highlighted by more than 156.000 publications containing either “SARS-CoV-2” or “COVID-19” listed on PubMed between December 2019 and July 2021.

Strong and persistent adaptive immune responses against SARS-CoV-2 were reported (Peng et al., 2020; Sekine et al., 2020; Wajnberg et al., 2020). This good news further fueled the development of several vaccines in record time (Krammer, 2020). However, several independent studies described the emergence of novel SARS-CoV-2 variants that were associated with decreased antibody responses and even partial antibody escape (Greaney et al., 2021; Li et al., 2021; Liu et al., 2020; McCarthy et al., 2021; Zhou et al., 2021). This thesis expands the potential of mutations in SARS-CoV-2 to evade immune responses to CD8$^+$ T cell responses and led to the first study published on potential T cell evasion of SARS-CoV-2.

The introduction will be divided in the following subchapters:

1.1 Epidemiology and virology of SARS-CoV-2
1.2 Antiviral immune responses
1.3 T cell responses and
1.4 Immune responses to SARS-CoV-2 infection
1.5 Mechanisms of immune escape

1.1 Epidemiology and virology of SARS-CoV-2

SARS-CoV-2 is an RNA virus belonging to the Sarbecovirus family of Coronaviruses (V'kovski et al., 2020). RNA viruses are classified into different groups according to the Baltimore classification by their genome organization and replication strategy: double-stranded RNA viruses, positive-sense single-stranded RNA viruses and negative-sense single-stranded RNA viruses (Lostroh, 2019). As the causative agent for the COVID-19 pandemic SARS-CoV-2 received much attention and much is known about its virology, epidemiology and pathogenesis.

1.1.1 RNA Viruses

Viruses can be roughly divided into RNA and DNA viruses based on the organization of their genome. The group of RNA viruses is further classified into double-stranded RNA viruses, positive- and negative-sense single-stranded RNA viruses. For the replication of their RNA genome RNA viruses require a specialised RNA-dependent RNA polymerase (RdRP), which lacks – in most cases – proofreading activity (Villa et al., 2020). Therefore, RNA viruses generally harbor high mutation rates, leading to high genetic diversity (Villa et al., 2020). Eigen and Schuster coined the term "quasispecies" to describe this cloud of mutants present in an infected individual (Eigen and Schuster, 1977). Importantly, viral evolution acts on the level of quasispecies, possibly selecting for advantageous mutations in short time periods. This was observed for Hepatitis-C virus (HCV), as well as the retrovirus Human Immunodeficiency Virus-1 (HIV-1), both of which can quickly adapt and thus escape selection pressures, such as antiviral treatments or the immune response (Bowen and Walker, 2005; Deng et al., 2015; Goulder and Watkins, 2004; Goulder et al., 2001; Pircher et al., 1990; Timm and Walker, 2015). Intriguingly, most of the viruses that emerged in the last century and cause disease in humans are RNA viruses, such as the different subtypes of Influenza A viruses, Ebola virus, as well as the Coronaviruses SARS-CoV, MERS and SARS-CoV-2, highlighting the high pathogenic potential of RNA viruses (Woolhouse et al., 2013).

1.1.2 History of Coronaviruses

The family of Coronaviruses in the order of Nidovirales received much attention in recent years due to the emergence of several epidemics and pandemics caused by coronaviruses. Coronaviruses are positive-sense single stranded RNA viruses with large genomes (compared to other RNA viruses) of up to 32 kB, are known to cause infections in animals and humans and are responsible for several disease outbreaks in these species (Cui et al., 2019; Gorbalenya et al., 2006). The first coronavirus infections were identified in poultry in the early

1930's (Fabricant, 1998). Since then, coronavirus infections have been observed in rodents, cats, pigs, bats and human (Perlman and Netland, 2009). Among these, bats have been shown to be an important reservoir and potentially the natural host for many coronaviruses (Anthony et al., 2017). As such, they play an important role in the emergence of novel coronaviruses with the potential to cause infections in human and livestock. Human coronavirus infections were first discovered in the 1960's as one of the causative agents of the common cold (Garbino et al., 2006). Due to the structural similarities with infectious bronchitis virus (IBV), the causative agent for poultry infections identified in the 1930's and their appearance under an electron microscope these viruses were combined together in the new group of coronaviruses (Becker et al., 1967). The name coronavirus stems from the fact that these viruses appear to be surrounded by a crown-like structure in electron-micrographs.

Up until the year 2002 coronaviruses did not receive much attention, until several cases of atypical pneumonia of unknown etiology occurred in November 2002 in the Guangdong province in China (Zhong et al., 2003). The disease was termed severe acute respiratory syndrome (SARS) by the Center for Disease Control and Prevention (CDC) (Center for Disease Control and Prevention, 2003). Shortly thereafter several groups suggested that the etiologic agent for SARS is a novel coronavirus (Drosten et al., 2003; Ksiazek et al., 2003; Peiris et al., 2003). This led to the sequencing of the genome sequence of this novel coronavirus. Importantly, the sequence was only moderately related to other known coronaviruses and it was proposed that SARS-CoV defines a new group in the family of coronaviruses (Marra et al., 2003). Efforts were targeted to the identification of the natural or intermediate host that enabled transmission of SARS-CoV to humans. Because the first infections arose in restaurant workers and the surroundings of animal markets (Zhong et al., 2003), focus was put on wild animals that were sold on wet markets for culinary purposes. Several apparently healthy civet cats and raccoon dogs were tested positive for SARS-CoV and sequence analysis revealed high homology to SARS-CoV sequenced from patients (Guan et al., 2003). However, no SARS-CoV was detected in farmed or wild civet cats, suggesting that they might be an intermediary host for zoonotic transmission, whereas the natural host remained elusive (Perlman and Netland, 2009). This led to the large culling of civet cats, in an effort to remove the intermediary host and reduce the risk of reintroduction into human populations (Anderson et al., 2004). This was combined by contact tracing and isolation of infected individuals as well as their contact persons. These measures were highly effective, partly because the majority of patients became infectious only after the onset of symptoms and there were little cases of asymptomatic infection (Anderson et al., 2004). Nevertheless, SARS-CoV spread to over 8000 individuals in 25 countries and caused 774 deaths (Peiris et al., 2004). After the end of the pandemic the search for the natural reservoir of SARS-CoV

continued and finally it was suggested that horseshoe bats might be the origin for SARS-CoV (Lau et al., 2005; Li et al., 2005).

Approximately 10 years after the occurrence of SARS-CoV, another novel coronavirus was found to cause disease in humans. In April and June 2012 cases of severe respiratory disease were identified in the Middle East (Hijawi et al., 2013; Zaki et al., 2012). Briefly after the occurrence of these cases, MERS-CoV, a coronavirus phylogenetically distinct from other coronaviruses known at the time (Graham et al., 2013). MERS-CoV caused similar symptoms as SARS-CoV, including acute respiratory distress syndrome (ARDS), but showed increased mortality rates of ~36% (De Wit et al., 2016). MERS-CoV infection was confirmed for more than 2400 cases and caused more than 850 deaths (World Health Organization, 2019). Interestingly, human to human was often linked to nosocomial infections, whereas there was evidence for multiple introduction events into the human population (De Wit et al., 2016). Serological analyses suggested that MERS-CoV circulated in dromedary camels and was transmitted to humans by close contact (Reusken et al., 2013). Retrospective analysis of serum taken from Northern and Eastern Africa, as well as the Middle East suggested MERS-like coronaviruses have been circulating in dromedary camels as early as 1983 (Müller et al., 2014). This suggested that a MERS related ancestral virus crossed the species border from bats to dromedary camels, in which it acquired the potential to cross to and cause disease in humans (De Wit et al., 2016).

The two examples of SARS-CoV and MERS-CoV highlight the potential of coronaviruses to cross species barriers and cause severe disease in humans. As a response, research focused on the identification of novel coronaviruses in bats as well as potential treatment strategies, including antivirals and vaccines (Cui et al., 2019).

1.1.3 SARS-CoV-2 epidemiology and COVID-19

Despite all efforts, yet another coronavirus crossed the species barrier to humans in December 2019. In the city of Wuhan in the Chinese Hubei province several cases of pneumonia of unknown etiology were reported in December (Wu et al., 2020). While the first cases were connected to a so-called wet market, there was ample evidence that human to human transmission plays a critical role in the transmission of the disease (Guo et al., 2020). In record time the causative agent was identified as a novel coronavirus and its sequence published on the GISAID database on January 12th (Shu and McCauley, 2017). Due to its high sequence homology to SARS-CoV the virus was called SARS-CoV-2 (Coronaviridae Study Group of the International Committee on Taxonomy of Viruses, 2020). The Chinese government quickly took strict measures to contain the spread of SARS-CoV-2 and the entire city of Wuhan was

quarantined and all travel to and from the city was shut down on January 23rd (Hu et al., 2020). These measures slowed viral spread in Wuhan, however due to high travel activity connected to lunar New Year SARS-CoV-2 infections were reported all across China and in several countries and quickly spread all over the world (Hu et al., 2020). The WHO declared SARS-CoV-2 to be a pandemic in March 2020 (World Health Organization, 2020). Business travel and tourism played a major role in the early spread to countries all over the world. For instance, we showed in a landmark study how tourism in Austrian skiing resorts acted as central hub for the transmission of SARS-CoV-2 to European countries, as well as the USA (Popa et al., 2020). Compared to SARS-CoV the novel coronavirus shows increased human to human transmission, partly because SARS-CoV-2 can be transmitted before the onset of symptoms, making contact tracing and containment measures complicated (Wölfel et al., 2020). In addition, many SARS-CoV-2 infections are thought to be asymptomatic (Li et al., 2020). As a consequence, several countries worldwide imposed unprecedent countermeasures and limited social life with stay-at-home orders and lockdown strategies, combined with widespread testing strategies. Despite these widespread countermeasures, 191 Million cases and 4.1 Million associated deaths were reported, as of 15th July 2021 (Dong et al., 2020).

The clinical manifestations of SARS-CoV-2 infection were called coronavirus disease 2019 (COVID-19) by the WHO. Most commonly COVID-19 manifests in mild to moderate symptoms including fever, fatigue and dry cough (Cevik et al., 2020). Additional reported sy mptoms include headache, diarrhoea, nausea and vomiting, as well as sore throat and chest pain (Wang et al., 2020). Interestingly transient lack of taste and smell have been reported as well (Giacomelli et al., 2020). A subset of patients develops severe symptoms of respiratory failure, ARDS, multiorgan failure and acute cardiac injury and as a result require ventilation and intensive care (Berlin et al., 2020). As of now the mortality rate of COVID-19 is 2-3%, although this number is only an approximation and the actual mortality rate should be lower due to the unknown number of asymptomatic cases (Hu et al., 2020). Age was identified to be the major risk factor for severe disease and death, as well as co-morbidities, such as hypertension, cardiovascular disease, diabetes and lung related illnesses, although 28% of patients requiring intensive care did not have any co-morbidities (Cevik et al., 2020; Wang et al., 2020). Typically, symptoms develop after a median of 5 days post infection and severe illness presents at 7 days after initial symptom onset (Berlin et al., 2020). It has become apparent that severe disease is often accompanied by immune dysregulation and a hyperinflammatory state (Hu et al., 2020; Huang et al., 2020). In addition, the lungs of deceased COVID-19 patients are often lacking virus but are heavily infiltrated by immune cells (Merad and Vabret, 2021). Several studies revealed an overactivation of the myeloid compartment and increased levels of pro-inflammatory cytokines in severely ill patients, further suggesting that

hyperinflammation plays an important role in disease severity (Lucas et al., 2020a; Mathew et al., 2020; Silvin et al., 2020; Del Valle et al., 2020).

1.1.4 Post-acute COVID-19 syndromes

In addition to acute COVID-19 symptoms several studies have described post-acute symptoms that arise and persist up to 6 months after virus clearance (Nalbandian et al., 2021). These manifestations were termed post-acute COVID-19 or long COVID. The number of COVID-19 patients that develop post-acute COVID symptoms ranges from 13% to 76%, partially depending on the severity of the primary SARS-CoV-2 infection (Chopra et al., 2021; Huang et al., 2021; Nalbandian et al., 2021; Sudre et al., 2021). Affected organ systems include pulmonary, hematologic, cardiovascular, renal, gastro-intestinal, endocrine and neuropsychiatric systems (Nalbandian et al., 2021). The most common symptoms include dyspnoea, fatigue, depression, anxiety and thromboembolic events (Huang et al., 2021; Nalbandian et al., 2021). The pathophysiological mechanisms are only poorly understood, but include effects of virus-induced tissue damage, immunological damage and hyperinflammation (Nalbandian et al., 2021).

A special syndrome related to cleared SARS-CoV-2 infection is multisystem inflammatory syndrome in children (MIS-C) that occurs in children and young adults (Henderson and Yeung, 2021; Nalbandian et al., 2021). MIS-C is characterized by fever, hyperinflammation and multiple organ dysfunction (Henderson and Yeung, 2021). Pathophysiologically, MIS-C is distinct from acute COVID-19 and characterized in part by increased autoantibodies (Gruber et al., 2020). Further research is required to describe long COVID and MIS-C in greater detail to further our understanding of these syndromes and address these health issues in the future.

1.1.5 SARS-CoV-2 virology

The viral life cycle of SARS-CoV-2 begins with the binding of the Spike (S) protein to its cognate receptor, angiotensin converting enzyme 2 (ACE2). ACE2 protein is expressed on cells in the upper and lower respiratory tract, kidney, intestinal tract, gallbladder, testis and heart (Hikmet et al., 2020). These expression patterns might in part explain some of the clinical symptoms that were observed in COVID-19. The S protein consists of two functional parts: S1 is presented on the surface of the virus and contains the receptor binding domain (RBD) that interacts with ACE2 (Letko et al., 2020). The transmembrane S2 domain contains two heptad repeats and the fusion peptide, which is required for the fusion of viral and cellular membranes and thus, viral entry (Li, 2016). In addition to the cellular receptor ACE2, host cell-mediated cleavage of the S protein is required for cellular entry (Li, 2016; Shang et al., 2020). SARS-

CoV-2 utilizes the serine protease TMPRSS2, which can be targeted by the protease inhibitor camostat mesylate, a strategy that is used in the clinic to restrict SARS-CoV-2 infection (Hoffmann et al., 2020; Shang et al., 2020). An interesting feature of the SARS-CoV-2 S protein is the acquisition of a polybasic cleavage site (PRRAR) between S1 and S2 that facilitates cleavage by the enzyme furin (V'kovski et al., 2020). This cleavage results in increased infectivity and likely represents a crucial step in SARS-CoV-2 evolution, that sets it apart from SARS-CoV and other members of the sarbecovirus genus, which lack such a furin cleavage site (V'kovski et al., 2020).

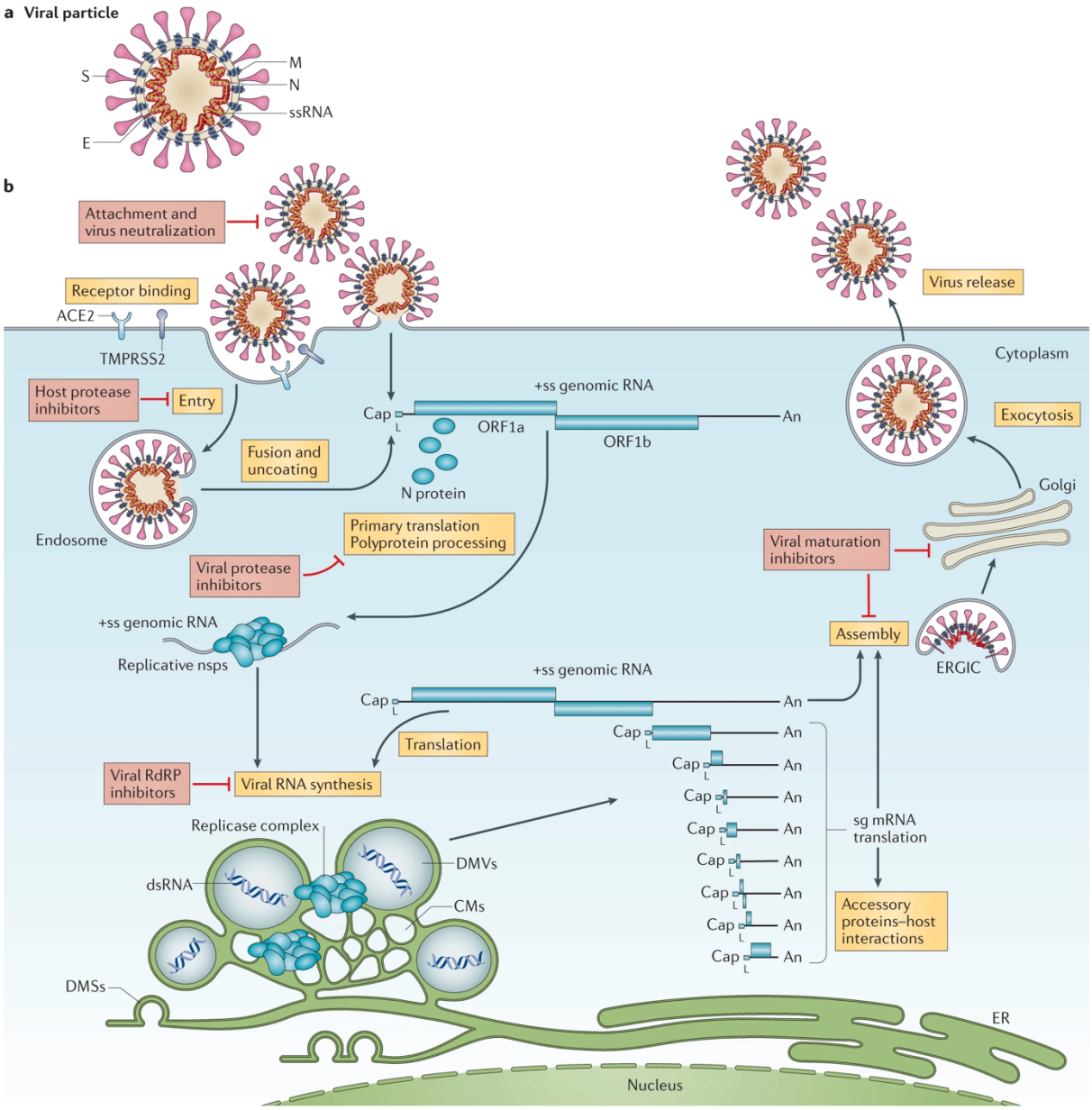

Figure 1. The coronavirus life cycle. Upon cell entry the viral RNA genome is released into the host cell, where translation of ORF1ab is initiated. The resulting polyproteins are cleaved into several nsps that make up the RTC and viral RNA synthesis is initiated to generate copies of the RNA genome, as well as structural proteins, which

are then used to assemble new virions that are then released from the cell to start the next infection cycle. Figure taken from (V'kovski et al., 2020). License number 5093141236498.

Upon cellular entry and membrane fusion the positive-strand RNA genome is released into the host cell (Figure 1). As a first step, open reading frame (ORF) 1a and ORF1b are translated into two large polyproteins, pp1a and pp1ab, that are further cleaved into 16 non-structural proteins (nsps) by two viral proteases: papain-like protease (PL^{pro}) that is located in nsp3 and main protease (M^{pro}), located in nsp5 (V'kovski et al., 2020). Nsp1 is quickly released from the polyproteins and interferes with the host translation machinery, thereby limiting translation of host factors, such as antiviral cytokines (Schubert et al., 2020; Thoms et al., 2020). The viral replication and transcription complex (RTC) consists of the remaining nsp2-16 (Snijder et al., 2016). Nsp12-16 represent the core enzymes for viral replication and transcription, whereas nsp2-11 have supporting functions (Snijder et al., 2016). RNA synthesis is carried out by the RNA-dependent RNAse polymerase (RdRP) nsp12 and nsp7 and nsp8, which serve as cofactors (Gao et al., 2020). An important feature of SARS-CoV-2 due to its large genome is its proofreading activity, that is conferred by the exonuclease nsp14 (Eckerle et al., 2007). The SARS-CoV-2 genome is further transcribed and replicated in replication organelles, that are in part generated by diverting host membranes by nsp3, nsp4 and nsp6 and play a role in the generation of double membrane vesicles (DMVs) (Knoops et al., 2008). Replication of the RNA genome occurs via an intermediary full-length negative-strand genome that serves as a template for the positive-strand genome, that is then either translated into pp1a and pp1ab or used to assemble new virions (V'kovski et al., 2020). In contrast, transcription of the remaining viral ORFs is characterized by discontinuous transcription, as described for other coronaviruses (Sawicki and Sawicki, 1995). This leads to the generation of a set of sub-genomic RNAs (sgRNAs) with shared 5' and 3' ends. During negative-strand synthesis the RTC stalls at transcription regulatory sequences (TRS), which are located in most ORFs downstream of ORF1ab (Di et al., 2018; Sawicki and Sawicki, 1995). Transcription is then continued at a TRS close to the 5' end of the genome, generating negative-strand RNAs that share the 5' leader sequence (Sawicki and Sawicki, 1995). These are then used to generate sets of nested positive-strand RNAs that are transcribed and translated to generate structural and accessory proteins (Kim et al., 2020). Structural proteins of SARS-CoV-2 are the spike (S), membrane (M), nucleocapsid (N) and envelope (E) proteins. Structural proteins play a role in the assembly and release of new virions. In contrast to most other coronaviruses, beta-coronaviruses use the lysosomal trafficking pathway to exit infected cells (Ghosh et al., 2020). In addition to the structural proteins so-called accessory proteins are encoded in the genome (Kim et al., 2020). The exact number of SARS-CoV-2 accessory proteins is still unclear, but it has been proposed that ORF3a, ORF6, ORF7a, ORF7b, ORF8 as well as potentially ORF3b,

ORF9 and ORF10 could be translated into functional proteins (Bojkova et al., 2020; Kim et al., 2020).

Several interactions between viral and host proteins have been suggested. For instance, a systematic interaction study identified more than 300 interactions between viral and host proteins (Gordon et al., 2020). One main purpose of such interactions is the evasion of innate antiviral immune responses. For example, SARS-CoV ORF3b, ORF6 and ORF9b have been shown to be type-1 interferon (IFN-I) antagonists on several levels (Kopecky-Bromberg et al., 2007; Liu et al., 2014). Interestingly, similar functions have been proposed for SARS-CoV-2 ORF3b, which has been shown to suppress IFN-I responses via suppression of interferon regulatory factor 3 (IRF3) signalling (Konno et al., 2020). Data from other coronaviruses suggest that also the RTC may contribute to innate immune evasion via different mechanisms. These include de-ubiquitination, de-ADP ribosylation, RNA modifications, and endo- as well as exonuclease activities (V'kovski et al., 2020). Additionally, it is thought that dsRNA intermediates that are strong triggers for innate immune signalling are hidden in DMVs and are thus not recognized by cellular receptors (V'kovski et al., 2020). It remains unclear to which extent these mechanisms also apply to SARS-CoV-2, but it is likely that it also utilizes several mechanisms to suppress innate immunity. A function that was not described in SARS-CoV is the ability of ORF8 to bind to and induce degradation of major-histocompatibility complex and thus confer some degree of immune evasion (Zhang et al., 2021). Another mechanism that has been described for SARS-CoV-2 is the suppression of host translation by nsp1, leading to decreased expression of type I and III interferons and other host immune factors (Thoms et al., 2020). Taken together, it is understood that COVID-19 is in part a consequence of virus-induced suppression of innate immune responses. This leads to a delayed IFN-I response and rapid early viral replication and, as a consequence, increased pro-inflammatory cytokine responses and cell infiltration inducing tissue damage and potentially contributes to the clinical symptoms of COVID-19, similar to what has been described for SARS (Channappanavar et al., 2016).

1.2 Antiviral immune responses

Mammals have evolved several lines of defense to combat pathogens. Classically, immune responses are divided into a quick acting, but less specific innate and a slower, but highly specific adaptive response. Innate immune responses serve as an essential first line of defense that keeps pathogens in check early in infection, alerts neighboring cells and ultimately is an important trigger for adaptive responses (McNab et al., 2015). Adaptive responses are often required to clear infection and confer memory to facilitate quicker and

stronger responses in case of pathogen re-encounter. This section will specifically focus on antiviral immune responses.

1.2.1 Pattern recognition

A first step in innate immune responses is the recognition of pathogens via pattern recognition receptors (PRRs) that recognize pathogen associated molecular patterns (PAMPs) (Cao, 2015). Such PAMPs are classically molecules absent on/in the host cell or only found in restricted compartments, such as the nucleus. As obligatory intracellular pathogens that rely on the host cell machinery for their reproduction, viral PAMPs are recognized by intracellular and endosomal PRRs (Takeuchi and Akira, 2010). Viruses are mainly recognized by non-host derived nucleic acids present in the cytoplasm or endosomes (Takeuchi and Akira, 2010).

The Toll-like receptor (TLR) family represents membrane bound PRRs that scan the extracellular environment (TLR1, 2, 4-6 and 11) or endosomes (TLR3, 7-10) for PAMPs. Virus derived nucleic acids in endosomes are recognized by dsRNA, ssRNA or unmethylated CpG, by the TLRs 3, 7 and 9 (Cao, 2015). Upon PAMP recognition, TLRs signal via recruitment of adapter proteins to their cytoplasmic Toll/IL-1R homology (TIR) domain, initiating downstream signaling (Akira et al., 2006). TLR3 signals via TIR-domain-containing adapter-inducing interferon-β (TRIF) that recruits TNF receptor associated factor 6 (TRAF6) and receptor-interacting serine/threonine-protein kinase 1 (RIP1), leading to the activation of the nuclear factor kappa-light-chain-enhancer of activated B cells (NF-κB) pathway (Takeuchi and Akira, 2010). NF-κB activation culminates in the activation of several downstream signaling pathways, including the expression of proinflammatory cytokines (Takeuchi and Akira, 2010). Additionally, TLR3 activation signals via TRAF3 that recruits the kinases TANK-binding kinase 1 (TBK1) and Inducible I kappa-B kinase (IKK-i) that lead to phosphorylation and subsequent activation of IRF3 and IRF7 (Kawai and Akira, 2010). This induces the expression of IFN-I, establishing antiviral responses (Figure 2A) (Kawai and Akira, 2010).

In contrast, TLR7 and TLR9 signal via myeloid differentiation primary response 88 (MyD88) by forming a complex with several interleukin-1 receptor-associated kinases (IRAK), TRAF6 and IRF7 (Takeuchi and Akira, 2010). This triggers a signaling cascade leading to the activation of NF-κB signaling and IFN-I expression via phosphorylation of IRF7 (Figure 2B) (Akira et al., 2006; Takeuchi and Akira, 2010).

Next to the membrane bound TLRs there are several additional cytosolic PRRs. The most important ones for the detection of viral PAMPs are retinoic acid inducible gene I (RIG-I) and melanoma differentiation-associated protein 5 (MDA5), that both recognize intracellular RNA

via different mechanisms. RIG-I recognizes shorter stretches of dsRNA and uncapped, phosphorylated ssRNA, whereas MDA5 typically recognizes longer stretches of dsRNA (Kato et al., 2006; Pichlmair et al., 2006; Yoneyama et al., 2004). Briefly, RIG-I and MDA5 rely on their Helicase domains to recognize their ligands, which induces a conformation change, exposing a so-called CARD domain (Takeuchi and Akira, 2010). RIG-I and MDA5 interact with MAVS via their CARD domains and subsequently activate TBK1, thus inducing transcription of IFN-I, as described for TLR3 (Figure 2C) (Akira et al., 2006; Schroder and Tschopp, 2010).

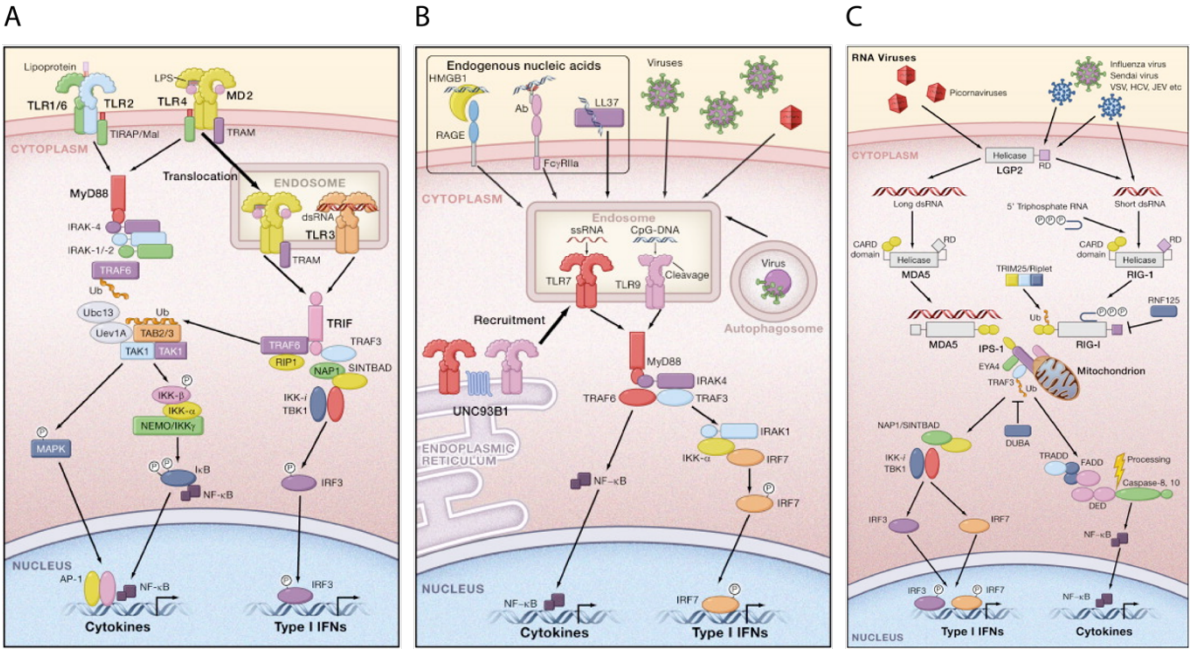

Figure 2. PRR signaling pathways for RNA viruses. A) Endosomal dsRNA is recognized via TLR3 that signals through TRIF. B) Endosomal ssRNA and unmethylated CpG is recognized by TLR7 and TLR9 that signal via MyD88. C) Intracellular RNAs are recognized by RIG-I and MDA5, signaling via MAVS and TBK1. Figures taken from (Takeuchi and Akira, 2010). License number 5093791502850.

In addition to RNA sensing mechanisms also intracellular DNA can be recognized by PRRs. The most important DNA sensors are cyclic GMP-AMP synthase (cGAS) and absent in melanoma 2 (AIM2). AIM2 signaling leads to the activation of caspase 1 and interleukin (IL)-1β production (Schroder and Tschopp, 2010). cGAS signals via Stimulator of Interferon Genes (STING) to activate TBK1 and subsequently induce an IFN-I response (Sun et al., 2013; Wu et al., 2013).

In conclusion, activation of PRRs by (viral) PAMPs leads to the initiation of NFκB signaling, resulting in the expression of pro-inflammatory cytokines, including IL-6 and tumor necrosis factor-α, resulting in the activation of immune cells including neutrophils, macrophages and dendritic cells (DCs) (Kany et al., 2019). Additionally, PRR signaling triggers the expression

of IFN-I, which leads to the induction of diverse gene expression programs conferring some degree of protection against viral infection (McNab et al., 2015).

1.2.2 Innate cytokine responses

As discussed above, signaling via PRRs leads to the expression of IFN-Is. These cytokines signal in an auto- and paracrine manner to increase antiviral signaling in the infected cell as well as to initiate an antiviral state in uninfected neighboring cells (McNab et al., 2015). This is achieved by downstream signaling upon binding of IFN-I to the IFN-I receptor, which consists of the two subunits IFNAR1 and IFNAR2 (McNab et al., 2015). This triggers a signaling cascade that culminates in the phosphorylation of signal transducer and activator of transcription (STAT) 1 and STAT2, allowing them to form heterodimers and associate with IRF9 to form the interferon stimulated gene factor 3 (ISGF3) (Kessler et al., 1988).

This complex translocates to the nucleus, where it binds to certain promoter elements called interferon stimulated response elements (ISRE) and initiates expression of a wide set of interferon stimulated genes (ISGs) (Figure 3) (Schoggins et al., 2011). Some of these ISGs, like interferon-induced GTP-binding protein Mx1 and 2'-5'-oligoadenylate synthase 1 have direct antiviral properties, the majority however remains incompletely characterized (McNab et al., 2015; Yan and Chen, 2012).

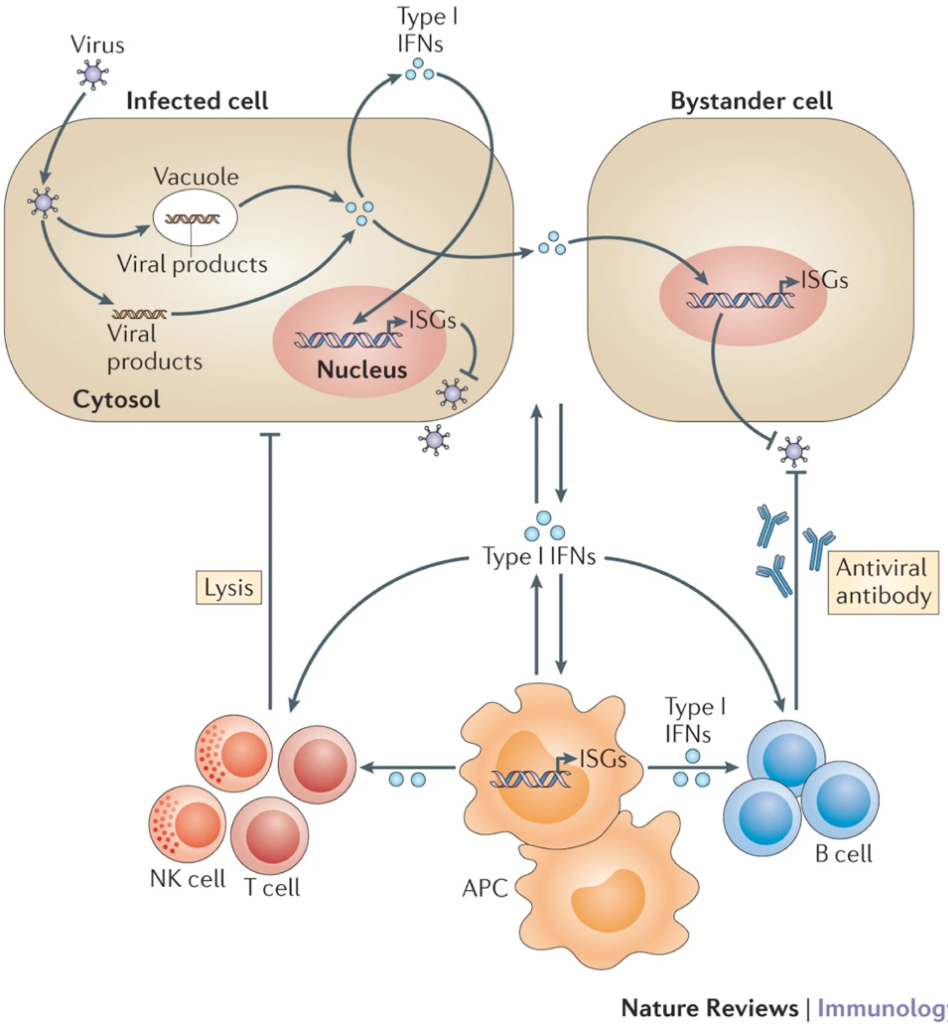

Figure 3. IFN-I has important antiviral functions. Upon viral PAMP recognition IFN-I is produced by the infected cell that signals in an autocrine and paracrine manner to induce the transcription of ISGs to establish an antiviral state. Additionally, IFN-I has effects on cells of the immune system, including APCs, B cells and T cells, where it plays a crucial role in the fine tuning of the immune response. Figure taken from (McNab et al., 2015). License number 5093801193254.

In addition to IFN-I responses PRR signaling can also induce the expression of pro-inflammatory cytokines. Importantly, PRR signaling in professional antigen presenting cells (APCs), such as DCs leads to their activation and serves as link between innate and adaptive responses (Iwasaki and Medzhitov, 2015). For instance, PRR signaling in DCs leads to their migration to draining lymph nodes, where they can interact with adaptive immune cells, like T cells (Ban et al., 2000; Rescigno et al., 2000; Sallusto and Lanzavecchia, 2000) and enhanced activation of cluster of differentiation (CD) 8^+ T cells (van Vliet et al., 2007; Watts et al., 2007). Additionally, PRR signaling triggers the expression of certain cytokines and co-stimulatory molecules, that are required to yield fully activated T cells which can then fight the ongoing viral infection (Werling and Jungi, 2003).

1.2.3 Adaptive responses

The adaptive arm of the immune system can broadly be divided into two parts: the cellular and humoral system. Both systems are able to generate highly antigen specific responses, as well as immune memory, which is crucial for long-lasting protection against certain pathogens and the basis of vaccination efforts (Hammarlund et al., 2003). Briefly, humoral responses are initiated by B cells that, upon antigen recognition, activation and maturation, differentiate into plasma cells, which produce large amounts of pathogen specific antibodies (Radbruch et al., 2006). Antibodies utilize different mechanisms to combat pathogens, including opsonization, antibody-dependent cellular cytotoxicity (ADCC), complement-mediated lysis and neutralization (Hangartner et al., 2006). Of these, neutralizing antibodies play a major role in long-lasting protection against viral infection (Corti and Lanzavecchia, 2013; Hangartner et al., 2006).

Cellular adaptive responses are conferred by T cells, that can broadly be divided into $CD4^+$ T helper cells (T_H) and $CD8^+$ cells. As their name implies, T_H cells function by "helping" other cell types to carry out their functions. An example for this is the T_H2 subset that is required for proper activation of antibody responses (Mosmann et al., 1986). Activated $CD8^+$ cells on the other hand have the ability to directly kill infected cells and are also referred to as cytotoxic T lymphocytes (CTLs) (Zinkernagel and Doherty, 1974). The next section will focus on detailed mechanisms of the activation, differentiation and function of CTLs.

1.3 Cytotoxic T cell responses and their regulation

T cells recognize antigens that are presented by cells via major histocompatibility complex (MHC) proteins (Zinkernagel and Doherty, 1974). Importantly, MHC-I is used by most cells to present intracellular antigens and interacts with the TCR of $CD8^+$ cells, whereas extracellular antigens are presented by APCs via MHC-II and are recognized by $CD4^+$ T cells (Kindred and Shreffler, 1972; Zinkernagel and Doherty, 1974). The T cell receptor (TCR) that is used for this interaction has an immense potential to recognize up to 10^{15} different antigens (Nikolich-Žugich et al., 2004). This high variability stems from the modular nature of the TCR locus, consisting of 3 segments that are present in several different versions (Nikolich-Žugich et al., 2004). These 3 segments are randomly recombined during T cell development by a process called V(D)J recombination to yield functional TCRs (de Villartay et al., 2003). Upon T cell activation by antigen encounter, T cells undergo rapid proliferation and differentiation into effector cells that will then exert their specific function, such as killing of infected cells (Kaech and Cui, 2012).

1.3.1 T cell activation

T cell activation is initiated in secondary lymphoid organs, where activated DCs present viral antigens via MHC-I (von Andrian and Mempel, 2003). There are two general mechanisms how DCs can present intracellular antigens: via the canonical pathway, that will be discussed later or by the so-called process of antigen cross-presentation. Briefly, DCs can take up remains of infected cells via endocytosis or phagocytosis and via a mechanism that is not completely understood shuttle the material that was taken up into the cytosol and process it via the proteasome to present it on MHC-I (Joffre et al., 2012). Antigen cross-presentation is crucial, because some viruses do not naturally infect DCs and thus their antigens could not be presented to $CD8^+$ T cells otherwise (Joffre et al., 2012). Naïve T cells scan DCs in the secondary lymphoid organs for antigens. In the event of a match between the TCR and the antigen that is presented on the DC the T cell gets activated (von Andrian and Mempel, 2003; Joffre et al., 2012). However, appropriate activation of the T cell requires the presence of co-stimulatory molecules, such as CD80/86 and a specific cytokine milieu (von Andrian and Mempel, 2003; Kaech and Cui, 2012). Importantly, some co-stimulatory receptors are only expressed by DCs upon pathogen encounter, as discussed previously, ensuring T cell responses only occur in response to pathogens (Watts et al., 2007). Upon activation T cells undergo rapid proliferation, a process called clonal expansion (Kaech and Cui, 2012). This yields a high number of pathogen specific T cells that further undergo maturation and differentiation into different T cell subsets, including, but not limited to, memory (T_{mem}) and effector (T_{eff}) T cells (Kaech and Cui, 2012). Following activation, T cells egress from the secondary lymphoid organ into the bloodstream, where they travel to the site of infection, recruited by specific chemokine signals (Krummel et al., 2016).

1.3.2 Antigen presentation via MHC-I

Infected cells present short viral antigens, so called epitopes, via MHC-I. In detail, intracellular proteins are constantly being degraded by the proteasome, which generates small peptide fragments (Rock et al., 1994). These peptides are then transported into the endoplasmic reticulum (ER) via the transporter associated with antigen processing (TAP) (Kelly et al., 1992). In the ER peptides are loaded on MHC-I molecules via the peptide loading complex (PLC) (Hansen and Bouvier, 2009; Neefjes et al., 2011). If a peptide efficiently binds to MHC-I it stabilizes the MHC-I complex and allows it to undergo ER processing and is transported to the cell membrane (Figure 4) (Neefjes et al., 2011).

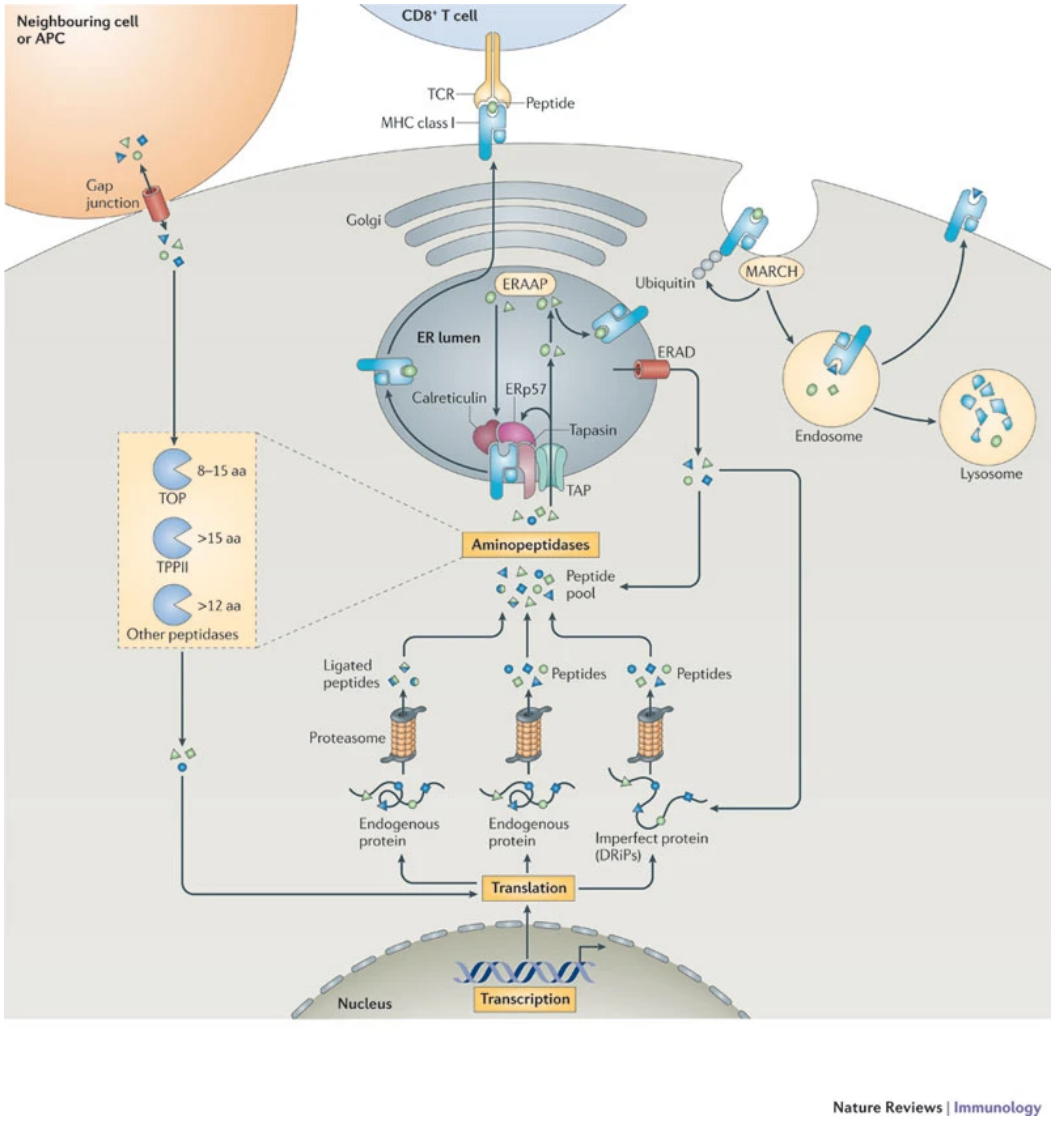

Figure 4. MHC-I presentation pathway. Cellular (and viral) proteins are degraded by the proteasome, thus generating peptide pools. These peptides are transported into the ER via TAP and - if possible - subsequently loaded onto MHC-I. The peptide-MHC-I complex is then transported to the cell membrane, where the epitope is presented and can be recognized by $CD8^+$ T cells. Figure taken from (Neefjes et al., 2011). License number 5093810331970.

Importantly, the genes encoding the heavy chain of MHC-I are highly polymorphic (Neefjes et al., 2011). In humans, these are encoded by the human leukocyte antigen (HLA) genes HLA-A, HLA-B and HLA-C and thousands of variants have been described (Gonzalez-Galarza et al., 2019). This is especially important, because each HLA has a unique binding groove, which will affect the peptides that can be presented by a given HLA molecule (Neefjes et al., 2011). This means that not every individual will present the same epitope repertoire, with potential implications for immunity (Trowsdale, 2005).

1.3.3 Antigen recognition and killing by CTL

An efficient interaction between a CTL via its TCR and an infected cell via MHC-I will trigger a signaling cascade in the CTL that culminates in the killing of the infected cell via the secretion of cytotoxic molecules like granzymes and perforins (Voskoboinik et al., 2015). Additionally, CTLs will secrete effector cytokines like IFNγ and TNFα that have additional functions in the antiviral immune response, like the activation of macrophages (Slifka and Whitton, 2000).

T cell signaling is highly controlled, to ensure appropriate activation and simultaneously prevent over-activation. Upon binding to their cognate antigen, TCRs form microclusters, which is an early event for the formation of the so-called immunological synapse (de La Roche et al., 2016). In this early step a central supramolecular activation cluster (cSMAC), consisting of TCR microclusters, forms and is the basis for downstream signaling (Monks et al., 1998). It has been demonstrated that the formation of the cSMAC heavily depends on cytoskeleton proteins, including F-actin and the microtubules (Beemiller et al., 2012; Hashimoto-Tane et al., 2011; Yi et al., 2012). TCR clustering triggers a signaling cascade involving the kinases LCK, ZAP70, that leads to the activation of 1-phosphatidylinositol 4,5-bisphosphate phosphodiesterase gamma-1 (PLCG1) that catalyzes the hydrolysis of phosphatidylinositol 4,5-bisphosphate (PIP_2) into the two second-messengers inositol-1,4,5-trisphosphate (IP3) and diacylglycerol (DAG) (de La Roche et al., 2016). Of these two DAG has been demonstrated to play an important role in the polarization of centrosomes, which is an essential step in CTL activation (Quann et al., 2009). DAG specifically activates some isoforms of protein kinase C (PKC), including PKCδ and PKCθ, that further signal to promote centrosome polarization (de La Roche et al., 2016; Quann et al., 2011). Upon the microtubule reorganization that is triggered by TCR clustering, secretory granules that were generated upon T cell activation and effector differentiation and stored in the CTLs, are transported to the immunological synapse where their content is released towards the target cell (Bossi and Griffiths, 2005). These granules contain several proteins that are responsible for killing of the target cell, the most important of which are granzymes and perforin (Voskoboinik et al., 2015).

Granzymes and perforin act together to kill target cells. Briefly, perforin forms a pore in the target membrane that enables granzymes to enter the cytoplasm of the target cell (Voskoboinik et al., 2015). It has been shown that although the pores formed by perforin are of sufficient size to allow passage of proteins, only small molecules could pass these pores (Browne et al., 1999). This and additional data suggest that granzymes do not enter the target cell via pores in the plasma membrane but via pores in endosomal vesicles that are internalized upon activation of endocytosis via perforin (Metkar et al., 2002; Thiery et al., 2010). However, more recently it has been shown that perforins could indeed form pores in

the plasma membrane that allow proteins to enter the target cell (Voskoboinik et al., 2015). Once granzymes enter the target cytoplasm they act as proteases that induce tightly controlled signaling cascades (Sutton and Trapani, 2010). The most well-known function of granzymes is to induce apoptotic cell death and the best studied granzyme in this regard is granzyme B (Voskoboinik et al., 2015). Human granzyme B activates the BID-dependent pathway of apoptosis, whereas murine granzyme B acts via direct activation of caspases (Kaiserman et al., 2006). In addition to direct cytotoxic effects several granzymes also influence inflammation via the release of pro-inflammatory cytokines (Anthony et al., 2010; Irmler et al., 1995; Metkar et al., 2008). In addition to the induction of target cell apoptosis via perforin and granzymes, activated CTLs also secrete several effector cytokines, including IFNγ and TNFα, that have additional important local and systemic functions in controlling infections (Slifka and Whitton, 2000).

1.4 Responses against SARS-CoV-2

Several studies have investigated various aspects of immune responses against SARS-CoV-2 including innate and adaptive responses to mild infection, immune responses, and their contribution to severe disease, as well as protection and immune memory (Brodin, 2021; Carvalho et al., 2021; Chen and John Wherry, 2020; Chvatal-Medina et al., 2021; Sette and Crotty, 2021; Vabret et al., 2020). Further, several lines of evidence – including this thesis - show the potential of SARS-CoV-2 to subvert immune responses on several levels (Agerer et al., 2021; Carvalho et al., 2021; Gupta, 2021; Lei et al., 2020; Xia et al., 2020).

1.4.1 Immune response to SARS-CoV-2 infection

Due to massive and coordinated research efforts much is already known about the immune responses to infection with SARS-CoV-2. It has been shown that an early, robust IFN-I response is crucial for the clearance of SARS-CoV-2 and subsequently mild disease (Bastard et al., 2020; Carvalho et al., 2021; Galani et al., 2021; Zhang et al., 2020). In the case of severe COVID-19, a delayed IFN-I response can lead to increased viral load and delayed clearance, which is associated with an elevated and sustained cytokine response (Blanco-Melo et al., 2020; Carvalho et al., 2021; Hadjadj et al., 2020). This is further highlighted by increased levels of interferons and ISGs for prolonged periods (Galani et al., 2021; Lucas et al., 2020b; Zhou et al., 2020). Overall, SARS-CoV-2 has been shown to be sensitive to IFN-I treatment *in vitro*, in contrast to SARS-CoV (Lokugamage et al., 2020; Mantlo et al., 2020). Additionally, it has been demonstrated that RIG-I acts as a restraining factor against SARS-CoV-2, independent of IFN-I induction (Yamada et al., 2021). As such, it binds to the viral RNA and prevents RdRP to access the RNAs for replication (Yamada et al., 2021).

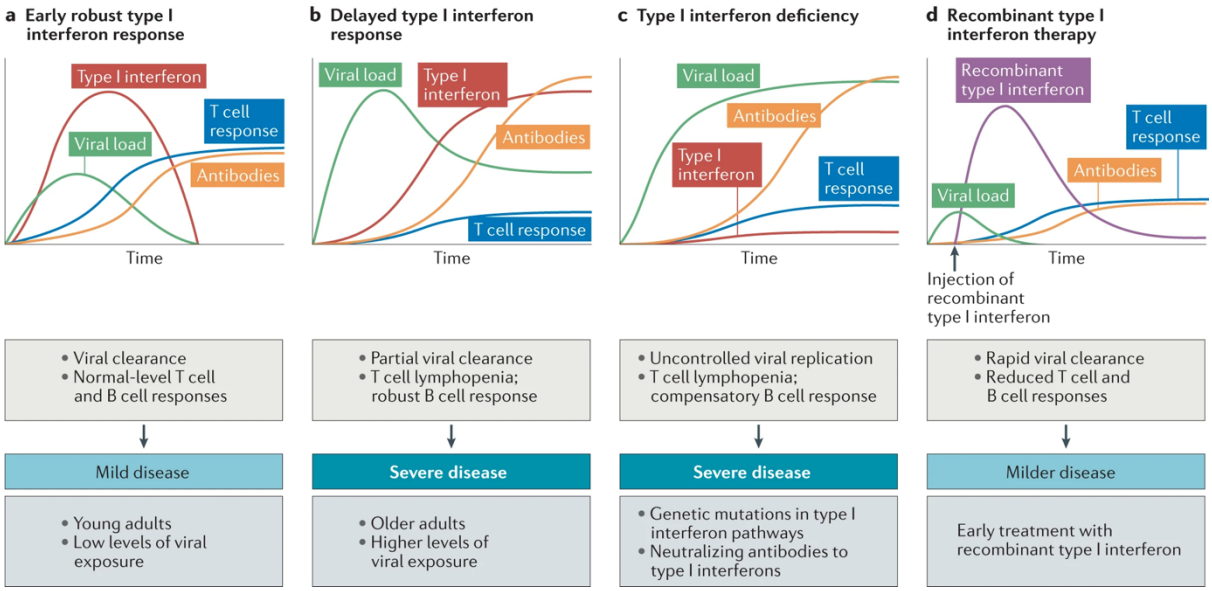

Figure 5. Delayed or aberrant IFN-I responses in severe COVID-19. A) A robust early IFN-I response is associated with timely viral clearance and robust antibody as well as T cell responses and mild disease. B and C) If IFN-I responses are delayed due to e.g. high viral loads or aberrant due to genetic defects, virus cannot be controlled efficiently, leading to sustained IFN-I signaling, reduced T cell responses, but elevated antibody levels. This is generally associated with more severe disease. D) Recombinant IFN-I can help to rapidly clear the virus and result in milder disease but might also lead to decreased adaptive immune responses. Figure taken from (Carvalho et al., 2021). License number 5093811204425.

In addition to innate immune responses, adaptive T and B cell responses have received a lot of attention. In response to SARS-CoV-2 infection the majority of people develop antibodies, as well as virus specific $CD4^+$ and $CD8^+$ T cells, suggesting an intact adaptive response (Sette and Crotty, 2021). Within 10 days post symptom onset virus specific antibodies are detectable in nearly all people tested (Long et al., 2020; Rydyznski Moderbacher et al., 2020; Suthar et al., 2020). Antibodies are mainly targeted to S and N protein, whereas S – and especially its receptor binding domain - is the target for neutralizing antibodies (Piccoli et al., 2020; Suthar et al., 2020). Importantly, these antibodies have been shown to be long lived and levels remained high for more than 8 months post infection (Dan et al., 2021).

Furthermore, robust $CD4^+$ and $CD8^+$ T cell responses have been described by several studies (Sette and Crotty, 2021). $CD4^+$ T cell responses are required for appropriate antibody responses and could be detected against most SARS-CoV-2 proteins (Grifoni et al., 2020a). Importantly, early and robust induction of $CD4^+$ T cell responses was associated with decreased severity and increased viral clearance (Rydyznski Moderbacher et al., 2020; Tan et al., 2021). $CD8^+$ T cell responses are less commonly observed than $CD4^+$ responses but have also been associated with better disease outcome (Grifoni et al., 2020a; Rydyznski Moderbacher et al., 2020). Several studies have mapped and functionally confirmed the

epitopes that are recognized by $CD8^+$ T cells, although this list is likely to be incomplete, due to the bias on HLA variants that have been assessed (le Bert et al., 2020; Ferretti et al., 2020; Grifoni et al., 2020b, 2020a; Nelde et al., 2020; Poran et al., 2020; Schulien et al., 2020; Shomuradova et al., 2020). Comparable to $CD4^+$ T cell epitopes $CD8^+$ epitopes are found across the whole SARS-CoV-2 genome (le Bert et al., 2020; Ferretti et al., 2020; Grifoni et al., 2020a; Nelde et al., 2020; Poran et al., 2020; Schulien et al., 2020; Shomuradova et al., 2020). Similar to antibodies T cell responses were shown to be long lasting (Dan et al., 2021). T cell responses might be impaired in severe COVID-19 and could contribute to disease severity (Chen and John Wherry, 2020). A recent study also suggested that there is higher activation of by-stander cells in mild disease, which could not be detected to the same extent in severe disease (Bergamaschi et al., 2021).

One of the most important aspects of immunity against pathogens is the definition of correlates of protection. For SARS-CoV-2 it has been demonstrated in rhesus macaques that previous infection protected against reinfection, which was promising in the light of vaccine development (Chandrashekar et al., 2020; Deng et al., 2020). Further studies in rhesus macaques and observative studies in humans have demonstrated that antibodies as well as $CD8^+$ T cells are required for complete protection (Brown, 2020; McMahan et al., 2020).

1.4.2 SARS-CoV-2 vaccines

The biggest hope to overcome the SARS-CoV-2 pandemic is the vaccination of a large proportion of the population to slow down viral spread and prevent severe disease (Krammer, 2020). No vaccine against SARS-CoV has been developed, due to the eradication of the virus from the human population (Krammer, 2020). Very early in the pandemic several companies started to develop vaccine candidates for SARS-CoV-2. The target for most of these vaccines is the S protein, against which neutralizing antibodies have also been detected following natural infection (Piccoli et al., 2020; Suthar et al., 2020). Thanks to the use of existing vaccination platforms and staggered trial design, vaccines were developed in record time and four vaccines have been approved by the European Medicines Agency (EMA) as of 20th June 2021 (Krammer, 2020). Interestingly, all approved vaccines utilize one of two novel vaccine technologies: RNA-based vaccines, like the vaccines from Biontech and Moderna, or replication-deficient Adenoviral vectors, like the AstraZeneca and Janssen vaccines (Forni and Mantovani, 2021; Krammer, 2020). Despite the unprecedented speed of development and approval, these vaccines have proven to be safe and efficacious in wide-spread vaccination programs (Forni and Mantovani, 2021; Soiza et al., 2021). The goal is now to vaccinate achieve a high seroprevalence in the population to slow the spread and eventually tame the pandemic virus (Forni and Mantovani, 2021; Krammer, 2020).

1.5 Mechanisms of immune escape

Viruses have evolved several mechanisms to evade or subvert host immune responses to ensure their undisturbed propagation. SARS-CoV-2 has been shown to inhibit innate immunity via various mechanisms. Two studies utilizing unbiased screens demonstrated the potential of several SARS-CoV-2 proteins to antagonize IFN-I responses at several levels (Lei et al., 2020; Xia et al., 2020). The induction of IFN-I expression is antagonized by inhibition of MDA5 activation via PL^{pro} (Liu et al., 2021), whereas the activation and translocation of IRF3 is suppressed by nsp6, nsp12, nsp13 and ORF6 (Lei et al., 2020; Wang et al., 2021b; Xia et al., 2020). Additionally, nsp1 nsp6, nsp13, ORF3a, ORF3b, ORF6, ORF7a, ORF7b and M have IFN-I antagonizing activity and prevent the induction of ISGs and thus the antiviral state (Konno et al., 2020; Xia et al., 2020). ORF8 on the other hand has been shown to induce the downregulation of MHC-I on the surface of the infected cell, thus preventing efficient epitope presentation and recognition by $CD8^+$ T cells (Zhang et al., 2021). An additional strategy to subvert innate responses is to prevent recognition by PRRs. As discussed previously, dsRNAs are shielded from PRRs in membrane compartments called DMVs (V'kovski et al., 2020). Additionally, SARS RNA is capped and 5' phosphorylated by various viral proteins, thus preventing efficient recognition by PRRs (Bouvet et al., 2010; Chen et al., 2009; Ivanov et al., 2004).

1.5.1 Antibody escape

Another potential mechanism for the evasion of immune responses is the prevention of antigen recognition via mutation of antibody recognition sites. This strategy is often observed in RNA viruses, due to their high mutation rates (Alcami and Koszinowski, 2000). SARS-CoV-2 has a relatively low mutation rate and thus has been found to utilize a slightly different strategy. Recurrent deletions in 4 regions in the S protein have been identified in several patients that were virus positive for prolonged periods of time (McCarthy et al., 2021). Importantly, some of these deletions were associated with decreased recognition by antibodies (McCarthy et al., 2021). In an independent study of a long-term infected patient similar mutations with decreased antibody recognition were identified (Kemp et al., 2021). Furthermore, using an unbiased yeast-display system several missense mutations that lead to antibody escape could be identified (Greaney et al., 2021). Strikingly, several new SARS-CoV-2 lineages emerged at the beginning of 2021 that harbored several of these mutations (Ribes et al., 2021). These lineages, including B.1.1.7, B.1.351 and P.1 carry mutations in the RBD as well as deletions in the regions described in the study by McCarthy et al (Ribes et al., 2021). B.1.1.7 can still be effectively neutralized by vaccine-induced antibodies (Muik et al., 2021; Xie et al., 2021).

The remaining two variants B.1.351 and P.1 on the other hand show decreased susceptibility to neutralization by vaccine-induced antibodies and convalescent plasma (Cele et al., 2021; Hoffmann et al., 2021; Xie et al., 2021). It must be noted however, that even though neutralization is reduced, it might still be sufficient to prevent severe disease. Nevertheless, it is possible that future vaccines might need to be adapted to induce sufficient protection against novel variants (Gupta, 2021).

1.5.2 T cell escape

Next to the evasion of antibody responses, viral escape from T cell responses has been shown for chronic infections with RNA viruses like HIV-1 and HCV (Cox et al., 2005; Deng et al., 2015; Goulder and Watkins, 2004; Goulder et al., 2001; Pircher et al., 1990). This is achieved by mutations in viral epitopes that can have different outcomes. One possibility is that the viral epitopes are mutated in a way that cannot be recognized by the TCR anymore and thus would not elicit a T cell response by wildtype specific T cells, but could elicit responses by new, mutant specific T cells (Sun et al., 2016). Another possible mode of action is the mutation of anchor residues - single, key residues that are required for efficient peptide loading to the MHC complex (Falk et al., 1991; Rammensee et al., 1993). This would lead to decreased peptide-MHC stability and result in the inability to present this peptide to the T cells. Furthermore, additional mechanisms have been described that utilize several viral proteins to suppress antigen processing or presentation (Hansen and Bouvier, 2009). One example that has been described for SARS-CoV-2 is the downregulation of MHC-I by ORF8, which results in decreased epitope presentation (Zhang et al., 2021). However, to what extent and how naturally occurring mutations in SARS-CoV-2 can append CTL responses was unknown and interrogating these questions was one goal of this thesis. To investigate this, we generated and analyzed deep viral sequencing data from 747 infected individuals and investigated missense mutations in viral CD8 epitopes. We further tested identified mutant epitopes for their potential to induce T cell responses with cell-free *in vitro* assays as well as with PBMCs isolated from SARS-CoV-2 convalescent individuals.

2. Aims

The aims of this study were the following:

1) Investigate and characterize mutations in the SARS-CoV-2 genome that might affect $CD8^+$ T cell epitopes.
2) Determine the potential of such mutations to evade $CD8^+$ T cell responses.
3) Investigate potential mechanisms of reduced $CD8^+$ T cell responses to mutated epitopes.

3. Results

3.1 Prelude

During the SARS-CoV-2 pandemic the virus spread all over the world and caused wide-spread infections. During the pandemic, mutations in the SARS-CoV-2 genome led to several new lineages with different properties. Additionally, intra-host diversity can be observed, adding to the genetic complexity (Popa et al., 2020). Several studies have shown that mutations in the S gene can lead to decreased antibody responses. In this study titled "**SARS-CoV-2 mutations in MHC-I-restricted epitopes evade CD8+ T cell responses**" we identify naturally occurring mutations in $CD8^+$ T cell epitopes and reveal their potential to evade recognition by $CD8^+$ T cells. Importantly, this study was the first to show that single amino-acid changes in the SARS-CoV-2 genome can lead to reduced CD8+ T cell responses and adds to the growing literature on immune evasion by SARS-CoV-2.

3.2 SARS-CoV-2 mutations in MHC-I-restricted epitopes evade CD8+ T cell responses

Science Immunology; 04 Mar 2021; Vol. 6, Issue 57, eabg6461

DOI: 10.1126/sciimmunol.abg6461

Benedikt Agerer[†], Maximilian Koblischke[†], Venugopal Gudipati[†], Luis Fernando Montaño-Gutierrez, Mark Smyth, Alexandra Popa, Jakob-Wendelin Genger, Lukas Endler, David M. Florian, Vanessa Mühlgrabner, Marianne Graninger, Stephan W. Aberle, Anna-Maria Hus, Lisa Ellen Shaw, Alexander Lercher, Pia Gattinger, Ricard Torralba-Gombau, Doris Trapin, Thomas Penz, Daniele Barreca, Ingrid Fae, Sabine Wenda, Marianna Traugott, Gernot Walder, Winfried F. Pickl, Volker Thiel, Franz Allerberger, Hannes Stockinger, Elisabeth Puchhammer-Stöckl, Wolfgang Weninger, Gottfried Fischer, Wolfgang Hoepler, Erich Pawelka, Alexander Zoufaly, Rudolf Valenta, Christoph Bock, Wolfgang Paster, René Geyeregger, Matthias Farlik, Florian Halbritter, Johannes B. Huppa[††], Judith H. Aberle[††] and Andreas Bergthaler[††]

[†, ††] equal contributions

ScienceImmunology

Submitted Manuscript: Confidential

Title: SARS-CoV-2 mutations in MHC-I-restricted epitopes evade CD8$^+$ T cell responses

Authors:

Benedikt Agerer[1,†], Maximilian Koblischke[2,†], Venugopal Gudipati[3,†], Luis Fernando Montaño-Gutierrez[4], Mark Smyth[1], Alexandra Popa[1], Jakob-Wendelin Genger[1], Lukas Endler[1], David M. Florian[2], Vanessa Mühlgrabner[3], Marianne Graninger[2], Stephan W. Aberle[2], Anna-Maria Husa[4], Lisa Ellen Shaw[5], Alexander Lercher[1,§], Pia Gattinger[6], Ricard Torralba-Gombau[1], Doris Trapin[7], Thomas Penz[1], Daniele Barreca[1], Ingrid Fae[8], Sabine Wenda[8], Marianna Traungott[9], Gernot Walder[10], Winfried F. Pickl[7,11], Volker Thiel[12,13], Franz Allerberger[14], Hannes Stockinger[3], Elisabeth Puchhammer-Stöckl[2], Wolfgang Weninger[5], Gottfried Fischer[7], Wolfgang Hoepler[9], Erich Pawelka[8], Alexander Zoufaly[8], Rudolf Valenta[3,6,11,15-16], Christoph Bock[1,17], Wolfgang Paster[4], René Geyeregger[4], Matthias Farlik[5], Florian Halbritter[4], Johannes B. Huppa[3,††], Judith H. Aberle[2,††], Andreas Bergthaler[1,††,*]

Affiliations:

[1] CeMM Research Center for Molecular Medicine of the Austrian Academy of Sciences, Vienna, Austria

[2] Center for Virology, Medical University of Vienna, Vienna, Austria

[3] Institute for Hygiene and Applied Immunology, Center for Pathophysiology, Infectiology and Immunology, Medical University of Vienna, Vienna, Austria

[4] St. Anna Children´s Cancer Research Institute (CCRI), Vienna, Austria

[5] Department of Dermatology, Medical University of Vienna, Vienna, Austria.

[6] Department of Pathophysiology and Allergy Research, Division of Immunopathology, Medical University of Vienna, Vienna, Austria

[7] Institute of Immunology, Center for Pathophysiology, Infectiology and Immunology, Medical University of Vienna, Vienna, Austria

[8] Department of Blood Group Serology and Transfusion Medicine, Medical University of Vienna, Vienna, Austria

[9] Department of Medicine 4, Clinic Favoriten, Vienna, Austria

[10] Division of Hygiene and Medical Microbiology, Medical University of Innsbruck, Innsbruck, Austria

[11] Karl Landsteiner University of Health Sciences, Krems, Austria

[12] Institute of Virology and Immunology, Bern and Mittelhäusern, Switzerland

[13] Department of Infectious Diseases and Pathobiology, Vetsuisse Faculty, University of Bern, Bern, Switzerland.

[14] Austrian Agency for Health and Food Safety (AGES), Vienna, Austria

[15] Laboratory for Immunopathology, Department of Clinical Immunology and Allergy, First Moscow State Medical University Sechenov, Moscow, Russia

[16] NRC Institute of Immunology FMBA of Russia, Moscow, Russia

[17] Department of Laboratory Medicine, Medical University of Vienna, Vienna, Austria.

§ present address: Laboratory of Virology and Infectious Disease, The Rockefeller University, New York, USA

†, †† Equal contributions

* Correspondence to: A.B. abergthaler@cemm.oeaw.ac.at.

One Sentence Summary: SARS-CoV-2 mutations in MHC-I epitopes identified by deep viral sequencing evade CTL responses through decreased peptide-MHC-I binding.

Abstract: $CD8^+$ T cell immunity to SARS-CoV-2 has been implicated in COVID-19 severity and virus control. Here, we identified nonsynonymous mutations in MHC-I-restricted $CD8^+$ T cell epitopes after deep sequencing of 747 SARS-CoV-2 virus isolates. Mutant peptides exhibited diminished or abrogated MHC-I binding in a cell-free in vitro assay. Reduced MHC-I binding of mutant peptides was associated with decreased proliferation, IFN-γ production and cytotoxic activity of $CD8^+$ T cells isolated from HLA-matched COVID-19 patients. Single cell RNA sequencing of ex vivo expanded, tetramer-sorted $CD8^+$ T cells from COVID-19 patients further revealed qualitative differences in the transcriptional response to mutant peptides. Our findings highlight the capacity of SARS-CoV-2 to subvert $CD8^+$ T cell surveillance through point mutations in MHC-I-restricted viral epitopes.

Introduction

SARS-CoV-2 infection elicits broad activation of the innate and adaptive arms of immunity (*1–4*). Major correlates of protection are neutralizing antibodies and cytotoxic $CD8^+$ T-lymphocytes (CTLs) (5). CTLs play an essential role in conferring immune memory and protection against viral pathogens (6–8). CTLs kill infected cells upon recognition of viral epitopes as they are displayed on the cell surface in the context of the class I major histocompatibility complex proteins (MHC-I). Certain positions in these epitopes have been shown to be critical for MHC-I presentation and mutations in these so-called anchor residues might interfere with peptide binding to MHC-I (9, 10). CTL responses have been described in great detail in SARS-CoV-2–infected patients (*3*, *4*, *11–15*). In acute SARS-CoV-2 infection, CTLs show high levels of cytotoxic effector molecules such as granzyme B, perforin and IFN-γ (*16*). Numerous human leukocyte antigen (HLA)-restricted CTL epitopes have been characterized for SARS-CoV-2 (*4*, *17–22*).

Compelling evolutionary evidence for CTL-mediated control of RNA viruses causing chronic infections like HIV and HCV is provided by mutations occurring in viral epitopes which directly interfere with MHC-I-restricted T cell antigen recognition and killing by CTLs (*24–27*). While several mutations in SARS-CoV-2 have recently been associated with an escape from antibody responses (*28–30*), the extent to which SARS-CoV-2 mutations may upend the presentation of virus-derived peptides via MHC-I remains to be determined. In this study, we used deep viral genome sequencing to identify nonsynonymous mutations in previously reported MHC-I epitopes. We applied a combination of cell-free in vitro assays, as well as functional and transcriptional characterization of COVID-19 patient-derived PBMCs to investigate the potential of single point mutations in MHC-I epitopes to evade CTL responses.

Results

Bioinformatic analysis of mutations in putative SARS-CoV-2 CD8$^+$ T cell epitopes

To assess a possible impact of virus mutations on SARS-CoV-2-specific CD8$^+$ T cell responses, we performed deep viral genome sequencing (> 20,000X coverage) (Fig. S1A) and bioinformatic analysis on 747 SARS-CoV-2 samples (21). We focused on 27 CTL epitopes, which had previously been reported as experimentally-validated epitopes restricted by HLA-A*02:01 (allele frequency 0.29 in Austria) or HLA-B*40:01 (allele frequency 0.03-0.05 in Austria) (*4*, *17–20*, *31*). Most of the selected epitopes are located in the S protein (N=13) and the remaining epitopes are distributed between the N (N=6), ORF1ab (N=4), M (N=3) and E (N=1) proteins. Detailed descriptions of peptides and their three-letter code are listed in Table S1. Among these epitopes we detected 194 nonsynonymous mutations present at frequencies of ≥ 0.02 in 229 samples (Fig. 1A-B). Of these 194 variants, 35 were found at frequencies between 0.1 to 0.5. Notably, 9 variants were fixed (frequency ≥ 0.9) and found in 53 different patient samples (Table S2). Due to overlaps in some epitopes, these 194 mutations result in 199 different epitope variants. Forty-one of these mutations were localized to anchor residues, and 21 mutations affected auxiliary residues, which are both integral to MHC-I peptide loading (Fig. S1B) (*9*, *10*). Prediction of the binding strength of the wild type and mutant peptides to HLA-A*02:01 and HLA-B*40:01 via NetMHCpan v4.1 (*32*) revealed weaker peptide binding to MHC-I, as indicated by an increase of NetMHCpan % ranks (Fig. S1C-F). For many of the investigated CTL epitopes, we detected multiple variants that independently emerged in different SARS-CoV-2 infected individuals (Fig. 1A). To corroborate these findings from low-frequency mutations in our deep sequencing dataset, we analyzed fixed mutations in >145,000 available global SARS-CoV-2 sequences from the public database GISAID (*33*). Mutations were observed in 0.0000689 - 7.336% epitope sequences (mean = 0.005106%)

(Fig. 1C). We found 10 to 11,717 viral genome sequences with a nonsynonymous mutation for each of the investigated 27 CTL epitopes (mean = 807.05). Importantly, we found fixed variants in GISAID that were also identified in our low-frequency analysis, highlighting the relevance of individual low-frequency mutations (Fig. 1D, S1G-S1H).

To examine the time dynamics of low-frequency epitope mutations in patients, we utilized serially-sampled viral genomes from COVID-19 patients. Suggestive of CTL-mediated selection pressures, mutations in viral epitopes arose typically later in infection (Fig. 1E). Based on our analysis of low-frequency and fixed mutations, we selected 11 wild type and 17 corresponding mutant peptides with predicted decreased HLA-binding strength for further biophysical and functional analyses (Table S3).

Mutations in CTL epitopes destabilize MHC-I complexes

To assess the MHC-I dependent immunogenic properties of nonsynonymous mutant peptides we produced MHC-I complexes with ultraviolet light cleavable peptides (UVCP) and performed peptide exchange reactions to destabilize and later reassemble MHC-I UVCP complexes (*34*). We next employed cell-free differential scanning fluorimetry (DSF) to measure the thermal stability of destabilized or reassembled MHC-I complexes (Fig. 2A-E, S2A-L) (*35–37*). As shown in Fig. S1A and S1B, HLA-A*02:01-UVCP complex is destabilized upon exposure to UV light and can be reassembled by adding UVCP peptide after UV exposure. The minima of the curves specify the melting temperature (T_m) of the HLA-peptide complexes. T_m values well above 37°C indicate strong peptide binding to MHC-I at physiological temperatures, whereas values around 37°C correlate only with weak and below 36°C with absent binding. For 9 of the 11 wild type peptides we observed binding to HLA-A*02:01 or HLA-B*40:01, indicating that these peptides can in

principle be presented by the respective HLA allele (Fig. S2C and S2D). In contrast, 11 analyzed mutants exhibited decreased stabilizing capacity towards MHC-I (Fig. 2A-E, S2D, S2F-S2L, Table S4). The HLA-B*40:01–restricted MEVTPSGTWL peptide featured specific binding to recombinant HLA-B*40:01 but not to HLA-A*02:01 (*4*) (Fig. 2C, S2L). An example of a weak binder is the mutant variant YFQPRTFLL (instead of YLQPRTFLL), whereas LFFNKVTLA (instead of LLFNKVTLA) represents a non-binder for HLA-A*02:01 (Fig. 2A, D). Of note, we did neither observe binding of the wild type nor the mutant peptides to HLA-A*02:01 for the published CTL epitopes LQLPQGTTL and LALLLLDRL (Fig. S2I and S2L).

To further corroborate these results, we generated peptide-loaded HLA-A*02:01 and HLA-B*40:01 tetramers presenting wild type and mutant peptides as a means to identify cognate $CD8^+$ T cells from expanded PBMCs of HLA-matched COVID-19 patients. As shown in Fig. 2F, tetramers loaded with mutant peptides stain cognate T cells in a T-cell receptor (TCR)-dependent fashion when kept at 4°C. However, when tetramers were incubated at 37°C prior to their use, T cell staining was abrogated, most likely due to peptide loss and structural disintegration of MHC-I. Taken together, these results imply that mutations found in SARS-CoV-2 genome sequences decrease peptide-MHC-I stability and subsequently could promote immune evasion from HLA-dependent recognition by CTLs.

Investigation of epitope responses in SARS-CoV-2 positive patient PBMCs

Next, we investigated peptide-specific $CD8^+$ T cell responses in PBMCs isolated from HLA-A*02:01 or HLA-B*40:01 positive COVID-19 patients (Fig. 3A, Table S5, Table S6). We first screened the 9 wild type peptides, which showed MHC-I binding in the DSF assay, using ex vivo ELISpot assays (Table S7). Of note, none of the 5 pre-pandemic healthy controls gave responses

to any of the peptides. Further, we could detect a positive response in at least one patient for four of the peptides, which were investigated in additional assays. To this end HLA-matched PBMCs from COVID-19 patients and 5 pre-pandemic controls were stimulated with peptides and cultured for 10-12 days followed by tetramer staining (Fig. 3B). This allowed us to confirm these wild type peptides as bona fide T cell epitopes in SARS-CoV-2. We further corroborated virus-specific CTL responses by intracellular cytokine staining (ICS) for IFN-γ after peptide-mediated restimulation (Fig. S3A, B). To investigate the extent to which identified mutations in viral epitopes affected T cell proliferation, we stained wild type or mutant peptide expanded PBMCs with wild type peptide-loaded HLA tetramers. We found fewer tetramer-positive $CD8^+$ T cells in PBMCs expanded in the presence of mutant peptides, indicating that mutant peptides featured significantly reduced immunogenicity (Fig. 3C-F). Consistent with this, ICS for IFN-γ revealed significantly diminished CTL responses after restimulation with mutant peptide as compared to the corresponding wild type peptides (Fig. 3G-J). We observed markedly diminished CTL responses to several mutant peptides both presented in the context of HLA-A*02:01 and HLA-B*40:01. This was further supported by peptide titration experiments involving wild type peptides and their mutant counterparts for T cell stimulation (Fig. S3C). To complement intracellular cytokine measurements, we also carried out ex vivo ELISpot assays after stimulating PBMCs with wild type or mutant peptides without extended expansion. These experiments confirmed that stimulation with mutant peptides resulted in significantly fewer cytokine-producing cells than with wild type peptides (Fig. 3K, S3D). To further corroborate these results, we performed functional cytotoxicity assays with PBMCs isolated from four COVID-19 patients expanded for 10-12 days in the presence of wild type or mutant YLQPRTFLL (YLQ) peptide. We assessed the ability of these cells to kill autologous Epstein-Barr virus (EBV)-transformed lymphoblastoid B cell lines (EBV^+ B cells) that were

pulsed with either wild type or mutant YLQ. While wild type expanded PBMCs showed specific killing of wild type pulsed EBV^+ cells, they failed to kill EBV^+ B cells pulsed with mutant peptide (Fig. 3L), suggesting that mutant YLQ is not properly presented by the EBV^+ B cells. Furthermore, PBMCs expanded with mutant peptides failed to kill both wild type and mutant peptide pulsed EBV^+ B cells (Fig. 3L and S3E). These results further underline that expansion with the mutant peptide failed to mount a functional CTL response.

Transcriptional single T cell analysis upon stimulation with wild type or mutant peptides

To further characterize our results from patient PBMCs we expanded PBMCs isolated from two patients (SARS042 and SARS060) for 10-12 days in the presence of wild type or mutant YLQ peptide. We sorted equal numbers of YLQ tetramer-positive and tetramer-negative $CD8^+$ T cells for each condition, labeled them with oligonucleotide-barcoded antibodies (TotalSeq anti-human Hashtag) and performed single-cell RNA sequencing (scRNA-seq) combined with TCR sequencing on a total of 17635 cells (Fig 4A, S4A). We again noted that expansion elicited by the mutant YLQ peptide resulted in reduced numbers of YLQ tetramer positive cells, consistent with our previous results (Fig. 4B). This unbiased sequencing approach led to the identification of 10 distinct clusters, showing a clear division between tetramer negative and tetramer positive cells (Fig. 4C, S4B). For tetramer positive (responding) cells we identified differential clustering between wild type- and mutant-stimulated cells, indicating that stimulation with mutant peptides not only leads to reduced expansion, but also altered gene expression in tetramer-specific $CD8^+$ T cells (Fig. 4D). In contrast, tetramer negative (nonresponding) wild type and mutant-stimulated cells clustered in mixed neighborhoods, further suggesting that differences can only be found in responding cells.

We next analyzed the TCR sequences of these cells. In tetramer negative cells we found a high diversity of TCR sequences for both wild type and mutant peptide conditions (Fig. 4E, S4C). In response to peptide stimulation, we found that the pool of cells consisted of a subset of clones, with 5 T cell clones making up more than 50% of T cells in both patients (Fig. 4E). Importantly, we found the TRAV12-1 gene to be the dominant TRAV variant for both patients, as well as the two TRBV variants TRBV7-9 and TRBV2 to be prominent, which were all recently found to be part of public TCRs specific for YLQ (*19*, *22*) (Fig. 4F). We further asked whether there are T cell clones that specifically expand in response to the mutant peptide. Interestingly, we discovered expansion of the same T cell clones upon stimulation with either wild type or mutant peptide (Fig. 4E).

We next investigated gene expression signatures associated with cytotoxic activity and exhaustion (*38*). Importantly, cytotoxic gene signatures were found enriched in tetramer positive cells (as compared to tetramer negative cells). In line with our cytotoxicity assay results we found upregulated expression of cytotoxicity associated genes, such as *GZMB*, *PRF1* and *NKG7*, and decreased expression of genes associated with naïve T cell states, such as *IL7R* and *TCF7* (Fig. S4D and S4E). To further our understanding of qualitative differences we performed differential gene expression analysis to compare wild type and mutant peptide-stimulated cells (Fig 4G). We identified lower expression levels of several cytotoxicity- and exhaustion-associated transcripts such as *GZMB*, *GNLY*, the coinhibitory receptors *LAG3* and *HAVCR2,* the cytokines *IFNG*, *CCL3* and *CCL4* and the costimulatory gene *SIRPG* in mutant-stimulated T cells (Fig. 4G, 4H and S4G). This is in line with a more profound exhaustion gene signature, that has recently been identified in SARS-CoV-2-specific $CD8^+$ T cells in cells stimulated with wild type peptide (Fig. S4F). This signature was linked in the literature to a higher expression of cytotoxicity-associated genes (*38*).

These findings further underline qualitative differences in the response to expansion with mutant peptide and are in line with the results from the killing assay presented earlier (Fig. 3L). In contrast, we found a set of genes including *GZMK, LTB, CD74*, *SELL*, *IFITM1*, *IFITM2* and *CX3CR1* expressed at higher levels in cells stimulated with mutant peptides (Fig S4F, S4H-S4K). Taken together, the scRNA-seq data indicate that stimulation with mutant peptide did not only lead to a reduced T cell response but also to altered gene expression patterns.

Discussion

The presented data demonstrate that SARS-CoV-2 may evade CTL surveillance through mutations in viral epitopes which lead to reduced peptide-MHC-I binding and quantitatively and qualitatively altered CTL responses. Deep SARS-CoV-2 genome sequencing results afford a valuable additional perspective that complements insights gained from numerous studies on SARS-CoV-2-specific T cell responses (*39*). Viruses employ numerous strategies to evade $CD8^+$ T cell immune responses (*40–42*). The SARS-CoV-2 encoded ORF8 protein is hypothesized to downregulate the surface expression of MHC-I molecules (*43*), and several reports linked mutations within the viral spike protein to the evasion of neutralizing antibody responses (*28–30*). Yet, we still lack a comprehensive understanding of the intrinsic capabilities of SARS-CoV-2 for immune evasion. Our study provides evidence that single nonsynonymous mutations in SARS-CoV-2 can subvert the immune response to $CD8^+$ T cell epitopes. The majority of nonsynonymous mutations found in the validated CTL escapes had not reached fixation, i.e. were present at frequencies between 0.02 and 0.42 (Fig. 1B). This could be explained by the shorter duration of infection with SARS-CoV-2 compared to HIV or HCV. It may also reflect on the degree to which HLA polymorphism

affects viral spreading within human populations. The impact of single anchor residue substitutions on the response of $CD4^+$ T cells is still unclear.

Our findings do not rule out that substitutions of residues facing the cognate T cell receptor may give rise to the emergence of CTL neoepitopes. Of note, we could show for the YLQ epitope that T cell clones that expanded in vitro in the presence of mutant peptides were identical to those expanded in response to the wild type peptide, suggesting a similar if not identical structural basis underlying TCR-epitope engagement.

This study does not allow direct conclusions to be drawn concerning potential selection pressures which shape the mutational landscape of $CD8^+$ T cell epitopes. This would invariably involve accounting for the HLA genotype of all individuals from whom SARS-CoV-2 genomes were sequenced. Moreover, how CTL escape mutations are maintained during transmission between individuals with differing HLA subtypes and how viruses carrying epitope mutations affect disease severity requires further investigation.

Many CTL epitopes for SARS-COV-2 have been described (*39*). Natural CTL responses against SARS-CoV-2 were associated with broad epitope recognition of on average 1.6 $CD8^+$ T cell epitopes per antigen per HLA allele (*23*), which raises the question whether and how mutations in single epitopes affect virus control. This may be of particular importance for SARS-CoV-2 subunit vaccines, such as the RNA vaccines currently in use, which contain the S gene only and thus induce responses against a limited number of CD8 epitopes (*44–46*). In summary, our results highlight the capacity of SARS-CoV-2 to evade adaptive immune responses through sporadically emerging mutations in MHC-I epitopes.

Materials and Methods

Study design

The objective of this study was to investigate mutations in SARS-CoV-2 for their potential to evade $CD8^+$ T cell responses. For this study, we performed deep sequencing on virus samples from Austria. To characterize identified mutants, we performed in vitro MHC-I binding assays. Further, we performed functional assays on PBMCs isolated from COVID-19 patients. PBMCs were only analyzed from patients who were positive for HLA-A*02:01 or HLA-B*40:01. This study was performed in accordance with the recommendations of the Declaration of Helsinki. The protocols were approved by the Ethics Committee of the Medical University of Vienna, Austria (2283/2019 and 1339/2017) and written informed consent was obtained from all patients.

Virus sample collection and processing

Virus samples were obtained from the Medical University of Vienna Institute of Virology, Medical University of Innsbruck Institute of Virology, Medical University of Innsbruck Department of Internal Medicine II and Division of Hygiene and Medical Microbiology, Central Institute for Medical-Chemical Laboratory Diagnostics Innsbruck, Klinikum Wels-Grieskirchen and the Austrian Agency for Health and Food Safety (AGES). Sample types included oropharyngeal swabs, nasopharyngeal swabs, tracheal secretion, bronchial secretion, serum and plasma. RNA was extracted using the following commercially available kits following the manufacturer's instructions: EasyMag (bioMérieux), MagMax (Thermo Fisher), MagNA Pure LC 2.0 (Roche), AltoStar Purification Kit 1.5 (Altona Diagnostics), MagNA Pure Compact (Roche) and

QIAsymphony (Qiagen). Viral RNA was reverse-transcribed with Superscript IV Reverse Transcriptase (Thermo Fisher) and viral sequences were amplified with modified primer pools (*47*). PCR reactions were pooled and processed for high-throughput sequencing.

PBMC sample collection and processing

Whole blood samples from hospitalized SARS-CoV-2-infected patients were collected at the Department of Medicine 4, Clinic Favoriten. Samples from the same individual were collected at 2- to 7-day time intervals to obtain sufficient blood volumes for different T cell analyses. Samples from healthy blood donors that were never exposed to SARS-CoV-2, were collected before the SARS-CoV-2 pandemic (June to November 2019). Peripheral blood mononuclear cells (PBMCs) were isolated by density gradient centrifugation and stored in liquid nitrogen until further use. HLA typing of PBMCs was carried out by next generation sequencing, as described previously (*48*).

Virus sequencing, data processing and analysis

AMPure XP beads (Beckman Coulter) at a 1:1 ratio were used for amplicon clean-up. Amplicon concentrations and size distribution were assessed with the Qubit Fluorometric Quantitation system (Life Technologies) and the 2100 Bioanalyzer system (Agilent), respectively. After normalization of amplicon concentrations, sequencing libraries were generated with the NEBNext Ultra II DNA Library Prep Kit for Illumina (New England Biolabs) according to the manufacturer's instructions. Library concentrations and size distribution were again assessed as indicated previously and pooled at equimolar ratios for sequencing. Sequencing was carried out

on the NovaSeq 6000 platform (Illumina) on a SP flow cell with a read length of 2x250bp in paired-end mode.

After demultiplexing, FASTQ files were quality controlled using FASTQC (v. 0.11.8)(*49*). Adapter sequences were trimmed with BBDUK from the BBTools suite (http://jgi.doe.gov/data-and-tools/bbtools). Overlaps of paired reads were corrected with the BBMERGE from BBTools. Read pairs were mapped on the combined GRCh38 and SARS-CoV-2 genome (RefSeq: NC_045512.2) using BWA-MEM with a minimal seed length of 17 (v 0.7.17) (*50*). Only reads uniquely mapping to the SARS-CoV-2 genome were retained. Primer sequences were masked with iVar (*51*). The consensus FASTA file was generated from the binary alignment map (BAM) file using Samtools (v 1.9) (*52*), mpileup, Bcftools (v 1.9) (*52*), and SEQTK (https://github.com/lh3/seqtk). The read alignment file was realigned with the Viterbi method from LoFreq (v 2.1.2) for low-frequency variant calling(*53*). InDel qualities were added and low-frequency variants were called with LoFreq. Variants were filtered with LoFreq and Bcftools (v 1.9) (*54*). We only considered variants with a minimum coverage of 75 reads, a minimum phred-value of 90 and indels (insertions and deletions) with a HRUN of at least 4. Based on the control experiments described earlier, all analyses were performed on variants with a minimum alternative frequency of 0.02 (*55*). Variants were annotated with SnpEff (v 4.3) (*56*) and SnpSift (v 4.3) (*57*).

The output of LoFreq was filtered for nonsynonymous variants with a frequency cut-off of 0.02. The resulting mutations were then filtered for positions in reported $CD8^+$ T cell epitopes. Data manipulation and plotting was carried out in R, with the packages dplyr, tidyr, ggplot2 and heatmap2.

Identification of epitope mutations in SARS-CoV-2 genomes

Mutations in epitope regions were identified in all available protein alignment files for the SARS-CoV-2 proteins non-structural protein 3 (NSP3, n=164,819), NSP6 (n=164,806), M (n=164,846), spike (S, n=165,249), N (n=164,876) and E (n=164,847) retrieved on October 30, 2020, from the global initiative on sharing all influenza data (GISAID) database (*33*). Protein alignment files were first filtered for protein sequences that have less than 5% unknown amino acid positions. Epitope regions were then extracted from the alignment files and misaligned entries (>4 misaligned positions in epitope region) and protein sequences with more than 4 unknown positions in epitope regions were removed. Mutations in epitope regions were identified based on sequence comparison to the reference sequence "Wuhan-Hu-1" (GenBank: MN908947.3) (*58*).

MHC-I binding predictions

To predict the binding strength of wild type and mutant peptides, NetMHCpan 4.1 was used (*32*). Briefly, wild type and mutant peptide sequences were interrogated for binding to HLA-A*02:01, HLA-A*02:06 and HLA-B*40:01 with the standard settings (strong binder % rank 0.5, weak binder % rank 2). The % ranks of wild type and mutant epitopes were then compared and plotted along the heatmap of variant frequencies.

Peptides

Peptides were purchased from JPT Peptide Technologies GmbH or synthesized in-house, as indicated in Table S2. Peptides were produced in-house by solid-phase synthesis with the 9-fluorenyl-methoxy carbonyl (Fmoc)-method (CEM-Liberty and Applied Biosystems) on PEG-PS preloaded resins (Merck, Darmstadt, Germany) as previously described (*59*, *60*) with the following

alterations. After synthesis the peptides were washed with 50 ml dichloromethane (Roth), cleaved from the resins using 28.5 ml trifluoroacetic acid (Roth), 0.75 ml silane (Sigma-Aldrich, St. Louis, MO, USA) and 0.575 ml H_2O for 2.5 hours at room temperature (RT) and precipitated into pre-chilled *tert*-butylmethylether (Merck). The peptides were purified by reversed-phase high-performance liquid chromatography in a 10–70% acetonitrile gradient using a Jupiter 4 µm Proteo 90 Å LC column (Phenomenex) and an UltiMate 3000 Pump (Dionex) to a purity >90%. Their identities and molecular weights were verified by mass spectrometry (Microflex MALDI-TOF, Bruker).

Synthesis of HLA/Peptide complexes.

cDNA encoding the extracellular domains of HLA-A*02:01 (UniProt: P01892) HLA-B*40:01 (UniProt: P01889) and beta-2-microglobulin (UniProt: P61769) were cloned without the leader sequence into pET-28b (HLA-A*02:01, HLA-B*40:01) and pHN1 (beta-2-microglobulin, β2m) for recombinant protein expression as inclusion bodies in *E. coli*. pET-28b was modified to encode a C-terminal 12x poly histidine tag (HIS_{12}) or AviTag. Single colonies of *E. coli* (BL21) transformed with individual vectors were grown in 8l Luria-Bertani (TB) media at 37°C to an OD600 of 0.5. Protein expression was induced by addition of isopropyl β-D-thiogalactoside (IPTG, Sigma-Aldrich) to a final concentration of 1 µM. Cells were harvested after 4 hours of induction. Inclusion bodies containing HLA and β2m protein were isolated, fully denatured and refolded in vitro in the presence of ultraviolet light-cleavable peptides (UVCP; GILGFVFJL for HLA-A*02:01; TEADVQJWL for HLA-B*40:01; J= 3-amino-3-(2-nitro)phenyl-propionic acid) to produce HLA/UVCP protein (UVCP peptides: GILGFVFJL for HLA-A*02:01, TEADVQJWL for HLA-B*40:01, J= 3-amino-3-(2-nitro)phenyl-propionic acid) (*34*, *61*, *62*). The refolding

reaction (500 ml) was dialyzed three times against 10 L of PBS. Dialyzed HLA/UVCP HIS_{12} tag proteins were purified by Ni^{2+}-NTA agarose chromatography (HisTrap excel, GE Healthcare) followed by size exclusion chromatography (SEC) (Superdex 200 10/300 GL, GE Healthcare). Dialyzed HLA/UVCP AviTag proteins were concentrated to 2 ml using spin concentrators and purified by SEC. Purified HLA/UVCP AviTag proteins were biotinylated using biotin protein ligase BirA as described (*63*) and further purified by SEC. The purity and integrity of all proteins was confirmed via SDS-PAGE followed by silver staining.

UV-mediated peptide exchange, Differential scanning fluorimetry (DSF) and tetramer synthesis

For peptide exchange, peptides were added to HLA/UVCP at an HLA/UVCP:peptide molar ratio of 1:20 (at a final concentration of 1.5 µM and 30 µM, respectively). For efficient cleavage, the reaction mix was placed within 5 cm from the CAMAG® UV Lamp 4 (Camag) and exposed to 366 nm UV light for 2h at 4ºC followed by 16h incubation at 4ºC.

For DSF, SYPRO Orange Protein Gel Stain (Thermo Fisher Scientific, 5000x stock solution) was diluted at 4°C into the solution containing UV-treated HLA/peptide HIS_{12} mixtures (see above) at a final concentration of 15x SYPRO Orange Protein Gel Stain. The reaction mix was immediately transferred to pre-chilled PCR tubes and placed on a CFX 96 Real-Time PCR system (BioRad) which had been precooled to 4 ºC. Samples were heated at a rate of 0.4ºC/20 s and relative fluorescence units (rfu) were measured every 20s in the FRET channel. Readings were plotted as negative derivative of fluorescence change vs. temperature -d(RFU)/dT.

For tetramer synthesis fluorescence-labeled streptavidin was added to UV-exchanged HLA/peptide AviTag protein solution in 10 steps as published (*64*).

Flow cytometry assays following 10-12d in vitro stimulation

For in vitro expansion, cryopreserved PBMCs were thawed in pre-warmed RPMI-1640 medium (R0883, Sigma) containing 10% FBS (FBS 12-A, Capricorn), 10 mM Hepes (Sigma), 2 mM GlutaMAX (Gibco), 50 IU/ml Pen-Strep (Sigma) and 50 IU IL-2 (Peprotech) at a concentration of 1×10^6 cells/ml. PBMCs were pulsed with peptides (1 µg/ml) and cultured for 10-12 days adding 100 IU IL-2 on day 5. In vitro expanded cells were analyzed by intracellular cytokine and cell surface marker staining. PBMCs were incubated with 2 µg/ml of peptide and 1 µg/ml anti-CD28/49d antibodies (L293 and L25, Becton Dickinson) or with CD28/49d antibodies alone (negative control) for 6h. After 2h, 0.01 µg/ ml brefeldin A (Sigma) was added. Staining was performed using APC/H7 anti-human CD3 (SK7, Becton Dickinson), Pacific Blue anti-human CD4 (RPA-T4, Becton Dickinson), PE anti-human CD8 (HIT8a, Becton Dickinson), FITC anti-human IFN-γ monoclonal antibodies (25723.11, Becton Dickinson), and Fix/Perm kit (Invitrogen). Viable cells were determined using live/dead cell viability assay kit (Invitrogen). Tetramer staining (10 µg/ml) was performed for 60 minutes at 4ºC followed by staining with anti-CD8α antibody (OKT8, Invitrogen) (10 µg/ml) for 30 minutes at 4ºC.

Flow-cytometric analyses were carried out on Cytek® Aurora (Cytek® Biosciences) or FACS Canto II (Becton Dickinson) instruments and evaluated using FlowJo software v. 7.2.5 (Tree Star). The gate for detection of IFN-γ in peptide-stimulated cell samples was set in the samples with costimulation only.

IFN-γ ELISpot assay

For ex vivo ELISpot assays, PBMCs were thawed and depleted of $CD4^+$ cells using magnetic microbeads coupled to anti-CD4 antibody and LD columns according to the manufacturer´s instructions (Miltenyi Biotec). A total of 1-2 x 10^5 CD4-depleted cells per well were incubated with 2 µg/ml single peptides, AIM-V medium (negative control) or PHA (L4144, Sigma; 0,5 µg/ml; positive control) in 96-well plates coated with 1.5 µg anti-IFN-γ (1-D1K, Mabtech). After 45h incubation, spots were developed with 0.1 µg biotin-conjugated anti-IFN-γ (7-B6-1, Mabtech), streptavidin-coupled alkaline phosphatase (Mabtech, 1:1000), and 5-bromo-4-chloro-3-indolyl phosphate/nitro blue tetrazolium (Sigma). Spots were counted in 2-3 wells per sample using a Bio-Sys Bioreader 5000 Pro-S/BR177 and Bioreader software generation 10. T cell responses were considered positive when mean spot counts were at least threefold higher than the mean spot counts of three unstimulated wells.

Generation of autologous EBV-transformed lymphoblastoid B cell lines

PBMCs were isolated from heparinized blood of four COVID-19 convalescent patients (SARS048, SARS047, SARS044, SARS050) by standard Ficoll density gradient centrifugation using Lymphoprep (Technoclone). EBV-transformed lymphoblastoid B cell lines (EBV^+ B cells) were generated by supplementing PBMCs with infectious marmoset P95-8 supernatant (ATCC) plus 200 ng/ml cyclosporin A (Sandimmune) in the presence of ODN2006 (1 µg/ml; InvivoGen) at 37°C in 5% CO_2. After 10 days of incubation, cells were replated 1:2 in fresh medium and further cultured in RPMI 1640 medium supplemented with 10% fetal calf serum, 2 mM *L*-glutamine and 100 µg/ml gentamicin sulfate.

Cellular cytotoxicity assay

The cytolytic activity of CTLs was tested in standard ^{51}Cr-release assays. Autologous EBV^+ B cell cells (2×10^6/2 ml, 24-well) were pulsed with YLQ wild type (YLQPRTFLL) or mutant peptide (YFQPRTFLL) or a negative control peptide (GVIMMFLSLGVGA, a non-immunogenic yellow fever virus peptide), respectively, at a concentration of 1µg/ml overnight. On the next day, cells were harvested, resuspended in 100 µl medium and labeled with 150 µCi of $Na^{51}CrO^4$ (PerkinElmer) at 37°C for 3 hours. After four washes, autologous EBV^+ B cells were added to round bottom 96-well plates that contained titrated numbers of wild type or mutant YLQ peptide specific PBMCs, generated as described under "Flow cytometry assays following 10-12d in vitro stimulation" (in duplicates). Subsequently, plates were centrifuged at 200 g for 5 minutes. After 5 h of incubation at 37°C, the supernatants were collected, and the radioactivity was determined in a γ-counter (Packard). The percentage of specific release was determined as follows: [CTL-induced release (cpm) − spontaneous release (cpm)]/[maximum release (cpm) − spontaneous release (cpm)] × 100.

Tetramer sorting, Hashtag labelling and single-cell RNA sequencing

PBMCs were harvested after 10-12d of in vitro expansion (as described under "Flow cytometry assays following 10-12d in vitro stimulation") with either YLQ wild type (YLQPRTFLL) or mutant peptide (YFQPRTFLL) and counted using TruCount tubes (Becton Dickinson) on a FACS Fortessa (Becton Dickinson). Cells were centrifuged at 400xg for 5 minutes at 4°C and washed in ice-cold FACS buffer (DPBS (Gibco) containing 1% Octaplas® LG, blood group AB (Octapharma). All staining and washing steps were performed on ice. After centrifugation, the cell pellet was resuspended in 50 µl FACS buffer and stained with HLA-A*02:01 YLQ wt (YLQPRTFLL) tetramer in PE at 10 µg/ml for 20 minutes. Cells were washed with ice-cold FACS

buffer followed by staining with FITC anti-human CD8 (SK1, Becton Dickinson) for 20 minutes. Cells were washed with ice-cold FACS buffer, resuspended in 200 µl FACS buffer and dead cells were counterstained with 2 µg/ml 4',6-diamidin-2-phenylindol (DAPI) (Sigma-Aldrich). Cell sorting was performed on a FACS Aria II Cell Sorter (Becton Dickinson). For each patient tetramer positive and tetramer negative cells of both wt peptide expanded and mutant peptide expanded cultures were sorted into 50 µl sorting buffer (DPBS (Gibco) with 0,08% bovine serum albumin (BSA) (Sigma-Aldrich). Cells were centrifuged and the supernatant was carefully discarded leaving 50 µl behind. To this residual 50 µl, 1 µl (0.5 µg) TotalSeq™-C0251 anti-human Hashtag Antibody 1 to 4, respectively, (394661, 394663, 394665, 394667, all BioLegend) was added and incubated for 20 minutes on ice. Cells were washed in 1 ml ice-cold sorting buffer and centrifuged and taken up in 1 ml sorting buffer. Cells were counted again using TruCount tubes.
For each patient volumes corresponding to 22,000 cells of each condition were pooled and centrifuged again. The cell pellet was resuspended in 80 µl sorting buffer and stored on ice until further preparation for sequencing.

Single-cell RNA-seq was performed on the live samples using the 10x Genomics Chromium Single Cell Controller with the Chromium Single Cell 5' v1.1 kit following the manufacturer's instructions. After cDNA amplification TCR enrichment and enrichment of feature barcoding sequences from the hashtag-antibodies were performed according to instructions by 10X Genomics manufacturer's guidelines for VDJ and feature barcoding enrichment. After quality control, libraries were sequenced on the Illumina NovaSeq sequencing platform using the SP flow cell in 2x150bp paired-end mode at the Biomedical Sequencing Facility (BSF) of the CeMM Research Center for Molecular Medicine of the Austrian Academy of Science.

Primary analysis was done using the CellRanger v5.0.1 software (10X Genomics). Alignment to the human reference transcriptome (refdata-gex-GRCh38-2020-A for gene expression and vdj_GRCh38_alts_ensembl-5.0.0 for VDJ analysis) was performed by the BSF. Hashtag Oligo identification was performed with the CITE-seq software (*65*) and demultiplexing was done with custom Python scripts by the BSF. We used the R statistics software to perform all further analysis using the Seurat package version 3.9.9.9038 (*66*). Briefly, CellRanger outputs from both patients were jointly loaded into R to perform quality control (removing cells with less than 1,000 genes, mitochondrial content more than 10%, as well as all cells without [negatives] or with two conflicting hashtag labels [doublets]). Preliminary clustering revealed two outlier clusters of cells shared across all conditions with higher number of counts (Fig. S5) which dominated the variance and were removed from downstream analysis. Patient-dependent batch effects were then removed by integration with Seurat's FindIntegrationAnchors and Integrate data (nfeatures=2000, dims=1:30). The dataset was then normalized (function NormalizeData, ScaleData) to generate corrected, log-transformed relative cell counts. Integrated data was used for low-dimensional projection using UMAP (*67*) based on the top 10 principal components and for clustering cells (resolution = 0.6). Differential gene expression analysis was performed using the FindMarkers function (method: MAST). The adjusted p-values returned by FindMarkers were further subjected to Bonferroni correction for the two tests applied (YLQ+ vs. YLQ- and WT YLQ+ vs. MUT YLQ+). For plotting, P-values smaller than 10^{-350} were capped to 10^{-350}. The results of the differential expression analysis on raw counts (|log2 fold-change| > 0.25) are reported in Table S7. Gene signatures for cytotoxic, viral, unhelped, IFN-γ and exhaustion responses were obtained from Kusnadi et al. (*38*), and enrichment was evaluated using R package AUCell (*68*).

For T cell clonotype analysis, the results from CellRanger were loaded into R and processed using the scRepertoire package and custom code. Clonotype identity was determined by the amino acid sequence of the assembled receptor sequences and we focused our analysis on the five most frequent clonotypes for each of the two individuals (Table S8).

Statistical Analysis

Statistical analysis of differences between the wild type and mutant $CD8^+$ T cell responses for ELISpot and ICS was done with Wilcoxon matched-pairs signed rank test. For comparison of >1 mutant responses, a Generalized Equation Estimations (GEE) model with peptide (fixed factor) and patient (random factor) was used. For analysis of CTL killing assays 2-way ANOVA followed by Dunnett's multiple comparison test was used. Differential gene expression analysis was performed using the FindMarkers function (method: MAST). The adjusted p-values returned by FindMarkers were further subjected to Bonferroni correction for the two tests applied (YLQ+ vs. YLQ- and WT YLQ+ vs. MUT YLQ+).

Supplementary Materials

Figure S1. Supplementary figures for mutation analysis

Figure S2. Controls and additional DSF assay results

Figure S3. Supplementary figures for PBMC analysis

Figure S4. Supplementary figures for scRNA-seq analysis

Figure S5. Quality control plots for scRNA-seq analysis and outlier clusters

Table S1. Wild type epitopes investigated in this study

Table S2. Samples with epitope mutations at allele frequency >0.02 (Excel spreadsheet)

Table S3. Peptides used in the study and their % rank predicted by netMHCpan v4.1

Table S4. T_m values for peptides tested in DSF assay

Table S5. Characteristics of HLA-A*02:01/HLA-B*40:01 positive patients

Table S6. HLA genotypes

Table S7. Overview of ELISpot results for wild type peptides

Table S8. DEGs from scRNA-seq analysis (Excel spreadsheet)

Table S9. Top clonotypes from TCR sequencing (Excel spreadsheet)

Table S10. Acknowledgments for sequences downloaded from GISAID (separate PDF file)

Table S11. Raw data (Excel spreadsheet)

References and Notes:

1. X. Zhang *et al.*, Viral and host factors related to the clinical outcome of COVID-19. *Nature* (2020), doi:10.1038/s41586-020-2355-0.

2. N. Vabret *et al.*, Immunology of COVID-19: current state of the science. *Immunity* (2020), doi:10.1016/j.immuni.2020.05.002.

3. D. Mathew *et al.*, Deep immune profiling of COVID-19 patients reveals distinct immunotypes with therapeutic implications. *Science (80-.).* **369**, eabc8511 (2020).

4. N. Le Bert *et al.*, SARS-CoV-2-specific T cell immunity in cases of COVID-19 and SARS, and uninfected controls. *Nature* (2020), doi:10.1038/s41586-020-2550-z.

5. K. McMahan *et al.*, Correlates of protection against SARS-CoV-2 in rhesus macaques. *Nature* (2020), doi:10.1038/s41586-020-03041-6.

6. P. J. Goulder, D. I. Watkins, Impact of MHC class I diversity on immune control of immunodeficiency virus replication. *Nat Rev Immunol*. **8**, 619–630 (2008).

7. J. E. Schmitz *et al.*, Control of viremia in simian immunodeficiency virus infection by CD8+ lymphocytes. *Science (80-.).* **283**, 857–860 (1999).

8. R. Thimme *et al.*, CD8(+) T cells mediate viral clearance and disease pathogenesis during acute hepatitis B virus infection. *J Virol*. **77**, 68–76 (2003).

9. K. Falk, O. Rötzschke, S. Stevanović, G. Jung, H.-G. Rammensee, Allele-specific motifs revealed by sequencing of self-peptides eluted from MHC molecules. *Nature*. **351**, 290–296 (1991).

10. H.-G. Rammensee, K. Falk, O. Rötzschke, MHC molecules as peptide receptors. *Curr.*

Opin. Immunol. **5**, 35–44 (1993).

11. J. Braun *et al.*, SARS-CoV-2-reactive T cells in healthy donors and patients with COVID-19. *Nature* (2020), doi:10.1038/s41586-020-2598-9.

12. T. Sekine *et al.*, Robust T cell immunity in convalescent individuals with asymptomatic or mild COVID-19. *Cell* (2020), doi:10.1016/j.cell.2020.08.017.

13. A. Grifoni *et al.*, Targets of T cell responses to SARS-CoV-2 coronavirus in humans with COVID-19 disease and unexposed individuals. *Cell* (2020), doi:10.1016/j.cell.2020.05.015.

14. I. Schulien *et al.*, Characterization of pre-existing and induced SARS-CoV-2-specific CD8+ T cells. *Nat. Med.* (2020), doi:10.1038/s41591-020-01143-2.

15. J. M. Dan *et al.*, *bioRxiv*, in press, doi:10.1101/2020.11.15.383323.

16. A. Sette, S. Crotty, Adaptive immunity to SARS-CoV-2 and COVID-19. *Cell* (2021), doi:10.1016/j.cell.2021.01.007.

17. A. Poran *et al.*, Sequence-based prediction of SARS-CoV-2 vaccine targets using a mass spectrometry-based bioinformatics predictor identifies immunogenic T cell epitopes. *Genome Med.* (2020), doi:10.1186/s13073-020-00767-w.

18. A. Grifoni *et al.*, A Sequence Homology and Bioinformatic Approach Can Predict Candidate Targets for Immune Responses to SARS-CoV-2. *Cell Host Microbe* (2020), doi:10.1016/j.chom.2020.03.002.

19. A. S. Shomuradova *et al.*, SARS-CoV-2 Epitopes Are Recognized by a Public and Diverse Repertoire of Human T Cell Receptors. *Immunity*. **53**, 1245-1257.e5 (2020).

20. A. Nelde *et al.*, SARS-CoV-2-derived peptides define heterologous and COVID-19-induced T cell recognition. *Nat. Immunol.* (2020), doi:10.1038/s41590-020-00808-x.

21. I. Schulien *et al.*, Characterization of pre-existing and induced SARS-CoV-2-specific CD8+ T cells. *Nat. Med.* (2020), doi:10.1038/s41591-020-01143-2.

22. A. P. Ferretti *et al.*, Unbiased Screens Show CD8+ T Cells of COVID-19 Patients Recognize Shared Epitopes in SARS-CoV-2 that Largely Reside outside the Spike Protein. *Immunity*. **53**, 1095-1107.e3 (2020).

23. A. Tarke *et al.*, Comprehensive analysis of T cell immunodominance and immunoprevalence of SARS-CoV-2 epitopes in COVID-19 cases. *Cell Reports Med.*, 100204 (2021).

24. H. Pircher *et al.*, Viral escape by selection of cytotoxic T cell-resistant virus variants in vivo. *Nature*. **346**, 629–633 (1990).

25. P. J. Goulder *et al.*, Evolution and transmission of stable CTL escape mutations in HIV infection. *Nature*. **412**, 334–338 (2001).

26. A. L. Cox *et al.*, Cellular immune selection with hepatitis C virus persistence in humans. *J Exp Med*. **201**, 1741–1752 (2005).

27. K. Deng *et al.*, Broad CTL response is required to clear latent HIV-1 due to dominance of escape mutations. *Nature*. **517**, 381–385 (2015).

28. K. R. Mccarthy *et al.*, *bioRxiv*, in press (available at https://doi.org/10.1101/2020.11.19.389916).

29. A. J. Greaney *et al.*, Complete Mapping of Mutations to the SARS-CoV-2 Spike Receptor-Binding Domain that Escape Antibody Recognition. *Cell Host Microbe*. **29**, 44-

57.e9 (2021).

30. P.-A. Koenig *et al.*, Structure-guided multivalent nanobodies block SARS-CoV-2 infection and suppress mutational escape. *Science (80-.).*, eabe6230 (2021).

31. F. F. Gonzalez-Galarza *et al.*, Allele frequency net database (AFND) 2020 update: gold-standard data classification, open access genotype data and new query tools. *Nucleic Acids Res.* **48**, D783–D788 (2019).

32. B. Reynisson, B. Alvarez, S. Paul, B. Peters, M. Nielsen, NetMHCpan-4.1 and NetMHCIIpan-4.0: improved predictions of MHC antigen presentation by concurrent motif deconvolution and integration of MS MHC eluted ligand data. *Nucleic Acids Res.* **48**, W449–W454 (2020).

33. Y. Shu, J. McCauley, GISAID: Global initiative on sharing all influenza data – from vision to reality. *Eurosurveillance*. **22** (2017), doi:10.2807/1560-7917.ES.2017.22.13.30494.

34. M. Toebes *et al.*, Design and use of conditional MHC class I ligands. *Nat. Med.* **12**, 246–251 (2006).

35. D. T. Blaha *et al.*, High-Throughput Stability Screening of Neoantigen/HLA Complexes Improves Immunogenicity Predictions. *Cancer Immunol. Res.* **7**, 50–61 (2019).

36. K. Gao, R. Oerlemans, M. R. Groves, Theory and applications of differential scanning fluorimetry in early-stage drug discovery. *Biophys. Rev.* **12**, 85–104 (2020).

37. F. H. Niesen, H. Berglund, M. Vedadi, The use of differential scanning fluorimetry to detect ligand interactions that promote protein stability. *Nat. Protoc.* **2**, 2212–2221 (2007).

38. A. Kusnadi *et al.*, Severely ill COVID-19 patients display impaired exhaustion features in

SARS-CoV-2-reactive CD8 + T cells. *Sci. Immunol.* **6**, eabe4782 (2021).

39. D. M. Altmann, R. J. Boyton, SARS-CoV-2 T cell immunity: Specificity, function, durability, and role in protection. *Sci. Immunol.* **5**, eabd6160 (2020).

40. T. H. Hansen, M. Bouvier, MHC class i antigen presentation: Learning from viral evasion strategies. *Nat. Rev. Immunol.* (2009), , doi:10.1038/nri2575.

41. A. Alcami, U. H. Koszinowski, Viral mechanisms of immune evasion. *Trends Microbiol.* (2000), , doi:10.1016/S0966-842X(00)01830-8.

42. P. J. R. Goulder, D. I. Watkins, HIV and SIV CTL escape: Implications for vaccine design. *Nat. Rev. Immunol.* (2004), , doi:10.1038/nri1417.

43. Y. Zhang *et al.*, *bioRxiv*, in press, doi:10.1101/2020.05.24.111823.

44. G. Liu, B. Carter, D. K. Gifford, Predicted Cellular Immunity Population Coverage Gaps for SARS-CoV-2 Subunit Vaccines and their Augmentation by Compact Peptide Sets. *Cell Syst.* (2020), doi:10.1016/j.cels.2020.11.010.

45. U. Sahin *et al.*, COVID-19 vaccine BNT162b1 elicits human antibody and TH1 T cell responses. *Nature*. **586**, 594–599 (2020).

46. K. S. Corbett *et al.*, SARS-CoV-2 mRNA vaccine design enabled by prototype pathogen preparedness. *Nature*. **586**, 567–571 (2020).

47. K. Itokawa, T. Sekizuka, M. Hashino, R. Tanaka, M. Kuroda, Disentangling primer interactions improves SARS-CoV-2 genome sequencing by multiplex tiling PCR. *PLoS One*. **15**, e0239403 (2020).

48. I. Faé, S. Wenda, C. Grill, G. F. Fischer, HLA-B*44:138Q : Evidence for a confined

deletion and recombination events in an otherwise unaffected HLA-haplotype. *HLA*. **93**, 89–96 (2019).

49. S. Andrews, FastQC - A quality control tool for high throughput sequence data. http://www.bioinformatics.babraham.ac.uk/projects/fastqc/. *Babraham Bioinforma.* (2010), (available at http://www.bioinformatics.babraham.ac.uk/projects/).

50. H. Li, R. Durbin, Fast and accurate short read alignment with Burrows-Wheeler transform. *Bioinformatics* (2009), doi:10.1093/bioinformatics/btp324.

51. N. D. Grubaugh *et al.*, An amplicon-based sequencing framework for accurately measuring intrahost virus diversity using PrimalSeq and iVar. *Genome Biol.* **20**, 8 (2019).

52. H. Li *et al.*, The Sequence Alignment/Map format and SAMtools. *Bioinformatics*. **25**, 2078–2079 (2009).

53. A. Wilm *et al.*, LoFreq: a sequence-quality aware, ultra-sensitive variant caller for uncovering cell-population heterogeneity from high-throughput sequencing datasets. *Nucleic Acids Res.* **40**, 11189–11201 (2012).

54. H. Li, A statistical framework for SNP calling, mutation discovery, association mapping and population genetical parameter estimation from sequencing data. *Bioinformatics* (2011), doi:10.1093/bioinformatics/btr509.

55. A. Popa *et al.*, Genomic epidemiology of superspreading events reveals mutational dynamics and transmission properties of SARS-CoV-2. *Sci. Transl. Med.* (2020), doi:10.1126/science.abe2555.

56. P. Cingolani *et al.*, A program for annotating and predicting the effects of single nucleotide polymorphisms, SnpEff. *Fly (Austin).* **6**, 80–92 (2012).

57. P. Cingolani *et al.*, Using Drosophila melanogaster as a model for genotoxic chemical mutational studies with a new program, SnpSift. *Front. Genet.* (2012), doi:10.3389/fgene.2012.00035.

58. F. Wu *et al.*, A new coronavirus associated with human respiratory disease in China. *Nature*. **579**, 265–269 (2020).

59. K. Niespodziana *et al.*, PreDicta chip-based high resolution diagnosis of rhinovirus-induced wheeze. *Nat. Commun.* **9**, 2382 (2018).

60. D. Gallerano *et al.*, HIV microarray for the mapping and characterization of HIV-specific antibody responses. *Lab Chip*. **15**, 1574–1589 (2015).

61. D. N. Garboczi, D. T. Hung, D. C. Wiley, HLA-A2-peptide complexes: refolding and crystallization of molecules expressed in Escherichia coli and complexed with single antigenic peptides. *Proc. Natl. Acad. Sci.* **89**, 3429–3433 (1992).

62. C. S. Clements *et al.*, The production, purification and crystallization of a soluble heterodimeric form of a highly selected T-cell receptor in its unliganded and liganded state. *Acta Crystallogr. Sect. D Biol. Crystallogr.* **58**, 2131–2134 (2002).

63. M. Fairhead, M. Howarth, in *Methods in Molecular Biology* (2015; http://link.springer.com/10.1007/978-1-4939-2272-7_12), pp. 171–184.

64. J. D. Altman *et al.*, Phenotypic Analysis of Antigen-Specific T Lymphocytes. *Science (80-.).* **274**, 94–96 (1996).

65. M. Stoeckius *et al.*, Simultaneous epitope and transcriptome measurement in single cells. *Nat. Methods*. **14**, 865–868 (2017).

66. T. Stuart *et al.*, Comprehensive Integration of Single-Cell Data. *Cell*. **177**, 1888-1902.e21

(2019).

67. L. McInnes, J. Healy, J. Melville, UMAP: Uniform manifold approximation and projection for dimension reduction. *arXiv*, 1–18 (2018).

68. S. Aibar *et al.*, Identification of expression patterns in the progression of disease stages by integration of transcriptomic data. *BMC Bioinformatics*. **17**, 432 (2016).

Acknowledgments: We would like to thank the Biomedical Sequencing Facility at CeMM for assistance with next-generation sequencing. We thank Ursula Sinzinger, Amelie Popovitsch and Maja Zabel for excellent technical assistance, Regina Sommer for helping us with UV-irradiation equipment and Judith Leitner for providing reagents used in cytotoxicity assays. We would like to thank Laura Domnanovich from the FACS Core Unit at CCRI for performing the tetramer sort; We thank Lukas Flatz, Giulio Superti-Furga, Martin Jäger, Laura Antonio Herrera, Dietmar Zehn and Rolf Zinkernagel for valuable feedback and comments. We thank the NIH Tetramer Core Facility for providing tetramer reagents that were used in preliminary experiments. We thank Sebastian Maurer-Stroh for providing help to generate the acknowledgment table for sequences downloaded from GISAID (Table S10).

Funding: BA was supported by the Austrian Science Fund (FWF) DK W1212. MS and AL were supported by DOC fellowships of the Austrian Academy of Sciences (No. 24813, No. 24158 and No. 24955 respectively). VG, VM and JBH received support from the Vienna Science and Technology Fund (WWTF, LS14-031). JHA was supported by the Medical-Scientific fund of the Mayor of the federal capital Vienna [grant COVID003]. W.F.P. was supported by the Medical-Scientific fund of the Mayor of the federal capital Vienna [grant COVID006]. C.B. and A.B. were

supported by ERC Starting Grants (European Union's Horizon 2020 research and innovation program, grant agreement numbers 679146 respectively 677006). This project was funded in part by two grants from the Vienna Science and Technology Fund (WWTF) as part of the WWTF COVID-19 Rapid Response Funding 2020 awarded to A.B. and R.G., respectively.

Competing interests: We declare that the research was conducted in the absence of any commercial or financial relationships that could be construed as a potential conflict of interest.

Data and materials availability: Raw BAM files were submitted for inclusion in the COVID-19 Data Portal hosted by the European Bioinformatics Institute under project numbers PRJEB39849 and PRJEB42987. Consensus virus sequences are deposited in the GISAID database. The pipeline used for calling low frequency mutations is available on GitHub (https://github.com/Bergthalerlab/SARSCoV2_Code). Single-cell RNA-seq data has been deposited at the European Genome-phenome Archive (EGA), under accession number EGAS00001005060. Processed single-cell RNA-seq data are available via Gene Expression Omnibus (GEO) under accession number GSE166651. The R code used for the analysis for single-cell RNA-seq data will be shared via GitHub (https://github.com/cancerbits).

Figure Captions

Fig. 1. Nonsynonymous mutations are detected in SARS-CoV-2 CTL epitopes. **A)** Allele frequency of low-frequency mutations detected in 27 CTL epitopes. Epitopes are indicated on the right. The heatmap to the left indicates change in % ranks predicted by netMHCpan 4.1(*32*). Bar plots below the large heatmap indicate viral loads as Ct values. **B)** Allele frequency of mutations in specified epitopes. Regions present in two epitopes are depicted separately. **C)** Frequency of global fixed mutations in CTL epitopes. **D)** Venn diagram depicting overlap between global fixed mutations and low-frequency variants. **E)** Mutations in CTL epitopes arise late in infection. Mutation frequency over time of two patients which were longitudinally sampled. Shown are variants that lead to nonsynonymous mutations in CTL epitopes. Patient 1 was sampled multiple times on the same day for some time points. Dashed lines indicate the detection limit for calling low-frequency mutations.

Fig. 2. Epitope variants lead to diminished MHC-I binding. **A-E**) Decreased thermostability of mutant peptide MHC-I complexes. Negative first derivative of relative fluorescence units (rfu) plotted against increasing temperatures. Curves for wild type peptides are black, mutated peptides are colored. The minimum point of the curves represents the melting temperature of peptide-MHC-I complexes. Dashed lines indicate SD. n=2-3 technical replicates. **F)** Tetramers featuring mutated peptides are unstable at 37°C. FACS plots showing staining of in vitro expanded PBMCs stained with tetramers containing wild type (top) or mutant (bottom) peptides incubated at 4°C (blue) or 37°C (red).

Fig. 3. SARS-CoV-2 epitope mutations are associated with decreased CTL responses. **A)** Experimental overview. **B)** CTL responses against wild type epitopes. PBMCs were isolated from HLA-A*02:01 or HLA-B*40:01 positive SARS-CoV-2 patients (black, n=35, 5, 3, or 13 respectively, or pre-pandemic controls with unknown HLA status (white, n=7), expanded 10-12 days with indicated peptides, and stained with wild type tetramers. Boxes show median ± 25^{th} and 75^{th} percentile and whiskers indicate 10^{th} and 90^{th} percentile. **C-E)** T cells expanded with mutant peptides do not give rise to wild type peptide-specific CTLs. PBMCs were isolated as in B), stimulated with wild type or mutant peptides and stained with tetramers containing the wild type peptide. (n=27, 25, and 2 patients per epitope). **F)** Representative FACS plots for C-E. **G-I)** Impact of mutations on CTL response. PBMCs expanded with wild type or mutant peptides as indicated, were analyzed for IFN-γ-production via ICS after restimulation with wild type or mutant peptide (n=14, 8, and 4 patients per epitope). **J)** Representative FACS plots for G-I. **K)** Ex vivo IFN-γ ELISpot assays from PBMCs stimulated with the YLQ peptide or the corresponding mutant (n=7, PBMCs obtained 2.7 ± 0.8 weeks after symptom onset) or the MEV peptide (marked in gray) or corresponding mutant (n=1, PBMCs obtained 3 weeks after symptom onset). Two or three wells were evaluated per sample and peptide. Patient ID is as indicated in Table S6. **L)** CTL killing assay. PBMCs from 4 patients were expanded with wild type or mutant YLQ peptide, mixed with autologous EBV^+ B cells that were pulsed with wild type or mutant YLQ peptide and specific killing was assessed (n=2 per patient). Error bars represent mean ± SD. Significance is indicated as $*P<0.05$, $**P<0.01$, $***P<0.001$, $****P<0.0001$, tested by Wilcoxon matched-pairs signed rank test (C,D,E,G,H,I,K) or 2-way ANOVA followed by Dunnett's multiple comparison test (L).

Fig. 4. Single cell transcriptomics and TCR sequencing of $CD8^+$ T cells reveals distinct transcritptional profiles in response to mutant peptide. **A)** Experimental setup. PBMCs were expanded for 10-12 days in the presence of wild type or mutant YLQ peptide, sorted for YLQ tetramer-positive and tetramer-negative $CD8^+$ cells, labeled with barcoded antibodies (TotalSeq anti-human Hashtag) and subjected to single-cell RNA sequencing (figure generated with BioRender.com). **B)** Percentages of YLQ tetramer-positive $CD8^+$ T cells in response to wild type or mutant peptide expansion from the two donors analyzed. **C-D)** UMAP plots displaying an embedding of single-cell transcriptomes in 2-dimensional space. The cells are colored according to their clusters (C), or experimental condition (D). **E)** Distribution of clonotypes for both patients and the indicated conditions. The top 5 clonotypes are colored. Connecting lines show clonotypes shared between conditions. **F)** Top 15 TRAV and TRVB genes. **G)** Volcano plot displaying differentially expressed genes between wild type-positive and mutant-positive cells. P-values of 0 were capped to 10^{-350} (indicated by gray dotted line). **H)** Violin plots showing expression levels in tetramer-negative and tetramer-positive cells expanded with mutant or wild type peptide. Expression levels given as log-normalized relative read counts (RC). All plots in C-H show combined data from both patients.

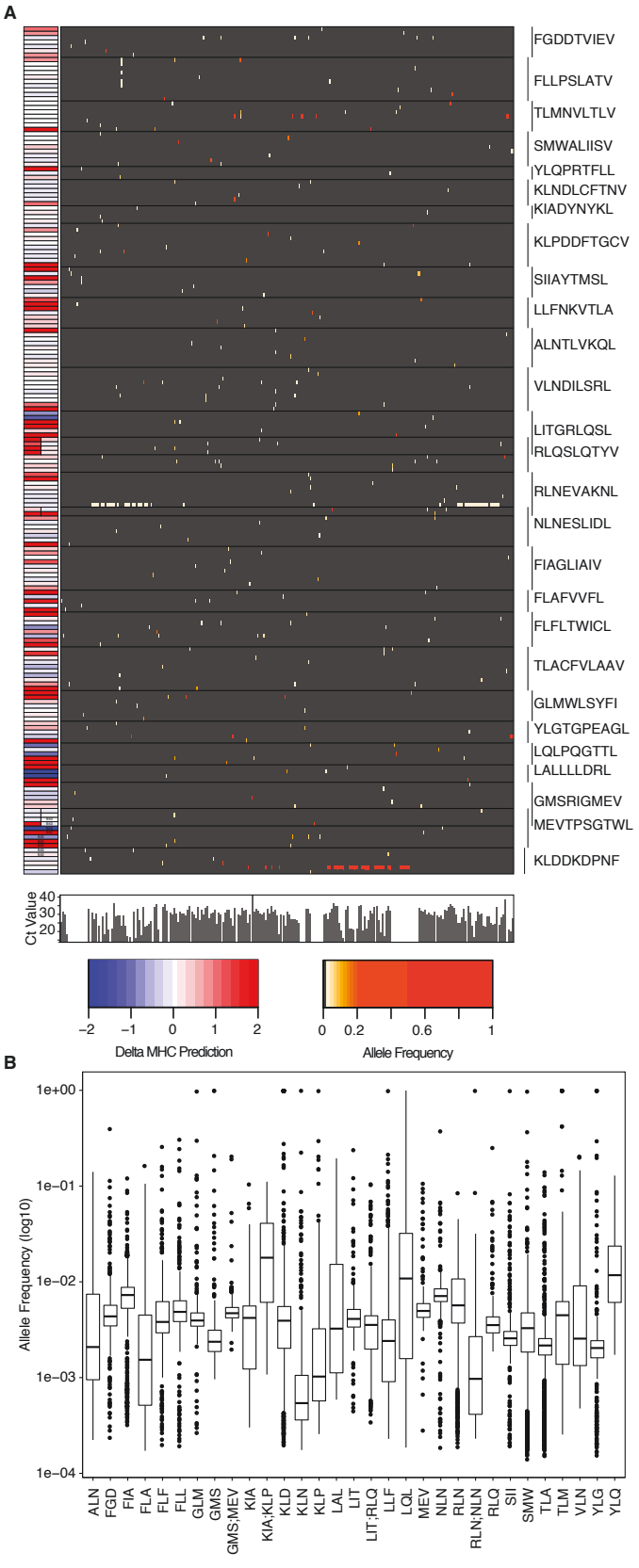
A
FGDDTVIEV
FLLPSLATV
TLMNVLTLV
SMWALIISV
YLQPRTFLL
KLNDLCFTNV
KIADYNYKL
KLPDDFTGCV
SIIAYTMSL
LLFNKVTLA
ALNTLVKQL
VLNDILSRL
LITGRLQSL
RLQSLQTYV
RLNEVAKNL
NLNESLIDL
FIAGLIAIV
FLAFVVFL
FLFLTWICL
TLACFVLAAV
GLMWLSYFI
YLGTGPEAGL
LQLPQGTTL
LALLLLDRL
GMSRIGMEV
MEVTPSGTWL
KLDDKDPNF
Ct Value
40
30
20
−2
−1
0
1
2
Delta MHC Prediction
0
0.2
0.6
1
Allele Frequency
B
Allele Frequency (log10)
1e+00
1e−01
1e−02
1e−03
1e−04
ALN
FGD
FIA
FLA
FLF
FLL
GLM
GMS
GMS;MEV
KIA
KIA;KLP
KLD
KLN
KLP
LAL
LIT
LIT;RLQ
LLF
LQL
MEV
NLN
RLN
RLN;NLN
RLQ
SII
SMW
TLA
TLM
VLN
YLG
YLQ
C
Gene
M
N
NSP3
NSP6
S
Frequency of mutants (log10)
1e−01
1e−02
1e−03
1e−04
1e−05
ALN
FGD
FLF
FLL
GLM
GMS
KIA
KLD
KLN
KLP
LAL
LLF
LQL
MEV
NLN
RLN
RLQ
SII
SMW
TLA
TLM
YLG
VLN
YLQ
D
Low-frequency mutations
Fixed mutations
115
(24.52%)
79
(16.84%)
275
(58.64%)
count
240
200
160
120
80
E
Patient 1
Position (Epitope)
2741 (FGD)
11481 (SMW)
24449 (ALN)
24581 (RLQ)
26607 (FLF)
Allele frequency
0.04
0.03
0.02
0.01
0.00
Mar 24
Mar 27
Mar 30
Apr 01
Apr 03
Patient 2
Position (Epitope)
11185 (FLL)
22730 (KLN)
24557 (LIT)
24570 (LIT/RLQ)
28773 LQL)
29239 (GMS)
29265 (MEV)
0.125
0.100
0.075
0.050
0.025
0.000
Mar 04
Mar 09
Mar 17

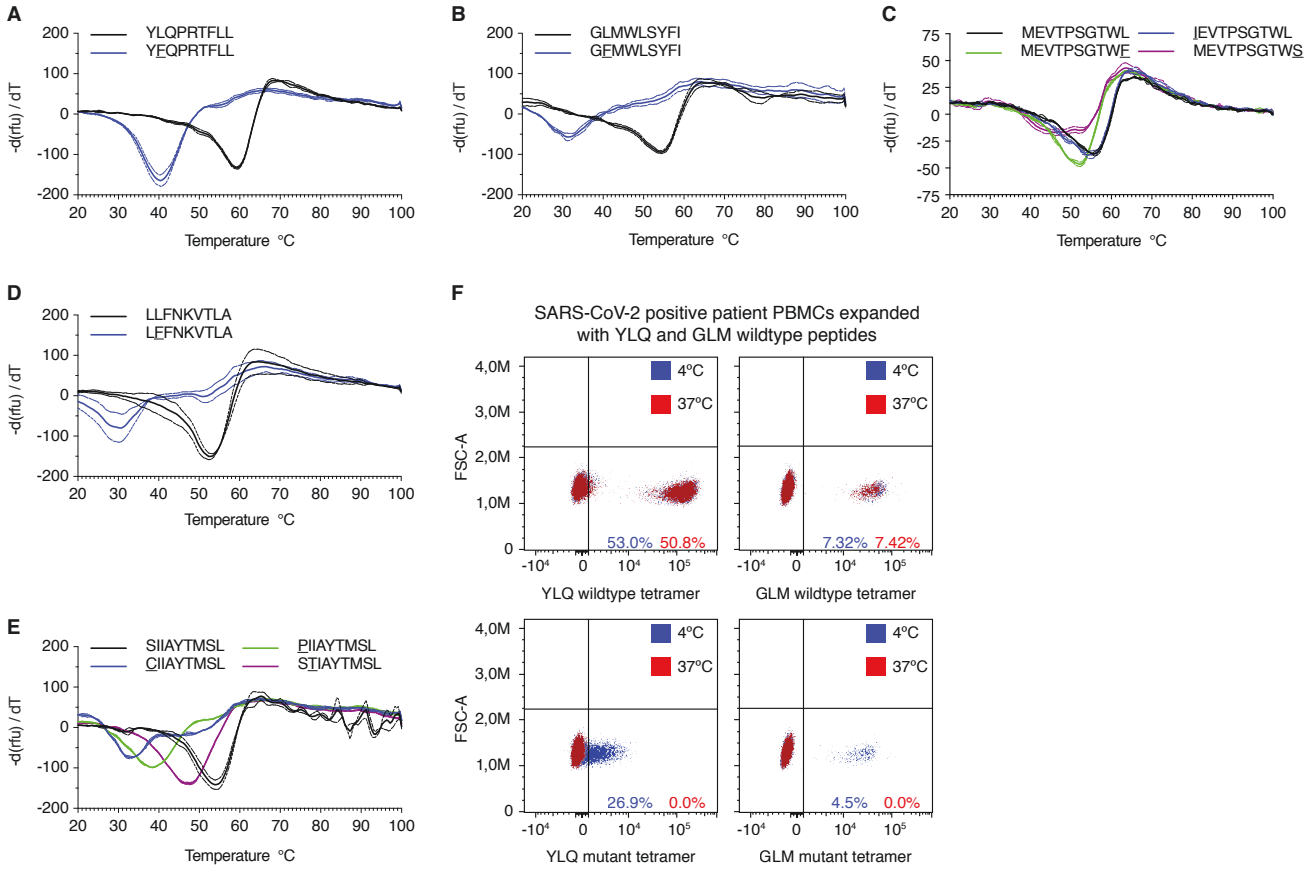
A
YLQPRTFLL
YFQPRTFLL
-d(rfu) / dT
Temperature °C
B
GLMWLSYFI
GFMWLSYFI
-d(rfu) / dT
Temperature °C
C
MEVTPSGTWL
MEVTPSGTWF
IEVTPSGTWL
MEVTPSGTWS
-d(rfu) / dT
Temperature °C
D
LLFNKVTLA
LFFNKVTLA
-d(rfu) / dT
Temperature °C
E
SIIAYTMSL
CIIAYTMSL
PIIAYTMSL
STIAYTMSL
-d(rfu) / dT
Temperature °C
F
SARS-CoV-2 positive patient PBMCs expanded
with YLQ and GLM wildtype peptides
4°C
37°C
FSC-A
53.0% 50.8%
YLQ wildtype tetramer
7.32% 7.42%
GLM wildtype tetramer
26.9% 0.0%
YLQ mutant tetramer
4.5% 0.0%
GLM mutant tetramer

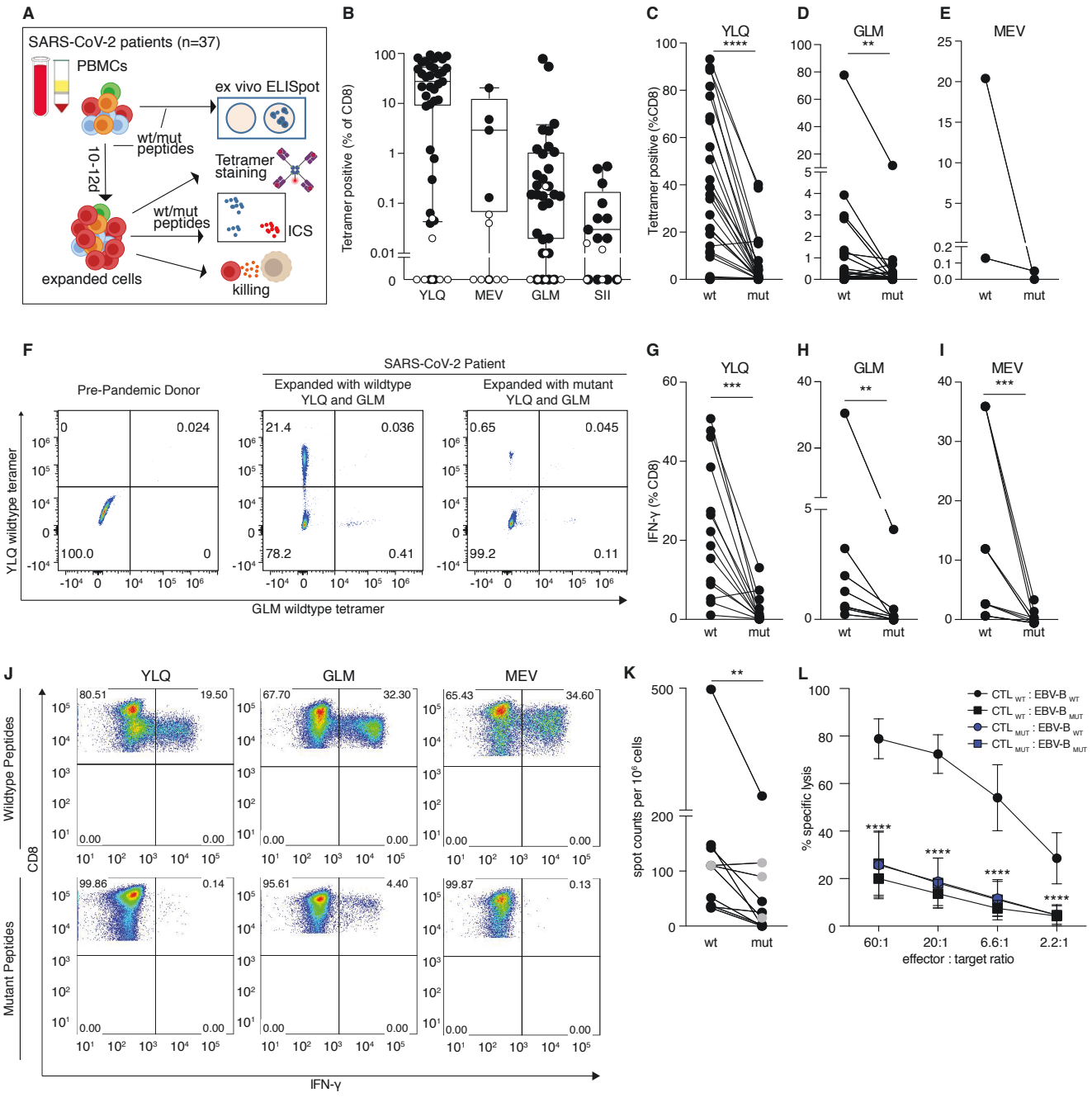
A
SARS-CoV-2 patients (n=37)
PBMCs
ex vivo ELISpot
wt/mut peptides
10-12d
Tetramer staining
wt/mut peptides
ICS
expanded cells
killing
B
Tetramer positive (% of CD8)
YLQ
MEV
GLM
SII
C
YLQ
****
Tettramer positive (%CD8)
wt
mut
D
GLM
**
wt
mut
E
MEV
wt
mut
F
SARS-CoV-2 Patient
Pre-Pandemic Donor
Expanded with wildtype YLQ and GLM
Expanded with mutant YLQ and GLM
YLQ wildtype teramer
GLM wildtype tetramer
0
0.024
100.0
0
21.4
0.036
78.2
0.41
0.65
0.045
99.2
0.11
G
YLQ
***
IFN-γ (% CD8)
wt
mut
H
GLM
**
wt
mut
I
MEV
***
wt
mut
J
YLQ
GLM
MEV
Wildtype Peptides
Mutant Peptides
CD8
80.51
19.50
67.70
32.30
65.43
34.60
0.00
99.86
0.14
95.61
4.40
99.87
0.13
IFN-γ
K
**
spot counts per 10⁶ cells
wt
mut
L
CTL WT : EBV-B WT
CTL WT : EBV-B MUT
CTL MUT : EBV-B WT
CTL MUT : EBV-B MUT
% specific lysis
****
60:1
20:1
6.6:1
2.2:1
effector : target ratio

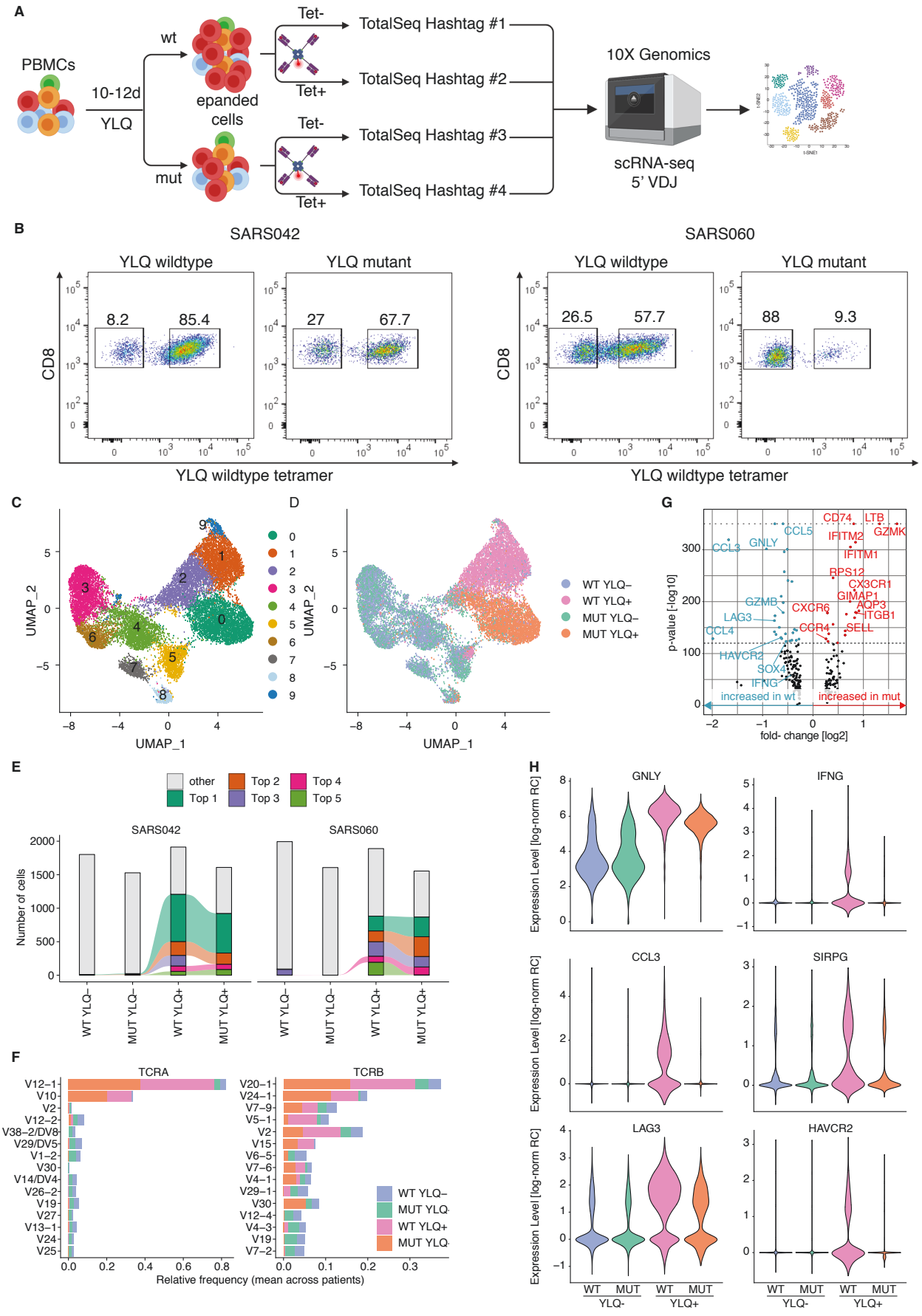
A
PBMCs
10-12d
YLQ
wt
mut
epanded cells
Tet-
Tet+
Tet-
Tet+
TotalSeq Hashtag #1
TotalSeq Hashtag #2
TotalSeq Hashtag #3
TotalSeq Hashtag #4
10X Genomics
scRNA-seq
5' VDJ
B
SARS042
SARS060
YLQ wildtype
YLQ mutant
CD8
8.2
85.4
27
67.7
26.5
57.7
88
9.3
YLQ wildtype tetramer
C
D
UMAP_1
UMAP_2
WT YLQ–
WT YLQ+
MUT YLQ–
MUT YLQ+
G
p-value [-log10]
fold- change [log2]
CD74
LTB
CCL5
GZMK
IFITM2
CCL3
GNLY
IFITM1
RPS12
CX3CR1
GIMAP1
GZMB
CXCR6
AQP3
ITGB1
LAG3
CCR4
SELL
CCL4
HAVCR2
SOX4
IFNG
increased in wt
increased in mut
E
other
Top 1
Top 2
Top 3
Top 4
Top 5
SARS042
SARS060
Number of cells
F
TCRA
TCRB
Relative frequency (mean across patients)
H
GNLY
IFNG
CCL3
SIRPG
LAG3
HAVCR2
Expression Level [log-norm RC]
WT
MUT
YLQ-
YLQ+

Supplementary Materials for

Title: SARS-CoV-2 mutations in MHC-I restricted epitopes evade CD8$^+$ T cell responses

Authors:

Benedikt Agerer[1,†], Maximilian Koblischke[2,†], Venugopal Gudipati[3,†], Luis Fernando Montaño-Gutierrez[4], Mark Smyth[1], Alexandra Popa[1], Jakob-Wendelin Genger[1], Lukas Endler[1], David M. Florian[2], Vanessa Mühlgrabner[3], Marianne Graninger[2], Stephan W. Aberle[2], Anna-Maria Husa[4], Lisa Ellen Shaw[5], Alexander Lercher[1,§], Pia Gattinger[6], Ricard Torralba-Gombau[1], Doris Trapin[7], Thomas Penz[1], Daniele Barreca[1], Ingrid Fae[8], Sabine Wenda[8], Marianna Traungott[9], Gernot Walder[10], Winfried F. Pickl[7,11], Volker Thiel[12,13], Franz Allerberger[14], Hannes Stockinger[3], Elisabeth Puchhammer-Stöckl[2], Wolfgang Weninger[5], Gottfried Fischer[7], Wolfgang Hoepler[9], Erich Pawelka[8], Alexander Zoufaly[8], Rudolf Valenta[3,6,11,15-16], Christoph Bock[1,17], Wolfgang Paster[4], René Geyeregger[4], Matthias Farlik[5], Florian Halbritter[4], Johannes B. Huppa[3,††], Judith H. Aberle[2,††], Andreas Bergthaler[1,††,*]

Correspondence to: abergthaler@cemm.oeaw.ac.at

This PDF file includes:

Table S1. Wildtype epitopes investigated in this study.

Table S2. Samples with epitope mutations at allele frequency >0.02.

Table S3. Peptides used in the study and their binding rank predicted by netMHC-pan v4.1. <0.5 strong binder, 0.5-2 weak binder, >2 non-binder.

Table S4. T_m values for peptides tested in DSF assay

Table S5. Characteristics of HLA-A*02:01/HLA-B*40:01 positive patients

Table S6. HLA genotypes

Table S7. Overview of ELISpot results for wildtype peptides

Table S8. DEGs from scRNA-seq analysis

Table S9. Top clonotypes from TCR sequencing

Table S10. Acknowledgments for sequences downloaded from GISAID

Table S11. Raw data

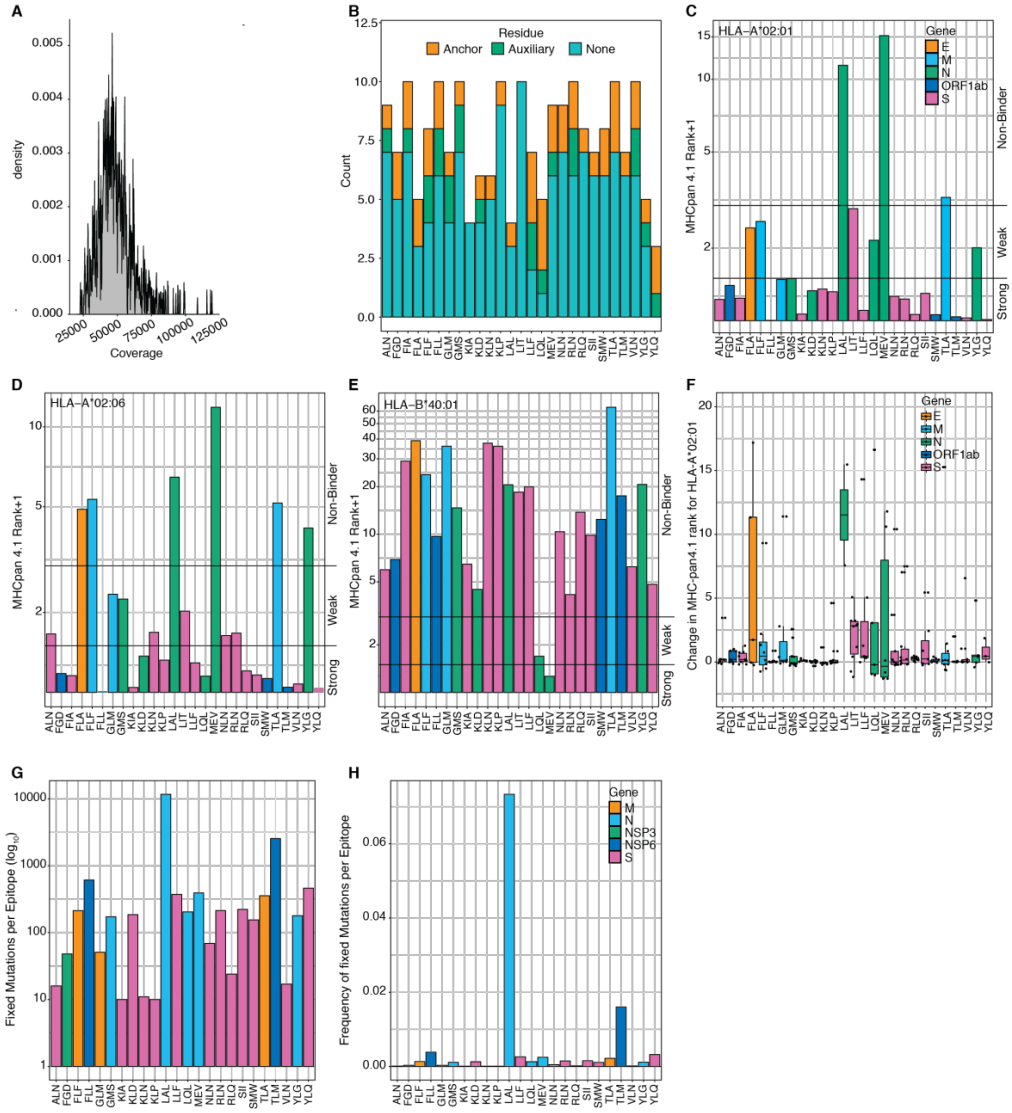
A
density
Coverage
B
Residue
Anchor
Auxiliary
None
Count
C
HLA−A*02:01
Gene
E
M
N
ORF1ab
S
MHCpan 4.1 Rank+1
Non-Binder
Weak
Strong
D
HLA−A*02:06
E
HLA−B*40:01
F
Change in MHC-pan4.1 rank for HLA-A*02:01
G
Fixed Mutations per Epitope (log10)
H
NSP3
NSP6
Frequency of fixed Mutations per Epitope

Fig. S1. Supplementary figures for bioinformatic analysis S1A) Coverage and read numbers of all sequenced samples. **S1B)** Mutation counts for specific residues of the epitopes. anchor = anchor residues, auxiliary = auxiliary residues, none = no special residue. **S1C-S1E)** netMHCpan binding predictions for the 27 wildtype epitopes to HLA-A*02:01, HLA-A*02:06 and HLA-B*40:01, respectively. **S1F)** change in netMHCpan binding predictions for the mutant epitopes to HLA-A*02:01. **S1G-S1H)** Total counts and frequency of fixed epitope mutations in the global samples.

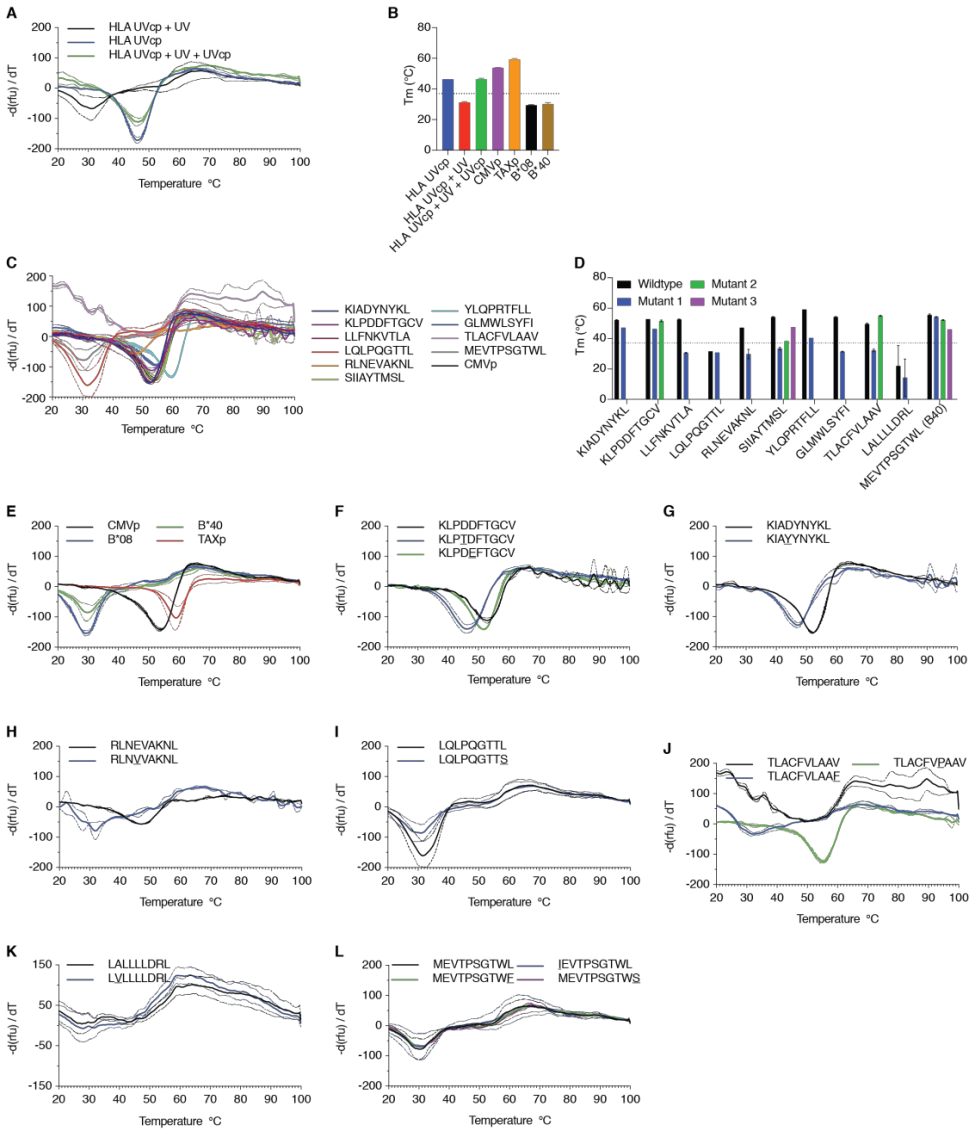

Fig. S2. Controls and additional DSF assay results S2A) Positive controls for the DSF assay. The black curve represents the complex of MHC and an UV cleavable peptide that was exposed to UV light, the blue curve represents the complex of MHC and an UV cleavable peptide not exposed to UV and the green curve represents the complex of MHC and an UV cleavable peptide exposed to UV light, prior to addition of another peptide. **S2B)** Bar graphs displaying T_m values

of peptide-MHC complexes for assay controls **S2C)** DSF curves for all wildtype peptides tested. **S2D)** Bar graphs displaying T_m values of peptide-MHC complexes for all wildtype and mutant peptides tested. **S2E)** Additional controls for the DSF assay. Two positive controls (CMV and TAX peptides), as well as two negative controls (HLA-B epitopes) complexed with HLA-A*02:01. **S2F-S2K)** DSF data for additional mutant peptides tested. Curves for wildtype peptides are black, mutated peptides are colored. The minimal point of the curves represents the melting temperature of peptide-MHC-I complexes. **S2L)** Additional negative control for the assay. A HLA-B*40:01 epitope and its mutant forms were complexed with HLA-A*02:01. Dashed lines for curves and error bars in bar-graphs represent mean ± SD. n=2-3 technical replicates for all graphs.

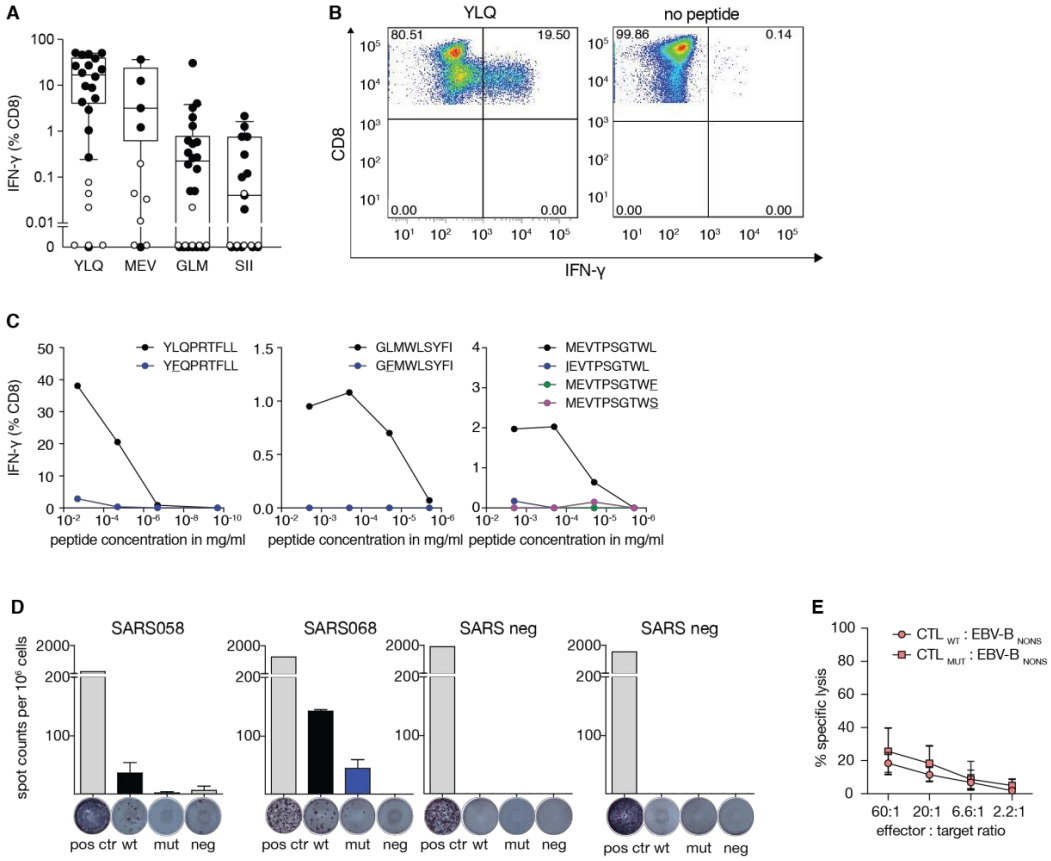

Fig. S3. Supplementary figures for PBMC analysis S3A) Intracellular cytokine staining of PBMCs from COVID-19 patients (black, n=18, 5, 22 and 15) or pre-pandemic controls with unknown HLA status (white, n=6) after 10-12 days *in vitro* expansion and restimulation with wildtype peptides as indicated. Boxes show median ± 25th and 75th percentile and whiskers indicate 10th and 90th percentile **S3B)** Representative FACS plots of the ICS shown for the YLQ epitope and an unstimulated control. **S3C)** Peptide titrations for three wildtype peptides and respective mutants. Peptides were tested in $\log_{10}$ and $\log_{100}$ dilutions in ICS assays. n=1 technical replicate. **S3D)** Representative *ex vivo* ELISpots for YLQ shown from two COVID19 patients and two healthy donors. Patient IDs are as indicated in Table S6. n=2-3 technical replicates. **S3E)** Negative

controls for cytotoxicity assay. PBMCs from 4 patients were expanded with wildtype or mutant YLQ peptide and co-cultured with autologous EBV^+ B cells that were pulsed with a nonsense peptide as negative control (n=2 technical replicates for each patient). All error bars represent mean ± SD

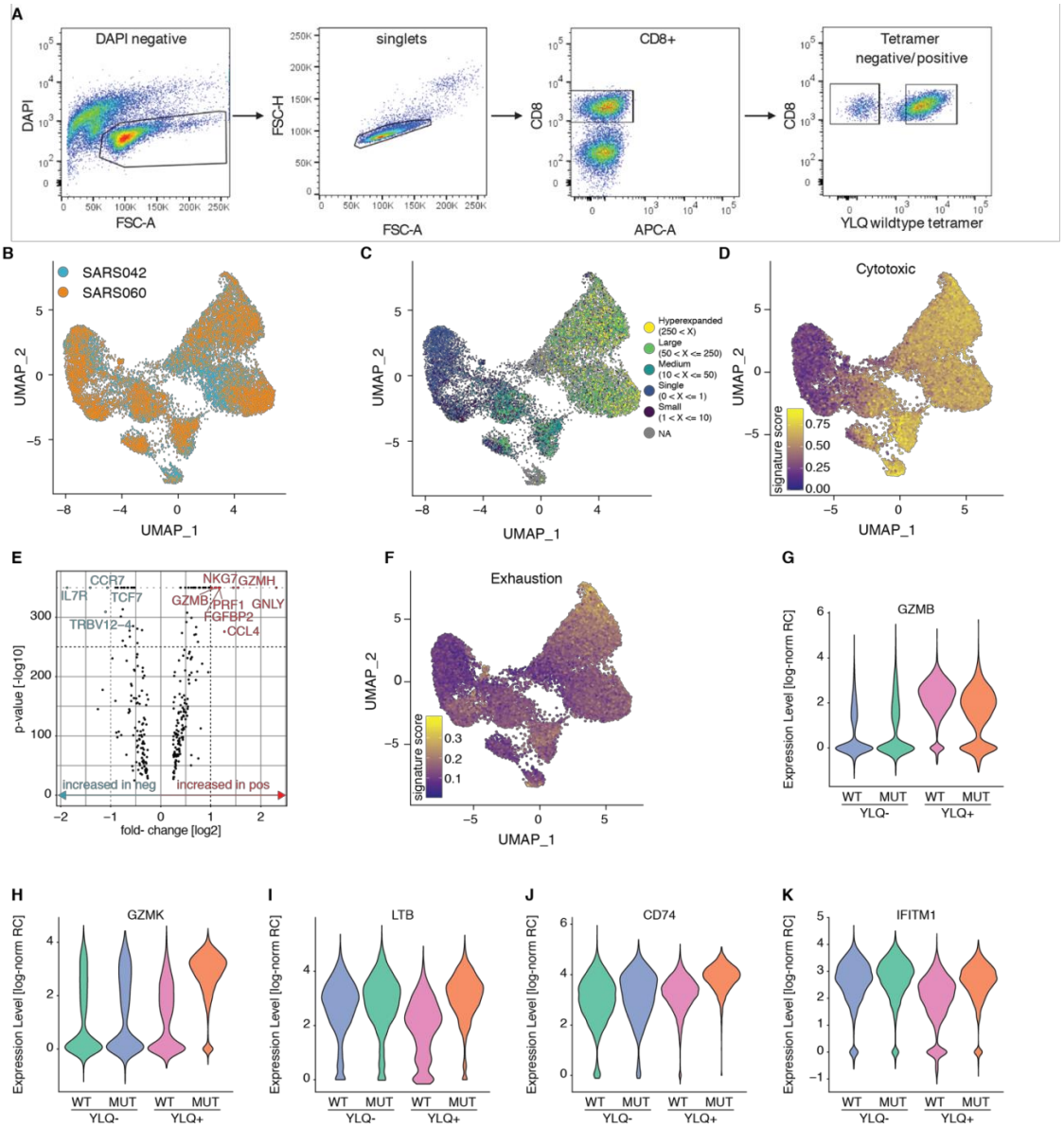

Fig. S4. Supplementary figures for scRNA-seq experiment. S4A) Gating strategy for sorting tetramer-positive and tetramer-negative CD8^{+} T cells **S4B-D)** UMAP plot displaying cells in 2-dimensional space. The cells are colored according to patient (B), to the number of cells with the same TCR as a measure for expansion (C), or the signature score (AUCell score) for the cytotoxic gene signature (D). **S4E)** Volcano plots displaying differentially expressed genes between

tetramer-positive and tetramer-negative. P-values of 0 were capped to 10^{-350} (indicated by grey dotted line) **S4F)** UMAP plot showing the signature score (AUCell Score) for the exhaustion gene signature.**S4G-S4K)** Violin plot showing expression levels in cells expanded with mutant or wildtype peptide. Expression levels given as log-normalized relative read counts (RC). All plots in B-K show combined data from both patients.

10

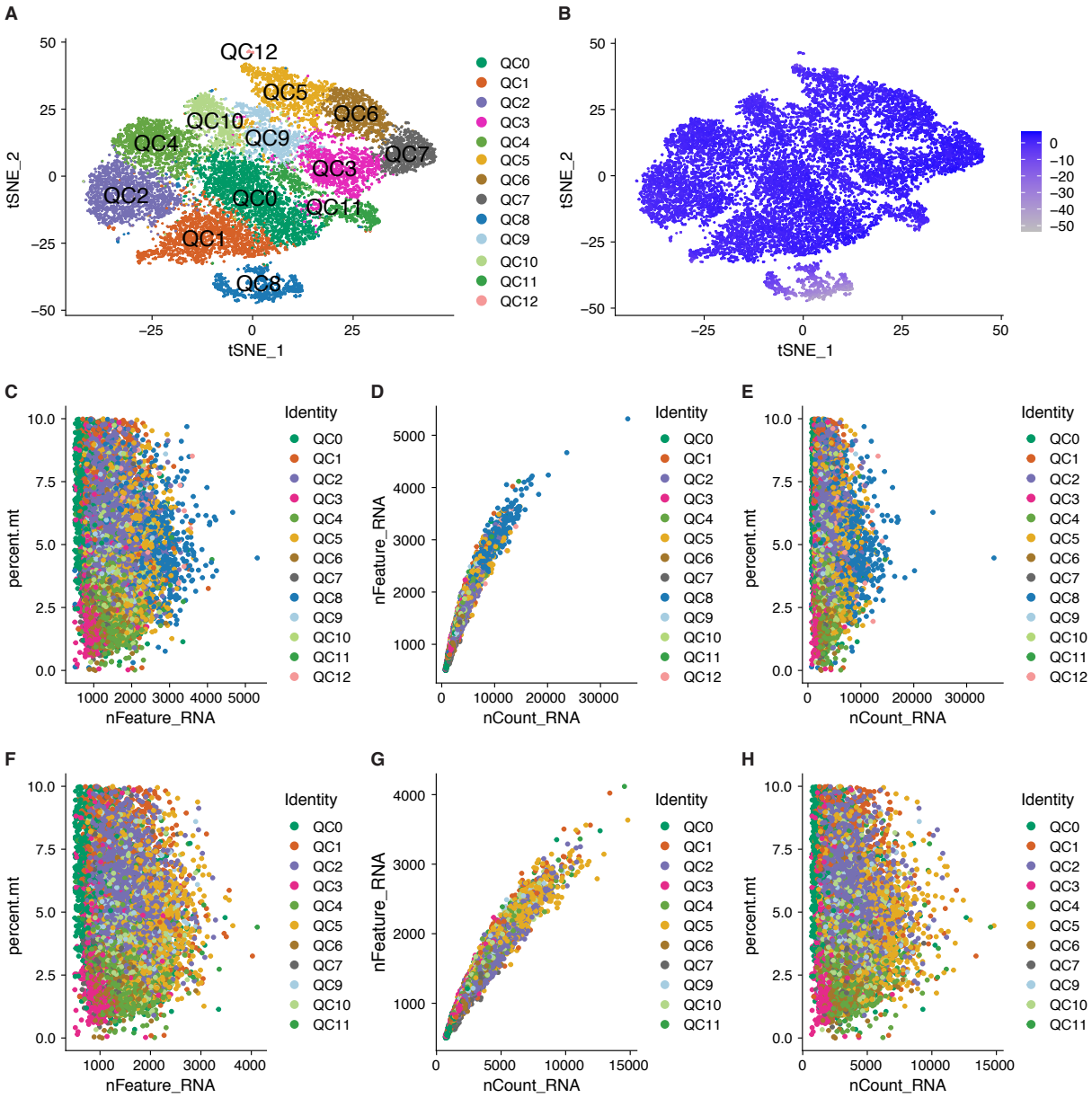

Fig S5. Quality control plots for scRNA-seq analysis and outlier clusters. A) Preliminary t-distributed Stochastic Neighbor Embedding (t-SNE) of single cells showing clusters in 2-dimensional space before removal of outliers. **B)** Differences between Cluster 8 and the rest of the cells dominate the variance in the data set, as reflected by each cell's values along the first component (PC_1) of a Principal Component Analysis (PCA). The plot shows PC_1 Values for each cell in the same t-SNE as in A. **C-E)** Quality control plots indicating outlier characteristics

of cluster 8 (shown in blue color). C) Number of genes per cell plotted against percentage of mitochondrial genes. D) Number of genes per cell plotted against counts per cell. E) Number of counts per cell plotted against percentage of mitochondrial genes. F-H) Same as C-E, but after removal of clusters 8 and 12.

12

Table S1. Wildtype epitopes investigated in this study.

Protein	Start AA	End AA	Sequence	Short	HLA	netMHCpan rank	Reference
ORF1ab	825	833	FGDDTVIEV	FGD	HLA-A*02:01	0.401	(*10*)
ORF1ab	3639	3647	FLLPSLATV	FLL	HLA-A*02:01	0.0047	(*10*)
ORF1ab	3710	3718	TLMNVLTLV	TLM	HLA-A*02:01, HLA-A*02:06	0.0398	(*12*)
ORF1ab	3732	3740	SMWALIISV	SMW	HLA-A*02:01, HLA-A*02:06, HLA-B*52:01	0.0603	(*11*)
S	269	277	YLQPRTFLL	YLQ	HLA-A*02:01	0.0129	(*12*)
S	386	395	KLNDLCFTNV	KLN	HLA-A*02:01	0.3539	(*10*)
S	417	425	KIADYNYKL	KIA	HLA-A*02:01	0.0671	(*12*)
S	424	433	KLPDDFTGCV	KLP	HLA-A*02:01, HLA-A*02:06	0.3198	(*11*, *12*)
S	691	699	SIIAYTMSL	SII	HLA-A*02:01	0.2998	(*11*, *12*)
S	821	829	LLFNKVTLA	LLF	HLA-A*02:01	0.1053	(*12*)
S	958	966	ALNTLVKQL	ALN	HLA-A*02:01, HLA-A*02:06	0.2258	(*11*, *12*)
S	976	984	VLNDILSRL	VLN	HLA-A*02:01, HLA-C*01:02	0.028	(*11*, *12*)
S	996	1004	LITGRLQSL	LIT	HLA-A*02:01	1.9126	(*11*, *12*)
S	1000	1008	RLQSLQTYV	RLQ	HLA-A*02:01	0.0622	(*10*, *12*)
S	1185	1193	RLNEVAKNL	RLN	HLA-A*02:01	0.2303	(*11*, *12*)

S	1192	1200	NLNESLIDL	NLN	HLA-A*02:01	0.2624	(*11*, *12*)
S	1220	1228	FIAGLIAIV	FIA	HLA-A*02:01, HLA-A*02:06	0.2409	(*10–12*)
E	20	27	FLAFVVFL	FLA	HLA-A*02:01	1.4245	(*10*)
M	26	34	FLFLTWICL	F:F	HLA-A*02:01	1.5782	(*10*)
M	61	70	TLACFVLAAV	TLA	HLA-A*02:01	2.2459	(*11*)
M	89	97	GLMWLSYFI	GLM	HLA-A*02:01, HLA-A*02:06	0.4829	(*11*)
N	112	121	YLGTGPEAGL	YLG	HLA-A*02:01	1.0066	(*10*)
N	159	167	LQLPQGTTL	LQL	HLA-A*02:01	1.1552	(*11*)
N	219	227	LALLLLDRL	LAL	HLA-A*02:01	10.4342	(*11*)
N	316	324	GMSRIGMEV	GMS	HLA-A*02:01	0.4967	(*11*)
N	322	331	MEVTPSGTWL	MEV	HLA-B*40:01, HLA-B*44:03	0.2638	(*4*)
N	338	346	KLDDKDPNF	KLD	HLA-A*02:01	0.3328	(*10*)

Table S2. Samples with epitope mutations at allele frequency >0.02.

Table S3. Peptides used in the study and their % rank predicted by netMHC-pan v4.1. <0.5 strong binder, 0.5-2 weak binder, >2 non-binder.

AA sequence	Variant	Residue	A*02:01	A*02:06	B*40:01	Source
YLQPRTFLL	Wildtype	NA	0.0129	0.0382	3.8259	JPT Peptide Technologies GmbH
YFQPRTFLL	Mutant	anchor	1.8892	2.3099	4.3899	JPT Peptide Technologies GmbH
KLPDDFTGCV	Wildtype	NA	0.3198	0.3235	35	JPT Peptide Technologies GmbH
KLPDEFTGCV	Mutant	unknown	0.2982	0.3191	35	JPT Peptide Technologies GmbH
KLPTDFTGCV	Mutant	unknown	0.298	0.319	35	JPT Peptide Technologies GmbH
SIIAYTMSL	Wildtype	NA	0.2998	0.1634	8.8673	JPT Peptide Technologies GmbH
PIIAYTMSL	Mutant	unknown	5.7413	5.9459	35	JPT Peptide Technologies GmbH
CIIAYTMSL	Mutant	unknown	2.7464	2.1016	31.75	JPT Peptide Technologies GmbH
STIAYTMSL	Mutant	unknown	1.1866	0.2433	5.6769	JPT Peptide Technologies GmbH
LLFNKVTLA	Wildtype	NA	0.1053	0.2926	18.9231	JPT Peptide Technologies GmbH
LFFNKVTLA	Mutant	anchor	5.1733	7.321	23.3333	JPT Peptide Technologies GmbH
TLACFVLAAV	Wildtype	NA	2.2459	4.1687	62.5	JPT Peptide Technologies GmbH
TLACFVPAAV	Mutant	none	1.6344	4.3485	49	JPT Peptide Technologies GmbH
TLACFVLAAF	Mutant	none	17.5355	19.9102	39.5	JPT Peptide Technologies GmbH
GLMWLSYFI	Wildtype	NA	0.4829	1.3444	35	JPT Peptide Technologies GmbH
GFMWLSYFI	Mutant	anchor	11.8902	19.8449	33	JPT Peptide Technologies GmbH
LQLPQGTTL	Wildtype	NA	1.1552	0.1519	0.6958	JPT Peptide Technologies GmbH
LQLPQGTTS	Mutant	anchor	17.8	6.8687	10.4104	JPT Peptide Technologies GmbH
LALLLLDRL	Wildtype	NA	10.4342	5.4673	19.5455	In-House
LVLLLLDRL	Mutant	anchor	4.6341	2.2488	22.6667	In-House

MEVTPSGTWL	Wildtype	NA	14.1747	10.8642	0.2638	JPT Peptide Technologies GmbH
IEVTPSGTWL	Mutant	unknown	12.8602	9.7767	0.2988	JPT Peptide Technologies GmbH
MEVTPSGTWS	Mutant	unknown	55.9091	42.7647	8.9259	JPT Peptide Technologies GmbH
MEVTPSGTWF	Mutant	unknown	34.7143	24.1466	0.8711	JPT Peptide Technologies GmbH
KIADYNYKL	Wildtype	NA	0.0671	0.0444	5.4725	JPT Peptide Technologies GmbH
KIAYYNYKL	Mutant	none	0.9743	1.1082	13.6447	JPT Peptide Technologies GmbH
RLNEVAKNL	Wildtype	NA	0.2303	0.674	3.156	JPT Peptide Technologies GmbH
RLNVVAKNL	Mutant	none	2.1559	4.3546	6.4438	JPT Peptide Technologies GmbH

Table S4. T_m values for peptides tested in DSF assay

Peptide	HLA tested	Tm (°C) Average	Tm (°C) SD
CMVp	A*02:01	53.80	0.2
KIADYNYKL	A*02:01	52.20	0.2
KIAYYNYKL	A*02:01	47.20	0
KLPDDFTGCV	A*02:01	52.80	0
KLPTDFTGCV	A*02:01	46.40	0
KLPDEFTGCV	A*02:01	51.60	0.4
LLFNKVTLA	A*02:01	52.60	0.2
LFFNKVTLA	A*02:01	30.60	0.2
LQLPQGTTL	A*02:01	31.60	0
LQLPQGTTS	A*02:01	30.80	0
MEVTPSGTWL (A2)	A*02:01	30.60	0.6
IEVTPSGTWL	A*02:01	30.40	0
MEVTPSGTWF	A*02:01	30.80	0
MEVTPSGTWS	A*02:01	31.20	0.4
RLNEVAKNL	A*02:01	47.20	0
RLNVVAKNL	A*02:01	29.80	2.2
SIIAYTMSL	A*02:01	54.20	0.2
CIIAYTMSL	A*02:01	33.40	0.6
PIIAYTMSL	A*02:01	38.40	0
STIAYTMSL	A*02:01	47.60	0
YLQPRTFLL	A*02:01	59.20	0
YFQPRTFLL	A*02:01	40.40	0
GLMWLSYFI	A*02:01	54.20	0.2
GFMWLSYFI	A*02:01	31.40	0.2
TLACFVLAAV	A*02:01	49.60	0.4
TLACFVLAAF	A*02:01	32.20	0.6
TLACFVPAAV	A*02:01	55.00	0.2
LALLLLDRL	A*02:01	22.00	10.87
LVLLLLDRL	A*02:01	14.27	9.99
MEVTPSGTWL	B*40:01	55.73	0.38
IEVTPSGTWL	B*40:01	54.53	0.5
MEVTPSGTWF	B*40:01	52.27	0.19
MEVTPSGTWS	B*40:01	46.00	0

Table S5. Characteristics of HLA-A*02:01/HLA-B*40:01 positive patients

Number of patients		**37**
Sex [n (%)]	Female	12 (32.4)
	Male	25 (67.6)
Age [years]	Range	22-91
	Median	69
Sample collection date	03/2020-11/2020	
Interval symptom onset to sample collection [weeks]	Range	1-16
Chronic comorbidities [n (%)]	Hypertension Lung disease Diabetes	21 (56.8) 3 (8.1) 15 (40.5)
Invasive ventilation [n (%)]		14 (37.8)
Death [n (%)]		5 (13.5)

Table S6. HLA genotypes

Patient ID	HLA-A	HLA-A	HLA-B	HLA-B	HLA-C	HLA-C
002	02:01	23:01	37:01	44:03	04:01	06:02
003	02:01	11:01	35:01	40:01	04:01	-
004	01:01	02:01	08:01	35:02	04:01	07:01
005	02:01	-	38:01	-	12:03	-
011	02:01	-	13:02	40:01	03:04	06:02
013	02:01	24:02	51:01	55:01	01:02	14:02
014	02:01	11:01	40:02	52:01	02:02	12:02
017	02:01	29:02	39:01	53:01	06:02	07:02
022	02:01	32:01	07:02	51:01	07:02	14:02
032	02:01	25:01	15:01	51:01	01:02	03:04
033	02:01	29:02	13:02	44:03	06:02	16:01
036	02:01	24:02	13:02	15:01	03:03	06:02
040	02:01	30:01	13:02	51:01	06:02	15:13
041	02:01	03:01	07:02	51:01	07:02	15:02
042	02:01	68:01	07:02	38:01	07:02	12:03
043	02:01	23:01	27:02	51:01	02:02	04:01
044	01:01	02:01	37:01	44:02	01:02	06:02
047	02:01	29:01	07:05	35:03	04:01	15:05
048	02:01	31:01	13:02	37:01	06:02	-
049	02:01	24:02	07:02	51:01	07:02	14:02
050	02:01	24:02	51:01	58:01	03:02	15:04
055	02:01	33:03	15:01	40:01	03:03	03:04
056	24:02	29:02	08:01	40:01	03:04	07:01
058	01:01	02:01	15:01	51:01	03:04	15:02
059	02:01	32:01	15:01	57:01	01:02	06:02
060	02:01	26:01	18:01	38:01	07:01	12:03
061	02:01	32:01	18:01	35:01	04:01	07:01
063	02:01	24:02	35:02	39:01	04:01	12:03
064	02:01	11:01	13:02	35:03	06:02	12:03
066	02:01	29:01	07:05	35:03	04:01	15:05
067	02:01	-	07:02	15:01	01:02	07:02
068	02:01	-	27:05	40:01	02:02	03:04
069	02:01	26:01	27:05	51:01	02:02	14:02
070*	2*	*Donor HLA-typed by flow cytometry				
081	23:01	31:01	40:01	51:01	03:04	12:03

083	02:01	30:01	08:01	13:02	06:02	07:01
085	02:01	68:01	08:01	44:05	07:01	07:02

Table S7. Overview of ELISpot results for wildtype peptides

Protein	Start aa	End aa	Sequence	Short	SARS-CoV-2 patients [positive/tested (%)]	Pre-pandemic controls [positive/tested (%)]
S	269	277	YLQPRTFLL	YLQ	2/13 (15%)	0/5 (0%)
S	417	425	KIADYNYKL	KIA	0/10 (0%)	0/5 (0%)
S	424	433	KLPDDFTGCV	KLP	0/10 (0%)	0/5 (0%)
S	691	699	SIIAYTMSL	SII	5/13 (38%)	0/5 (0%)
S	821	829	LLFNKVTLA	LLF	0/10 (0%)	0/5 (0%)
S	1185	1193	RLNEVAKNL	RLN	0/13 (0%)	0/5 (0%)
M	61	70	TLACFVLAAV	TLA	0/12 (0%)	0/5 (0%)
M	89	97	GLMWLSYFI	GLM	1/14 (7%)	0/5 (0%)
N	322	331	MEVTPSGTWL	MEV	1/3 (33%)	0/5 (0%)

Table S8. Differentially expressed genes from scRNA-seq analysis

Table S9. Top clonotypes from TCR sequencing

Table S10. Acknowledgments for sequences downloaded from GISAID

Table S11. Raw data

4. Discussion

4.1 General discussion

An essential characteristic of SARS-CoV-2 is its capability to subvert host immune responses. This has been shown for innate responses, where the virus efficiently suppresses IFN-I responses (Lei et al., 2020; Xia et al., 2020). More recently, several studies have shown that novel SARS-CoV-2 variants are less sensitive to neutralization by antibodies, causing concerns about ongoing vaccination efforts (Greaney et al., 2021; Gupta, 2021; Liu et al., 2020; McCarthy et al., 2021). In this study, we demonstrated that naturally occurring, low-frequency mutations can alter $CD8^+$ T cell epitopes and, consequently, diminish $CD8^+$ T cell responses against these mutated epitopes. The mechanisms behind this reduction in $CD8^+$ T cell responses are associated with decreased stability of the peptide-MHC-I complex, as demonstrated by cell-free *in vitro* assays. This was consolidated by staining with MHC-I tetramers complexed with wildtype and mutant peptide. Cells could be stained with mutant containing tetramers at low temperatures, which was abolished at physiological temperatures, likely due to disintegration of the complex. Such a decrease in peptide-MHC-I stability did not lead to the formation neoepitopes, because the mutant epitope cannot be efficiently presented. This is in line with our TCR sequencing data, where T cell clones greatly overlap between wildtype and mutant stimulated T cells. Importantly, a recent pre-print reported similar results, further strengthening the notion that single amino-acid mutations can affect $CD8^+$ T cell responses (Qiu et al., 2021). Of note, the sequences that we analysed in our study were sampled before July 2020, at a time where vaccinations have not started yet. It would be interesting to compare mutations with possible effects on T cell responses from populations with high vaccination rates. Such an approach would even allow to compare the rates of mutations within the S gene, against which vaccine-induced responses are targeted and the rest of the viral genome. This could allow to draw some conclusions on potential selection pressures exerted by global mass vaccination strategies.

4.2 T cell selection pressure

T cell immunity is often impaired in chronic infections like HIV-I and HCV due to sequence variation in viral epitopes (Timm and Walker, 2015). One key component of this is the concept of viral quasispecies, which describes a “cloud” of viral variants that is present in the host at the same time (Lauring and Andino, 2010). External selection pressures have a strong effect on the quasispecies and restrict the sequence space that can be explored (Lauring and Andino, 2010). In HIV-I and HCV infections selection pressure by $CD8^+$ T cells has been

shown to play a crucial role in shaping the viral quasispecies (Timm and Walker, 2015). This was achieved by comparing the rate of non-synonymous mutation within T cell epitopes and other regions of the genome, combined with functional characterization of these mutants (Cox et al., 2005; Timm et al., 2004). However, such viral escape mechanisms do generally not occur in acute infections (Grifoni et al., 2021). It needs to be mentioned that the study presented in this thesis does not allow to draw conclusions about T cell selection pressures that might be exerted on SARS-CoV-2.

There are several ways this could be addressed in future studies. One possibility resembles the strategy described above for HCV: sequencing the viral genome at different timepoints of infection and the comparison of mutation rates within and outside of $CD8^+$ T cell epitopes. A prerequisite for this approach is the prior knowledge of the HLA repertoire of each infected individual, since the HLA repertoire defines the epitope repertoire that can be presented (Neefjes et al., 2011). However, such data was not available to us for the current study, as viral sequences were derived from samples obtained via an epidemiological surveillance system. In an ideal scenario such a study would be carried out in a prospective setting, where participants are sampled at the beginning of infection, as well as at later timepoints, combined with sequencing of their HLA loci. Although more than 1000 T cell epitopes have been identified with various methods, this list might still be incomplete and potentially biased for some HLA isotypes (Grifoni et al., 2021). In addition, some epitopes might be more important for the T cell response as others, which also needs to be considered when investigating potential T cell related selection pressures.

A second strategy to investigate if T cells exert selection pressure on SARS-CoV-2 is to compare the rate of epitope mutations for specific HLA isotypes in regions with high allele frequency for these HLAs in comparison to regions with low HLA allele frequencies. This approach is challenging for several reasons: First, the distribution of HLAs is complex and few HLA isotypes and populations would allow for such a comparison. Second, international travel, although restricted, can strongly influence the viral strains present in a geographic region. Third, escape mutations might develop in single individuals, but could not get fixed or be passed on to the next host, because the mutation might have an advantage intra-host, but a disadvantage in transmission. To conclude, additional studies will be required to answer the question whether the observed mutations that evade T cell responses occurred due to selection pressure exerted by T cells or not.

4.3 Quantitative and qualitative differences of wildtype and mutant peptide-stimulated T cells

Upon T cell expansion we observed a decrease in the numbers of cells expanded in the presence of mutant peptide. TCR sequencing on the single-cell level revealed that the same T cell clones expand in the presence of wildtype and mutant peptides. Thus, the investigated mutation did not lead to the generation of neo-epitopes that could trigger the activation of novel T cell clones. However, if and how other mutations might affect the expansion of T cell clones remains to be investigated. Two recent studies investigated the TCRs of T cell clones reacting to the YLQ epitope from several individuals (Ferretti et al., 2020; Shomuradova et al., 2020). These studies revealed that for some epitopes TCRs are shared between individuals. Of note, the two most prominent V genes of TCRA and TCRB, respectively, that were identified in our study were also reported in these studies. These results further highlight that there is a public TCR recognising the YLQ epitope. However, we also identified additional V genes present at lower abundance, suggesting that there are additional TCRs capable of recognising this epitope. Such public TCRs have been shown to play a crucial role in the response against HIV and their abundance was associated with better virus control (Price et al., 2009). It is tempting to speculate that mutations in epitopes recognized by such public TCRs could have implications for viral evasion of $CD8^+$ T cell responses in multiple individuals. It remains to be determined if public TCRs are found for additional epitopes and if and how mutations in these epitopes affect T cell immunity.

In addition to the quantitative differences observed upon T cell expansion, our unbiased single-cell RNA sequencing (scRNA-seq) approach also revealed qualitative differences in the cells that responded to the mutant peptide. For example, cells stimulated with mutant peptide had higher expression of lymphotoxin-beta (LTB), which plays a crucial role in the development and maintenance of T cell responses (Gommerman et al., 2014). Interestingly, LTB signalling to DCs leads to an induction of IFN-beta, thus promoting antiviral immunity (Ng et al., 2015; Summers deLuca et al., 2011). Increased IFN-I signalling might also explain the higher levels of certain ISGs, such as IFITM1 and IFITM2 that were observed in cells stimulated with mutant peptide (Schoggins et al., 2011). This might represent a compensatory mechanism, by which weakly activated cells try to achieve better activation. Interestingly, granzyme K (GZMK) was also expressed at higher levels in mutant peptide stimulated T cells. In contrast to granzyme A, GZMK is not cytotoxic *in vivo*, but has pro-inflammatory properties (Bouwman et al., 2021; Joeckel et al., 2011). Furthermore, it has recently been shown to be a hallmark of aging T cells (Mogilenko et al., 2021). In this study the authors showed that GZMK expressing aged T cells have clonally expanded and shared some characteristics with exhausted T cells, including

decreased expression of effector molecules (Mogilenko et al., 2021). It is unlikely that the changes that were observed in our study reflect immune aging, but the observed overlap is interesting and might hint towards shared mechanisms behind T cell aging and expansion with a suboptimal MHC-I epitope.

The fact that we observed quantitative and qualitative differences upon stimulation with mutant peptides is in line with the fact that weak TCR ligands induce distinctive signalling events and have various outcomes on T cell activation (Edwards and Evavold, 2011). Various escape mutants for different viruses have been shown to act as T cell antagonists and thus not only prevent T cells from reacting to the mutant epitope, but also render them unable to react to the wildtype epitope at the same time (Bertoletti et al., 1994; Frasca et al., 1999; Klenerman et al., 1994; Kubota et al., 2000). This has implications for emerging escape mutations *in vivo*, as already low frequencies of such mutations might affect T cell responses also against the wildtype epitopes. To what extent the mutant epitopes described in this thesis represent TCR antagonists remains to be determined.

4.4 Epitope mutations and the importance for antiviral immunity

On average, we identified mutations in 1.56 tested epitopes for individuals that had at least one mutation. Of note, most epitopes included in our study are HLA-A*02:01 epitopes, which is the most common HLA in the Austrian population (Gonzalez-Galarza et al., 2019). However, on average individuals are able to recognize 17 SARS-CoV-2 MHC-I epitopes (Tarke et al., 2021a). This raises the question to what extent mutations in one or a few of these epitopes affect T cell immunity to SARS-CoV-2. In this context it is important to note, that while theoretically, many epitopes can be recognized, immune responses to many viral infections are often dominated by a few epitopes, to which the majority of responses are generated. This concept of immunodominance has been described for lymphocytic choriomeningitis virus (LCMV), cytomegalovirus (CMV), Influenza A virus, HBV, HCV, HIV-I and also SARS-CoV-2 (Akram and Inman, 2012; Tarke et al., 2021a; Yewdell, 2006). The YLQ epitope, which much of this thesis is focussed on was also reported to be a dominant epitope (Shomuradova et al., 2020; Tarke et al., 2021a). If the immune response is largely dominated by one epitope, mutations in this epitope could promote viral escape. It has been described in HIV-I infection, that some escape mutations are associated with disease progression (Kelleher et al., 2001). However, in elite suppressors, which can effectively control HIV-I, escape mutations also accumulated, but some of these mutations could still trigger an efficient T cell response (Bailey et al., 2006). Additionally, in a recent study from our lab we describe escape mutations in the murine infection model LCMV, where mutations in a dominant T cell epitope accumulated

(Smyth et al., 2021). Upon infection with a virus carrying this escape mutation the responses against the remaining epitopes were not affected and as a result, no differences in viral load or disease severity were observed between infection with wildtype and mutant virus (Smyth et al., 2021). In lights of this it is unlikely that mutations in few T cell epitopes will affect the overall response to SARS-CoV-2 infection.

Additionally, the large HLA diversity on the population level would make it very hard for such escape mutations to establish and be transmitted, as it is likely that the next infectee has a different set of HLAs and thus recognizes different epitopes (Gonzalez-Galarza et al., 2019; Grifoni et al., 2021).

Furthermore, the rapid proliferation and transmissibility of SARS-CoV-2 enable it to be transmitted before the original host can mount an efficient T cell response, which takes few days to develop, while transmissions often occur before the onset of symptoms (Chen and John Wherry, 2020; Grifoni et al., 2021). Thus, escape mutations might arise in individual patients, but are unlikely to be passed on and establish in new viral lineages on the population level.

The situation might look a bit different in the light of ongoing vaccination efforts. Currently, all EMA approved vaccines contain only the S gene of SARS-CoV-2 (Forni and Mantovani, 2021; Krammer, 2020). Thus, T cell responses following vaccination can only target epitopes in the S gene, and it has been demonstrated that per HLA allele individuals react to 1.6 epitopes per antigen on average (Tarke et al., 2021a). Assuming 4 different HLA-A and HLA-B alleles per individual, this results in around 6 epitopes recognized per individual upon vaccination with an S containing vaccine. This highly reduces the number of epitopes that need to be changed in order to escape the T cell response. Additionally, high vaccination rates might increase the selection pressure on the population level and could potentially lead to the selection of variants that are less efficiently recognized by T cells. To date, all circulating variants still induce robust T cell responses (Geers et al., 2021; Redd et al., 2021; Riou et al., 2021; Tarke et al., 2021b). However, a recent preprint that analyzed more than 300.000 genomes sampled during the first year of the pandemic across the world, found that epitopes for certain HLA types accumulated specific mutational patterns, providing evidence for potential selection of such mutations (Hamelin et al., 2021). Of note, some mutations that were identified in this preprint were also identified in our study and demonstrated to induce decreased T cell responses.

4.5 New SARS-CoV-2 variants and potential immune escape

The SARS-CoV-2 lineage B.1.1.7, now denominated Alpha, first emerged in the United Kingdom in September 2020 and then quickly spread to and beyond the rest of Europe (Gupta, 2021) (Meng et al., 2021) This variant was associated with increased infectivity (Hamelin et al., 2021). Importantly, pseudovirus containing S protein from the Alpha variant showed decreased neutralization against serum derived from individuals that received the mRNA vaccine from Pfizer/Biontech (Collier et al., 2021). Furthermore, the mutation E484K in S was reported to be acquired in some cases of Alpha infection, which is also present in other SARS-CoV-2 variants and was associated with reduced neutralization by monoclonal antibodies (Wang et al., 2021a). Similarly, Alpha variant carrying the E484K mutation showed reduced neutralization by vaccine-induced serum as compared to Alpha alone (Collier et al., 2021). In addition to the Alpha variant new variants independently emerged in South Africa and Brazil, named Beta and Gamma, which were both associated with increased infectivity, (Faria et al., 2021; Tegally et al., 2021). Both these variants are characterized by a great number of mutations, including the shared mutations K417T/N, E484K, N501Y (which is also seen in Alpha) in S (Faria et al., 2021; Tegally et al., 2021). This convergent evolution within a short timeframe might indicate altered selection pressures. Indeed, a recent preprint suggests that there was a global shift in selection pressures in October 2020 that coincided with the establishment of these variants (Martin et al., 2021). What exactly caused this shift in selection pressure is still unclear, but one possibility is an increase in seropositivity and thus immunity against the virus in the population (Martin et al., 2021). At the time of emergence of these variants global vaccinations have not started yet or were only about to pick up speed. In fact, both the Beta and Gamma variant show decreased neutralization by vaccine-induced, as well as convalescent sera (Cele et al., 2021; Wang et al., 2021a). More recently, an additional variant Delta arose, that is associated with even higher transmissibility and also reduced neutralization by vaccine-induced sera (Wall et al., 2021b, 2021a).

There is ample evidence that certain newly emerged variants are associated with decreased neutralization by antibody responses. T cell responses might be important to still confer protection in the context of decreased antibody responses. Thus, a crucial question is if and how the mutations found in these variants affect T cell responses. Although some mutations lie withing T cell epitopes, overall T cell responses against the discussed variants are still intact (Geers et al., 2021; Riou et al., 2021; Tarke et al., 2021b). Nevertheless, some studies have highlighted the possibilities that some variants could lead to decreased T cell responses, further showing the importance for ongoing surveillance of viral variants for potential immune escape (Pretti et al., 2021; de Silva et al., 2021).

4.6 Immunosuppressed patients as incubators for new variants

In most patients SARS-CoV-2 causes acute infection, with the majority of individuals clearing the virus within 2-3 weeks post symptom onset (He et al., 2020; To et al., 2020; Zou et al., 2020). In this period some degree of intra-patient variability for virus mutations is seen (Popa et al., 2020). However, a growing number of reports indicates that immunosuppressed patients can carry infectious virus for extended periods of time (Agarwal et al., 2020; Avanzato et al., 2020; Choi et al., 2020; Clark et al., 2021; Damiano D'Ardes et al., 2020; Kemp et al., 2021). Growing concern about such long-term infected patients arose with reports that the Alpha variant could have first developed in an immunosuppressed patient (Kemp et al., 2021). Additional studies highlighted the ongoing viral evolution in long-term infected individuals (Avanzato et al., 2020; Choi et al., 2020; Clark et al., 2021; Kemp et al., 2021). Since these patients cannot mount an immune response on their own, treatment often encompassed the administration of convalescent serum or monoclonal antibodies targeting SARS-CoV-2. However, this was associated with the occurrence of recurrent deletions and other mutations that were shown to decrease the neutralisation by these antibodies (Kemp et al., 2021; McCarthy et al., 2021). We obtained serial sequences from a patient that was virus positive from September 2020 until March 2021. In this patient we could observe increased frequencies of insertions and deletions in the S gene that coincided with treatment with convalescent serum (unpublished data). Together with data published by others this raises concerns about the selection of antibody escape mutations via treatment of immunosuppressed patients with serum or antibodies.

If and how T cell escape mutations could accumulate in patients that are long-term positive for SARS-CoV-2 remains to be determined. However, in our long-term infected patient we identified potential escape mutations for the HLA-B*07:02 (the patient carries the HLA-B*07:02 allele) epitope SPRRARSVA. Additional functional readouts need to be performed to confirm that the observed mutation can evade T cell responses. It is unclear how T cell escape mutations can be selected in a patient that has consistently low numbers of T cell in the blood. To further investigate if T cell responses directed against SARS-CoV-2 are present in this patient functional T cell readouts are required.

Another possibility for the accumulation of mutations in immunosuppressed patients is that drugs that are used in immunosuppressed might have an effect on the mutation rate of SARS-CoV-2. Many of these patients have an underlying malignant disease and drugs that are used to treat these often interact with or are analogs of nucleic acids and might affect viral replication. Additionally, some drugs that are used to suppress the immune system or to treat

other virus infections, like HIV-I have similar modes of action like the chemotherapeutics mentioned. To investigate this hypothesis, we are currently setting up a screening strategy to test the potential of such drugs to change the mutation rate of SARS-CoV-2 (unpublished data).

4.7 Conclusion and outlook

To conclude, the work presented in this thesis provided the first evidence that naturally occurring single amino-acid mutations in SARS-CoV-2 have the potential to subvert $CD8^+$ T cell responses. The mutations we investigated reduced the binding to MHC-I and thus, mutant peptides cannot be efficiently presented to $CD8^+$ T cells. As a result, $CD8^+$ T cells stimulated with mutant peptide show quantitative and qualitative differences as compared to cells stimulated with wildtype peptide.

Until today, there is no strong evidence for the accumulation of such mutations that subvert T cell responses in circulating SARS-CoV-2 variants. However, some reports suggest that mutations present in SARS-CoV-2 variants could affect T cell responses (Pretti et al., 2021; de Silva et al., 2021). As global vaccination efforts progress, this might introduce additional selection pressures in the future that could lead to the accumulation of some mutations in certain populations.

As an outlook, there is the need for the implementation of global surveying mechanisms to detect potential immune escape early on. Such global variant monitoring will allow to quickly react to local outbreaks of variants that might evade the immune system. Additionally, it will inform how to adapt future vaccines to increase immunogenicity, or which variants to include in next generation vaccines. Lastly, to induce a T cell that is as broad as possible and makes the emergence of complete escape variants unlikely it could be beneficial to include additional SARS-CoV-2 proteins – or full-length SARS-CoV-2 – in future vaccines.

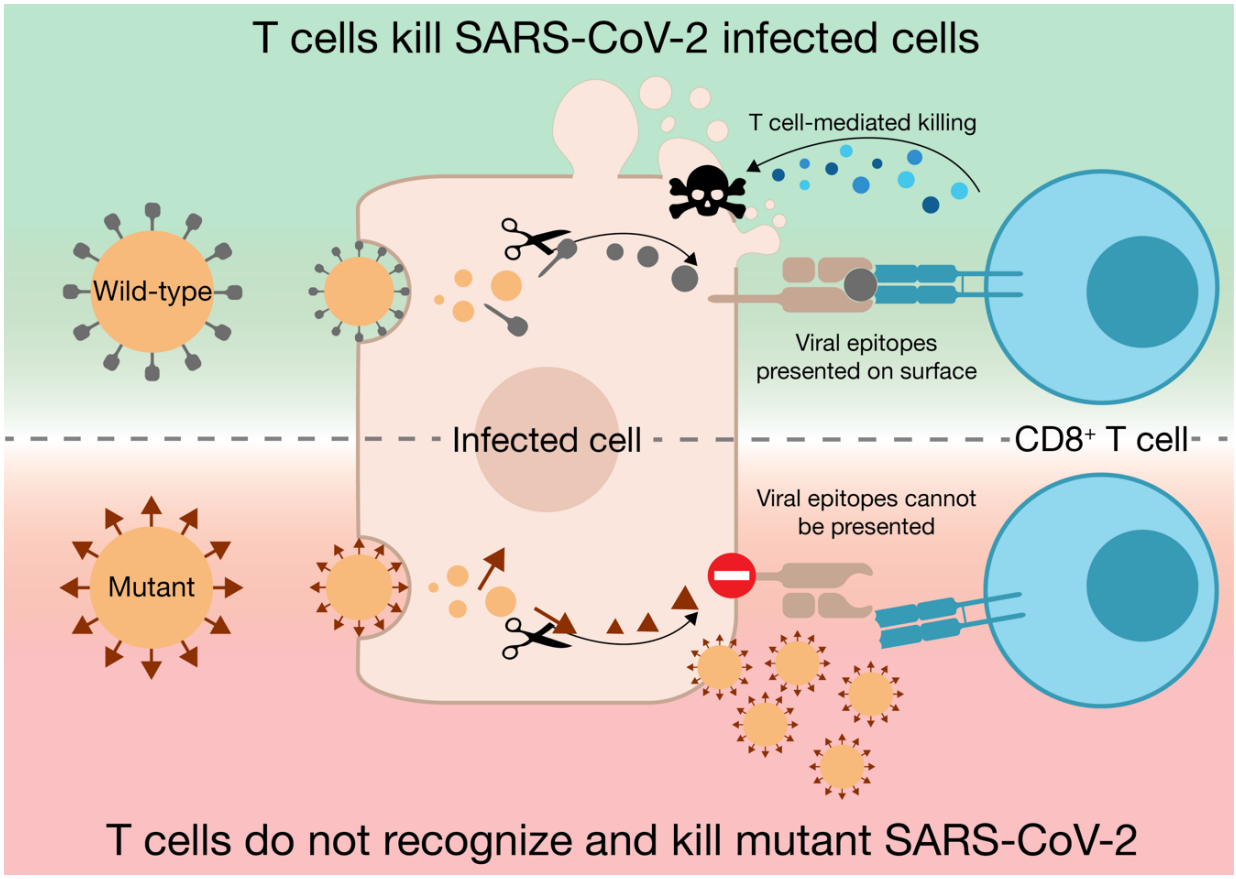

Figure 6 Graphical abstract. © Benedikt Agerer

5. Materials and Methods

The materials and methods relating to this thesis are described in the “Materials and Methods” section of the published manuscript “SARS-CoV-2 mutations in MHC-I-restricted epitopes evade CD8+ T cell responses”. See also page 37 – 48 in section 3.2 of this thesis.

6. References

Agarwal, V., Venkatakrishnan, A.J., Puranik, A., Kirkup, C., Lopez-Marquez, A., Challener, D.W., Theel, E.S., O'Horo, J.C., Binnicker, M.J., Kremers, W.K., et al. (2020). Long-term SARS-CoV-2 RNA shedding and its temporal association to IgG seropositivity. Cell Death Discovery *6*, 138.

Agerer, B., Koblischke, M., Gudipati, V., Montaño-Gutierrez, L.F., Smyth, M., Popa, A., Genger, J.W., Endler, L., Florian, D.M., Mühlgrabner, V., et al. (2021). SARS-CoV-2 mutations in MHC-I-restricted epitopes evade CD8+ T cell responses. Science Immunology *6*, 17–22.

Akira, S., Uematsu, S., and Takeuchi, O. (2006). Pathogen Recognition and Innate Immunity. Cell *124*, 783–801.

Akram, A., and Inman, R.D. (2012). Immunodominance: A pivotal principle in host response to viral infections. Clinical Immunology *143*, 99–115.

Alcami, A., and Koszinowski, U.H. (2000). Viral mechanisms of immune evasion. Trends in Microbiology.

Anderson, R.M., Fraser, C., Ghani, A.C., Donnelly, C.A., Riley, S., Ferguson, N.M., Leung, G.M., Lam, T.H., and Hedley, A.J. (2004). Epidemiology, transmission dynamics and control of SARS: The 2002-2003 epidemic. Philosophical Transactions of the Royal Society B: Biological Sciences *359*, 1091–1105.

von Andrian, U.H., and Mempel, T.R. (2003). Homing and cellular traffic in lymph nodes. Nature Reviews Immunology *3*, 867–878.

Anthony, D.A., Andrews, D.M., Chow, M., Watt, S. v., House, C., Akira, S., Bird, P.I., Trapani, J.A., and Smyth, M.J. (2010). A Role for Granzyme M in TLR4-Driven Inflammation and Endotoxicosis. The Journal of Immunology *185*, 1794–1803.

Anthony, S.J., Johnson, C.K., Greig, D.J., Kramer, S., Che, X., Wells, H., Hicks, A.L., Joly, D.O., Wolfe, N.D., Daszak, P., et al. (2017). Global patterns in coronavirus diversity. Virus Evolution *3*, 1–15.

Avanzato, V.A., Matson, M.J., Seifert, S.N., Pryce, R., Williamson, B.N., Anzick, S.L., Barbian, K., Judson, S.D., Fischer, E.R., Martens, C., et al. (2020). Case Study: Prolonged Infectious SARS-CoV-2 Shedding from an Asymptomatic Immunocompromised Individual with Cancer. Cell *183*, 1901-1912.e9.

Bailey, J.R., Williams, T.M., Siliciano, R.F., and Blankson, J.N. (2006). Maintenance of viral suppression in HIV-1–infected HLA-B*57+ elite suppressors despite CTL escape mutations. Journal of Experimental Medicine *203*, 1357–1369.

Ban, E., Dupré, L., Hermann, E., Rohn, W., Vendeville, C., Quatannens, B., Ricciardi-Castagnoli, P., Capron, A., and Riveau, G. (2000). CpG motifs induce Langerhans cell migration in vivo. International Immunology *12*, 737–745.

Bastard, P., Rosen, L.B., Zhang, Q., Michailidis, E., Hoffmann, H.-H., Zhang, Y., Dorgham, K., Philippot, Q., Rosain, J., Béziat, V., et al. (2020). Autoantibodies against type I IFNs in patients with life-threatening COVID-19. Science *370*, eabd4585.

Becker, W.B., McIntosh, K., Dees, J.H., and Chanock, R.M. (1967). Morphogenesis of avian infectious bronchitis virus and a related human virus (strain 229E). Journal of Virology *1*, 1019–1027.

Beemiller, P., Jacobelli, J., and Krummel, M.F. (2012). Integration of the movement of signaling microclusters with cellular motility in immunological synapses. Nature Immunology *13*, 787–795.

Bergamaschi, L., Mescia, F., Turner, L., Hanson, A.L., Kotagiri, P., Dunmore, B.J., Ruffieux, H., de Sa, A., Huhn, O., Morgan, M.D., et al. (2021). Longitudinal analysis reveals that delayed bystander CD8+ T cell activation and early immune pathology distinguish severe COVID-19 from mild disease. Immunity *54*, 1257-1275.e8.

Berlin, D.A., Gulick, R.M., and Martinez, F.J. (2020). Severe Covid-19. New England Journal of Medicine *383*, 2451–2460.

le Bert, N., Tan, A.T., Kunasegaran, K., Tham, C.Y.L., Hafezi, M., Chia, A., Chng, M.H.Y., Lin, M., Tan, N., Linster, M., et al. (2020). SARS-CoV-2-specific T cell immunity in cases of COVID-19 and SARS, and uninfected controls. Nature.

Bertoletti, A., Sette, A., Chisari, F. v, Penna, A., Levrero, M., Carli, M. de, Fiaccadori, F., and Ferrari, C. (1994). Natural variants of cytotoxic epitopes are T-cell receptor antagonists for antiviral cytotoxic T cells. Nature *369*, 407–410.

Blanco-Melo, D., Nilsson-Payant, B.E., Liu, W.-C., Uhl, S., Hoagland, D., Møller, R., Jordan, T.X., Oishi, K., Panis, M., Sachs, D., et al. (2020). Imbalanced Host Response to SARS-CoV-2 Drives Development of COVID-19. Cell *181*, 1036-1045.e9.

Bojkova, D., Klann, K., Koch, B., Widera, M., Krause, D., Ciesek, S., Cinatl, J., and Münch, C. (2020). Proteomics of SARS-CoV-2-infected host cells reveals therapy targets. Nature *583*, 469–472.

Bossi, G., and Griffiths, G.M. (2005). CTL secretory lysosomes: Biogenesis and secretion of a harmful organelle. Seminars in Immunology *17*, 87–94.

Bouvet, M., Debarnot, C., Imbert, I., Selisko, B., Snijder, E.J., Canard, B., and Decroly, E. (2010). In Vitro Reconstitution of SARS-Coronavirus mRNA Cap Methylation. PLoS Pathogens *6*, e1000863.

Bouwman, A.C., van Daalen, K.R., Crnko, S., ten Broeke, T., and Bovenschen, N. (2021). Intracellular and Extracellular Roles of Granzyme K. Frontiers in Immunology *12*.

Bowen, D.G., and Walker, C.M. (2005). Mutational escape from CD8+ T cell immunity. Journal of Experimental Medicine *201*, 1709–1714.

Brodin, P. (2021). Immune determinants of COVID-19 disease presentation and severity. Nature Medicine *27*, 28–33.

Brown, M. (2020). Immune correlates of SARS-CoV-2 protection. Nature Reviews Immunology *20*, 593–593.

Browne, K.A., Blink, E., Sutton, V.R., Froelich, C.J., Jans, D.A., and Trapani, J.A. (1999). Cytosolic Delivery of Granzyme B by Bacterial Toxins: Evidence that Endosomal Disruption, in Addition to Transmembrane Pore Formation, Is an Important Function of Perforin. Molecular and Cellular Biology *19*, 8604–8615.

Cao, X. (2015). Self-regulation and cross-regulation of pattern-recognition receptor signalling in health and disease. Nature Reviews Immunology *16*, 35–50.

Carvalho, T., Krammer, F., and Iwasaki, A. (2021). The first 12 months of COVID-19: a timeline of immunological insights. Nature Reviews Immunology *21*, 245–256.

Cele, S., Gazy, I., Jackson, L., Hwa, S.H., Tegally, H., Lustig, G., Giandhari, J., Pillay, S., Wilkinson, E., Naidoo, Y., et al. (2021). Escape of SARS-CoV-2 501Y.V2 from neutralization by convalescent plasma. Nature *593*, 142–146.

Center for Disease Control and Prevention (2003). Severe acute respiratory syndrome (SARS).

Cevik, M., Bamford, C.G.G., and Ho, A. (2020). COVID-19 pandemic—a focused review for clinicians. Clinical Microbiology and Infection *26*, 842–847.

Chandrashekar, A., Liu, J., Martinot, A.J., McMahan, K., Mercado, N.B., Peter, L., Tostanoski, L.H., Yu, J., Maliga, Z., Nekorchuk, M., et al. (2020). SARS-CoV-2 infection protects against rechallenge in rhesus macaques. Science *369*, 812–817.

Channappanavar, R., Fehr, A.R., Vijay, R., Mack, M., Zhao, J., Meyerholz, D.K., and Perlman, S. (2016). Dysregulated Type I Interferon and Inflammatory Monocyte-Macrophage Responses Cause Lethal Pneumonia in SARS-CoV-Infected Mice. Cell Host & Microbe *19*, 181–193.

Chen, Z., and John Wherry, E. (2020). T cell responses in patients with COVID-19. Nature Reviews Immunology *20*, 529–536.

Chen, Y., Cai, H., Pan, J., Xiang, N., Tien, P., Ahola, T., and Guo, D. (2009). Functional screen reveals SARS coronavirus nonstructural protein nsp14 as a novel cap N7 methyltransferase. Proceedings of the National Academy of Sciences *106*, 3484–3489.

Choi, B., Choudhary, M.C., Regan, J., Sparks, J.A., Padera, R.F., Qiu, X., Solomon, I.H., Kuo, H.-H., Boucau, J., Bowman, K., et al. (2020). Persistence and Evolution of SARS-CoV-2 in an Immunocompromised Host. New England Journal of Medicine *383*, 2291–2293.

Chopra, V., Flanders, S.A., O'Malley, M., Malani, A.N., and Prescott, H.C. (2021). Sixty-Day Outcomes Among Patients Hospitalized With COVID-19. Annals of Internal Medicine *174*, 576–578.

Chvatal-Medina, M., Mendez-Cortina, Y., Patiño, P.J., Velilla, P.A., and Rugeles, M.T. (2021). Antibody Responses in COVID-19: A Review. Frontiers in Immunology *12*, 1–14.

Clark, S.A., Clark, L.E., Pan, J., Coscia, A., McKay, L.G.A., Shankar, S., Johnson, R.I., Brusic, V., Choudhary, M.C., Regan, J., et al. (2021). SARS-CoV-2 evolution in an immunocompromised host reveals shared neutralization escape mechanisms. Cell *184*, 2605-2617.e18.

Collier, D.A., de Marco, A., Ferreira, I.A.T.M., Meng, B., Datir, R.P., Walls, A.C., Kemp, S.A., Bassi, J., Pinto, D., Silacci-Fregni, C., et al. (2021). Sensitivity of SARS-CoV-2 B.1.1.7 to mRNA vaccine-elicited antibodies. Nature *593*, 136–141.

Coronaviridae Study Group of the International Committee on Taxonomy of Viruses (2020). The species Severe acute respiratory syndrome-related coronavirus: classifying 2019-nCoV and naming it SARS-CoV-2. Nature Microbiology *5*, 536–544.

Corti, D., and Lanzavecchia, A. (2013). Broadly Neutralizing Antiviral Antibodies. Annual Review of Immunology *31*, 705–742.

Cox, A.L., Mosbruger, T., Mao, Q., Liu, Z., Wang, X.-H., Yang, H.-C., Sidney, J., Sette, A., Pardoll, D., Thomas, D.L., et al. (2005). Cellular immune selection with hepatitis C virus persistence in humans. Journal of Experimental Medicine *201*, 1741–1752.

Cui, J., Li, F., and Shi, Z.L. (2019). Origin and evolution of pathogenic coronaviruses. Nature Reviews Microbiology *17*, 181–192.

Damiano D'Ardes, Andrea Boccatonda, Ilaria Rossi, Michela Pontolillo, Giulio Cocco, Cosima Schiavone, Francesca Santilli, Maria Teresa Guagnano, Marco Bucci, and Francesco Cipollone (2020). Long-term Positivity to SARS-CoV-2: A Clinical Case of COVID-19 with Persistent Evidence of Infection. European Journal of Case Reports in Internal Medicine.

Dan, J.M., Mateus, J., Kato, Y., Hastie, K.M., Yu, E.D., Faliti, C.E., Grifoni, A., Ramirez, S.I., Haupt, S., Frazier, A., et al. (2021). Immunological memory to SARS-CoV-2 assessed for up to 8 months after infection. Science *371*, eabf4063.

Deng, K., Pertea, M., Rongvaux, A., Wang, L., Durand, C.M., Ghiaur, G., Lai, J., McHugh, H.L., Hao, H., Zhang, H., et al. (2015). Broad CTL response is required to clear latent HIV-1 due to dominance of escape mutations. Nature *517*, 381–385.

Deng, W., Bao, L., Liu, J., Xiao, C., Liu, J., Xue, J., Lv, Q., Qi, F., Gao, H., Yu, P., et al. (2020). Primary exposure to SARS-CoV-2 protects against reinfection in rhesus macaques. Science *369*, 818–823.

Di, H., McIntyre, A.A., and Brinton, M.A. (2018). New insights about the regulation of Nidovirus subgenomic mRNA synthesis. Virology *517*, 38–43.

Dong, E., Du, H., and Gardner, L. (2020). An interactive web-based dashboard to track COVID-19 in real time. The Lancet Infectious Diseases *20*, 533–534.

Drosten, C., Günther, S., Preiser, W., van der Werf, S., Brodt, H.-R., Becker, S., Rabenau, H., Panning, M., Kolesnikova, L., Fouchier, R.A.M., et al. (2003). Identification of a Novel

Coronavirus in Patients with Severe Acute Respiratory Syndrome. New England Journal of Medicine *348*, 1967–1976.

Eckerle, L.D., Lu, X., Sperry, S.M., Choi, L., and Denison, M.R. (2007). High Fidelity of Murine Hepatitis Virus Replication Is Decreased in nsp14 Exoribonuclease Mutants. Journal of Virology *81*, 12135–12144.

Edwards, L.J., and Evavold, B.D. (2011). T cell recognition of weak ligands: roles of signaling, receptor number, and affinity. Immunologic Research *50*, 39–48.

Eigen, M., and Schuster, P. (1977). A principle of natural self-organization. Naturwissenschaften *64*, 541–565.

Fabricant, J. (1998). The Early History of Infectious Bronchitis. Avian Diseases *42*, 648.

Falk, K., Rötzschke, O., Stevanović, S., Jung, G., and Rammensee, H.-G. (1991). Allele-specific motifs revealed by sequencing of self-peptides eluted from MHC molecules. Nature *351*, 290–296.

Faria, N.R., Mellan, T.A., Whittaker, C., Claro, I.M., Candido, D. da S., Mishra, S., Crispim, M.A.E., Sales, F.C.S., Hawryluk, I., McCrone, J.T., et al. (2021). Genomics and epidemiology of the P.1 SARS-CoV-2 lineage in Manaus, Brazil. Science *372*, 815–821.

Ferretti, A.P., Kula, T., Wang, Y., Nguyen, D.M.V., Weinheimer, A., Dunlap, G.S., Xu, Q., Nabilsi, N., Perullo, C.R., Cristofaro, A.W., et al. (2020). Unbiased Screens Show CD8+ T Cells of COVID-19 Patients Recognize Shared Epitopes in SARS-CoV-2 that Largely Reside outside the Spike Protein. Immunity *53*, 1095-1107.e3.

Forni, G., and Mantovani, A. (2021). COVID-19 vaccines: where we stand and challenges ahead. Cell Death & Differentiation *28*, 626–639.

Frasca, L., del Porto, P., Tuosto, L., Marinari, B., Scottà, C., Carbonari, M., Nicosia, A., and Piccolella, E. (1999). Hypervariable region 1 variants act as TCR antagonists for hepatitis C virus-specific CD4+ T cells. The Journal of Immunology *163*, 650–658.

Galani, I.-E., Rovina, N., Lampropoulou, V., Triantafyllia, V., Manioudaki, M., Pavlos, E., Koukaki, E., Fragkou, P.C., Panou, V., Rapti, V., et al. (2021). Untuned antiviral immunity in COVID-19 revealed by temporal type I/III interferon patterns and flu comparison. Nature Immunology *22*, 32–40.

Gao, Y., Yan, L., Huang, Y., Liu, F., Zhao, Y., Cao, L., Wang, T., Sun, Q., Ming, Z., Zhang, L., et al. (2020). Structure of the RNA-dependent RNA polymerase from COVID-19 virus. Science (New York, N.Y.).

Garbino, J., Crespo, S., Aubert, J. -D., Rochat, T., Ninet, B., Deffernez, C., Wunderli, W., Pache, J., Soccal, P.M., and Kaiser, L. (2006). A Prospective Hospital-Based Study of the Clinical Impact of Non–Severe Acute Respiratory Syndrome (Non-SARS)–Related Human Coronavirus Infection. Clinical Infectious Diseases *43*, 1009–1015.

Geers, D., Shamier, M.C., Bogers, S., den Hartog, G., Gommers, L., Nieuwkoop, N.N., Schmitz, K.S., Rijsbergen, L.C., van Osch, J.A.T., Dijkhuizen, E., et al. (2021). SARS-CoV-2 variants of concern partially escape humoral but not T-cell responses in COVID-19 convalescent donors and vaccinees. Science Immunology *6*, eabj1750.

Ghosh, S., Dellibovi-Ragheb, T.A., Kerviel, A., Pak, E., Qiu, Q., Fisher, M., Takvorian, P.M., Bleck, C., Hsu, V.W., Fehr, A.R., et al. (2020). β-Coronaviruses Use Lysosomes for Egress Instead of the Biosynthetic Secretory Pathway. Cell *183*, 1520-1535.e14.

Giacomelli, A., Pezzati, L., Conti, F., Bernacchia, D., Siano, M., Oreni, L., Rusconi, S., Gervasoni, C., Ridolfo, A.L., Rizzardini, G., et al. (2020). Self-reported Olfactory and Taste Disorders in Patients With Severe Acute Respiratory Coronavirus 2 Infection: A Cross-sectional Study. Clinical Infectious Diseases *71*, 889–890.

Gommerman, J.L., Browning, J.L., and Ware, C.F. (2014). The Lymphotoxin Network: Orchestrating a Type I interferon response to optimize adaptive immunity. Cytokine & Growth Factor Reviews *25*, 139–145.

Gonzalez-Galarza, F.F., McCabe, A., Santos, E.J.M. dos, Jones, J., Takeshita, L., Ortega-Rivera, N.D., Cid-Pavon, G.M. del, Ramsbottom, K., Ghattaoraya, G., Alfirevic, A., et al. (2019). Allele frequency net database (AFND) 2020 update: gold-standard data classification, open access genotype data and new query tools. Nucleic Acids Research *48*, D783–D788.

Gorbalenya, A.E., Enjuanes, L., Ziebuhr, J., and Snijder, E.J. (2006). Nidovirales: Evolving the largest RNA virus genome. Virus Research *117*, 17–37.

Gordon, D.E., Jang, G.M., Bouhaddou, M., Xu, J., Obernier, K., White, K.M., O'Meara, M.J., Rezelj, V. V., Guo, J.Z., Swaney, D.L., et al. (2020). A SARS-CoV-2 protein interaction map reveals targets for drug repurposing. Nature *583*, 459–468.

Goulder, P.J.R., and Watkins, D.I. (2004). HIV and SIV CTL escape: Implications for vaccine design. Nature Reviews Immunology.

Goulder, P.J., Brander, C., Tang, Y., Tremblay, C., Colbert, R.A., Addo, M.M., Rosenberg, E.S., Nguyen, T., Allen, R., Trocha, A., et al. (2001). Evolution and transmission of stable CTL escape mutations in HIV infection. Nature *412*, 334–338.

Graham, R.L., Donaldson, E.F., and Baric, R.S. (2013). A decade after SARS: Strategies for controlling emerging coronaviruses. Nature Reviews Microbiology *11*, 836–848.

Greaney, A.J., Starr, T.N., Gilchuk, P., Zost, S.J., Binshtein, E., Loes, A.N., Hilton, S.K., Huddleston, J., Eguia, R., Crawford, K.H.D., et al. (2021). Complete Mapping of Mutations to the SARS-CoV-2 Spike Receptor-Binding Domain that Escape Antibody Recognition. Cell Host & Microbe *29*, 44-57.e9.

Grifoni, A., Weiskopf, D., Ramirez, S.I., Mateus, J., Jennifer, M., Moderbacher, C.R., Rawlings, S.A., Sutherland, A., Premkumar, L., Jadi, R.S., et al. (2020a). Targets of T cell responses to SARS-CoV-2 coronavirus in humans with COVID-19 disease and unexposed individuals. Cell.

Grifoni, A., Sidney, J., Zhang, Y., Scheuermann, R.H., Peters, B., and Sette, A. (2020b). A Sequence Homology and Bioinformatic Approach Can Predict Candidate Targets for Immune Responses to SARS-CoV-2. Cell Host and Microbe.

Grifoni, A., Sidney, J., Vita, R., Peters, B., Crotty, S., Weiskopf, D., and Sette, A. (2021). SARS-CoV-2 Human T cell Epitopes: adaptive immune response against COVID-19. Cell Host & Microbe.

Gruber, C.N., Patel, R.S., Trachtman, R., Lepow, L., Amanat, F., Krammer, F., Wilson, K.M., Onel, K., Geanon, D., Tuballes, K., et al. (2020). Mapping Systemic Inflammation and Antibody Responses in Multisystem Inflammatory Syndrome in Children (MIS-C). Cell *183*, 982-995.e14.

Guan, Y., Zheng, B.J., He, Y.Q., Liu, X.L., Zhuang, Z.X., Cheung, C.L., Luo, S.W., Li, P.H., Zhang, L.J., Guan, Y.J., et al. (2003). Isolation and characterization of viruses related to the SARS coronavirus from animals in southern China. Science (New York, N.Y.) *302*, 276–278.

Guo, Y.-R., Cao, Q.-D., Hong, Z.-S., Tan, Y.-Y., Chen, S.-D., Jin, H.-J., Tan, K.-S., Wang, D.-Y., and Yan, Y. (2020). The origin, transmission and clinical therapies on coronavirus disease 2019 (COVID-19) outbreak – an update on the status. Military Medical Research *7*, 11.

Gupta, R.K. (2021). Will SARS-CoV-2 variants of concern affect the promise of vaccines? Nature Reviews Immunology *21*, 340–341.

Hadjadj, J., Yatim, N., Barnabei, L., Corneau, A., Boussier, J., Smith, N., Péré, H., Charbit, B., Bondet, V., Chenevier-Gobeaux, C., et al. (2020). Impaired type I interferon activity and inflammatory responses in severe COVID-19 patients. Science *369*, 718–724.

Hamelin, D.J., Fournelle, D., Grenier, J.-C., Schockaert, J., Kovalchik, K., Kubiniok, P., Mostefai, F., Duquette, J.D., Saab, F., Sirois, I., et al. (2021). The mutational landscape of SARS-CoV-2 variants diversifies T cell targets in an HLA supertype-dependent manner. BioRxiv 2021.06.03.446959.

Hammarlund, E., Lewis, M.W., Hansen, S.G., Strelow, L.I., Nelson, J.A., Sexton, G.J., Hanifin, J.M., and Slifka, M.K. (2003). Duration of antiviral immunity after smallpox vaccination. Nature Medicine *9*, 1131–1137.

Hangartner, L., Zinkernagel, R.M., and Hengartner, H. (2006). Antiviral antibody responses: the two extremes of a wide spectrum. Nature Reviews Immunology *6*, 231–243.

Hansen, T.H., and Bouvier, M. (2009). MHC class i antigen presentation: Learning from viral evasion strategies. Nature Reviews Immunology.

Hashimoto-Tane, A., Yokosuka, T., Sakata-Sogawa, K., Sakuma, M., Ishihara, C., Tokunaga, M., and Saito, T. (2011). Dynein-Driven Transport of T Cell Receptor Microclusters Regulates Immune Synapse Formation and T Cell Activation. Immunity *34*, 919–931.

He, X., Lau, E.H.Y., Wu, P., Deng, X., Wang, J., Hao, X., Lau, Y.C., Wong, J.Y., Guan, Y., Tan, X., et al. (2020). Temporal dynamics in viral shedding and transmissibility of COVID-19. Nature Medicine *26*, 672–675.

Henderson, L.A., and Yeung, R.S.M. (2021). MIS-C: early lessons from immune profiling. Nature Reviews Rheumatology *17*, 75–76.

Hijawi, B., Abdallat, M., Sayaydeh, A., Alqasrawi, S., Haddadin, A., Jaarour, N., Alsheikh, S., and Alsanouri, T. (2013). Novel coronavirus infections in Jordan, April 2012: epidemiological findings from a retrospective investigation. Eastern Mediterranean Health Journal *19 Suppl 1*, S12-8.

Hikmet, F., Méar, L., Edvinsson, Å., Micke, P., Uhlén, M., and Lindskog, C. (2020). The protein expression profile of ACE2 in human tissues. Molecular Systems Biology *16*.

Hoffmann, M., Kleine-Weber, H., Schroeder, S., Krüger, N., Herrler, T., Erichsen, S., Schiergens, T.S., Herrler, G., Wu, N.H., Nitsche, A., et al. (2020). SARS-CoV-2 Cell Entry Depends on ACE2 and TMPRSS2 and Is Blocked by a Clinically Proven Protease Inhibitor. Cell *181*, 271-280.e8.

Hoffmann, M., Arora, P., Groß, R., Seidel, A., Hörnich, B.F., Hahn, A.S., Krüger, N., Graichen, L., Hofmann-Winkler, H., Kempf, A., et al. (2021). SARS-CoV-2 variants B.1.351 and P.1 escape from neutralizing antibodies. Cell *184*, 2384-2393.e12.

Hu, B., Guo, H., Zhou, P., and Shi, Z.L. (2020). Characteristics of SARS-CoV-2 and COVID-19. Nature Reviews Microbiology.

Huang, C., Wang, Y., Li, X., Ren, L., Zhao, J., Hu, Y., Zhang, L., Fan, G., Xu, J., Gu, X., et al. (2020). Clinical features of patients infected with 2019 novel coronavirus in Wuhan, China. The Lancet *395*, 497–506.

Huang, C., Huang, L., Wang, Y., Li, X., Ren, L., Gu, X., Kang, L., Guo, L., Liu, M., Zhou, X., et al. (2021). 6-month consequences of COVID-19 in patients discharged from hospital: a cohort study. The Lancet *397*, 220–232.

Irmler, M., Hertig, S., MacDonald, H.R., Sadoul, R., Becherer, J.D., Proudfoot, A., Solari, R., and Tschopp, J. (1995). Granzyme A is an interleukin 1 beta-converting enzyme. Journal of Experimental Medicine *181*, 1917–1922.

Ivanov, K.A., Thiel, V., Dobbe, J.C., van der Meer, Y., Snijder, E.J., and Ziebuhr, J. (2004). Multiple Enzymatic Activities Associated with Severe Acute Respiratory Syndrome Coronavirus Helicase. Journal of Virology *78*, 5619–5632.

Iwasaki, A., and Medzhitov, R. (2015). Control of adaptive immunity by the innate immune system. Nature Immunology *16*, 343–353.

Joeckel, L.T., Wallich, R., Martin, P., Sanchez-Martinez, D., Weber, F.C., Martin, S.F., Borner, C., Pardo, J., Froelich, C., and Simon, M.M. (2011). Mouse granzyme K has pro-inflammatory potential. Cell Death & Differentiation *18*, 1112–1119.

Joffre, O.P., Segura, E., Savina, A., and Amigorena, S. (2012). Cross-presentation by dendritic cells. Nature Reviews Immunology *12*, 557–569.

Kaech, S.M., and Cui, W. (2012). Transcriptional control of effector and memory CD8+ T cell differentiation. Nature Reviews Immunology *12*, 749–761.

Kaiserman, D., Bird, C.H., Sun, J., Matthews, A., Ung, K., Whisstock, J.C., Thompson, P.E., Trapani, J.A., and Bird, P.I. (2006). The major human and mouse granzymes are structurally and functionally divergent. Journal of Cell Biology *175*, 619–630.

Kany, S., Vollrath, J.T., and Relja, B. (2019). Cytokines in Inflammatory Disease. International Journal of Molecular Sciences *20*, 6008.

Kato, H., Takeuchi, O., Sato, S., Yoneyama, M., Yamamoto, M., Matsui, K., Uematsu, S., Jung, A., Kawai, T., Ishii, K.J., et al. (2006). Differential roles of MDA5 and RIG-I helicases in the recognition of RNA viruses. Nature *441*, 101–105.

Kawai, T., and Akira, S. (2010). The role of pattern-recognition receptors in innate immunity: update on Toll-like receptors. Nature Immunology *11*, 373–384.

Kelleher, A.D., Long, C., Holmes, E.C., Allen, R.L., Wilson, J., Conlon, C., Workman, C., Shaunak, S., Olson, K., Goulder, P., et al. (2001). Clustered Mutations in HIV-1 Gag Are Consistently Required for Escape from Hla-B27–Restricted Cytotoxic T Lymphocyte Responses. Journal of Experimental Medicine *193*, 375–386.

Kelly, A., Powis, S.H., Kerr, L.-A., Mockridge, I., Elliott, T., Bastin, J., Uchanska-Ziegler, B., Ziegler, A., Trowsdale, J., and Townsend, A. (1992). Assembly and function of the two ABC transporter proteins encoded in the human major histocompatibility complex. Nature *355*, 641–644.

Kemp, S.A., Collier, D.A., Datir, R.P., Ferreira, I.A.T.M., Gayed, S., Jahun, A., Hosmillo, M., Rees-Spear, C., Mlcochova, P., Lumb, I.U., et al. (2021). SARS-CoV-2 evolution during treatment of chronic infection. Nature *592*.

Kessler, D.S., Levy, D.E., and Darnell, J.E. (1988). Two interferon-induced nuclear factors bind a single promoter element in interferon-stimulated genes. Proceedings of the National Academy of Sciences *85*, 8521–8525.

Kim, D., Lee, J.-Y., Yang, J.-S., Kim, J.W., Kim, V.N., and Chang, H. (2020). The Architecture of SARS-CoV-2 Transcriptome. Cell *181*, 914-921.e10.

Kindred, B., and Shreffler, D.C. (1972). H-2 dependence of co-operation between T and B cells in vivo. Journal of Immunology (Baltimore, Md. : 1950) *109*, 940–943.

Klenerman, P., Rowland-Jones, S., McAdam, S., Edwards, J., Daenke, S., Lalloo, D., Köppe, B., Rosenberg, W., Boyd, D., Edwards, A., et al. (1994). Cytotoxic T-cell activity antagonized by naturally occurring HIV-1 Gag variants. Nature *369*, 403–407.

Knoops, K., Kikkert, M., Worm, S.H.E. van den, Zevenhoven-Dobbe, J.C., van der Meer, Y., Koster, A.J., Mommaas, A.M., and Snijder, E.J. (2008). SARS-Coronavirus Replication Is Supported by a Reticulovesicular Network of Modified Endoplasmic Reticulum. PLoS Biology *6*, e226.

Konno, Y., Kimura, I., Uriu, K., Fukushi, M., Irie, T., Koyanagi, Y., Sauter, D., Gifford, R.J., Nakagawa, S., and Sato, K. (2020). SARS-CoV-2 ORF3b Is a Potent Interferon Antagonist Whose Activity Is Increased by a Naturally Occurring Elongation Variant. Cell Reports *32*, 108185.

Kopecky-Bromberg, S.A., Martínez-Sobrido, L., Frieman, M., Baric, R.A., and Palese, P. (2007). Severe Acute Respiratory Syndrome Coronavirus Open Reading Frame (ORF) 3b, ORF 6, and Nucleocapsid Proteins Function as Interferon Antagonists. Journal of Virology *81*, 548–557.

Krammer, F. (2020). SARS-CoV-2 vaccines in development. Nature *586*, 516–527.

Krummel, M.F., Bartumeus, F., and Gérard, A. (2016). T cell migration, search strategies and mechanisms. Nature Reviews Immunology *16*, 193–201.

Ksiazek, T.G., Erdman, D., Goldsmith, C.S., Zaki, S.R., Peret, T., Emery, S., Tong, S., Urbani, C., Comer, J.A., Lim, W., et al. (2003). A Novel Coronavirus Associated with Severe Acute Respiratory Syndrome. New England Journal of Medicine *348*, 1953–1966.

Kubota, R., Soldan, S.S., Martin, R., and Jacobson, S. (2000). An Altered Peptide Ligand Antagonizes Antigen-Specific T Cells of Patients with Human T Lymphotropic Virus Type I-Associated Neurological Disease. The Journal of Immunology *164*, 5192–5198.

de La Roche, M., Asano, Y., and Griffiths, G.M. (2016). Origins of the cytolytic synapse. Nature Reviews Immunology *16*, 421–432.

Lau, S.K.P., Woo, P.C.Y., Li, K.S.M., Huang, Y., Tsoi, H.-W., Wong, B.H.L., Wong, S.S.Y., Leung, S.-Y., Chan, K.-H., and Yuen, K.-Y. (2005). Severe acute respiratory syndrome coronavirus-like virus in Chinese horseshoe bats. Proceedings of the National Academy of Sciences of the United States of America *102*, 14040–14045.

Lauring, A.S., and Andino, R. (2010). Quasispecies theory and the behavior of RNA viruses. PLoS Pathogens *6*, 1–8.

Lei, X., Dong, X., Ma, R., Wang, W., Xiao, X., Tian, Z., Wang, C., Wang, Y., Li, L., Ren, L., et al. (2020). Activation and evasion of type I interferon responses by SARS-CoV-2. Nature Communications *11*, 1–12.

Letko, M., Marzi, A., and Munster, V. (2020). Functional assessment of cell entry and receptor usage for SARS-CoV-2 and other lineage B betacoronaviruses. Nature Microbiology *5*, 562–569.

Li, F. (2016). Structure, Function, and Evolution of Coronavirus Spike Proteins. Annual Review of Virology *3*, 237–261.

Li, Q., Nie, J., Wu, J., Zhang, L., Ding, R., Wang, H., Zhang, Y., Li, T., Liu, S., Zhang, M., et al. (2021). SARS-CoV-2 501Y.V2 variants lack higher infectivity but do have immune escape. Cell 1–10.

Li, R., Pei, S., Chen, B., Song, Y., Zhang, T., Yang, W., and Shaman, J. (2020). Substantial undocumented infection facilitates the rapid dissemination of novel coronavirus (SARS-CoV-2). Science *368*, 489–493.

Li, W., Shi, Z., Yu, M., Ren, W., Smith, C., Epstein, J.H., Wang, H., Crameri, G., Hu, Z., Zhang, H., et al. (2005). Bats are natural reservoirs of SARS-like coronaviruses. Science *310*, 676–679.

Liu, D.X., Fung, T.S., Chong, K.K.L., Shukla, A., and Hilgenfeld, R. (2014). Accessory proteins of SARS-CoV and other coronaviruses. Antiviral Research *109*, 97–109.

Liu, G., Lee, J.-H., Parker, Z.M., Acharya, D., Chiang, J.J., van Gent, M., Riedl, W., Davis-Gardner, M.E., Wies, E., Chiang, C., et al. (2021). ISG15-dependent activation of the sensor MDA5 is antagonized by the SARS-CoV-2 papain-like protease to evade host innate immunity. Nature Microbiology.

Liu, Z., VanBlargan, L.A., Rothlauf, P.W., Bloyet, L.-M., Chen, R.E., Stumpf, S., Zhao, H., Errico, J.M., Theel, E.S., Ellebedy, A., et al. (2020). Landscape Analysis of Escape Variants Identifies SARS-CoV-2 Spike Mutations that Attenuate Monoclonal and Serum Antibody Neutralization. SSRN Electronic Journal.

Lokugamage, K.G., Hage, A., de Vries, M., Valero-Jimenez, A.M., Schindewolf, C., Dittmann, M., Rajsbaum, R., and Menachery, V.D. (2020). Type I Interferon Susceptibility Distinguishes SARS-CoV-2 from SARS-CoV. Journal of Virology *94*.

Long, Q.-X., Liu, B.-Z., Deng, H.-J., Wu, G.-C., Deng, K., Chen, Y.-K., Liao, P., Qiu, J.-F., Lin, Y., Cai, X.-F., et al. (2020). Antibody responses to SARS-CoV-2 in patients with COVID-19. Nature Medicine *26*, 845–848.

Lostroh, P. (2019). Molecular and Cellular Biology of Viruses. In Molecular and Cellular Biology of Viruses, (Elsevier), pp. 11–13.

Lucas, C., Wong, P., Klein, J., Castro, T.B.R., Silva, J., Sundaram, M., Ellingson, M.K., Mao, T., Oh, J.E., Israelow, B., et al. (2020a). Longitudinal analyses reveal immunological misfiring in severe COVID-19. Nature *584*, 463–469.

Lucas, C., Wong, P., Klein, J., Castro, T.B.R., Silva, J., Sundaram, M., Ellingson, M.K., Mao, T., Oh, J.E., Israelow, B., et al. (2020b). Longitudinal analyses reveal immunological misfiring in severe COVID-19. Nature *584*, 463–469.

Mantlo, E., Bukreyeva, N., Maruyama, J., Paessler, S., and Huang, C. (2020). Antiviral activities of type I interferons to SARS-CoV-2 infection. Antiviral Research *179*, 104811.

Marra, M.A., Jones, S.J.M., Astell, C.R., Holt, R.A., Brooks-wilson, A., Butterfield, Y.S.N., Khattra, J., Asano, J.K., Barber, S.A., Chan, S.Y., et al. (2003). The Genome Sequence of the SARS-Associated Coronavirus. *300*, 1399–1405.

Martin, D.P., Weaver, S., Tegally, H., San, E.J., Shank, S.D., Wilkinson, E., Giandhari, J., Naidoo, S., Pillay, Y., Singh, L., et al. (2021). The emergence and ongoing convergent evolution of the N501Y lineages coincides with a major global shift in the SARS-CoV-2 selective landscape. MedRxiv 2021.02.23.21252268.

Mathew, D., Giles, J.R., Baxter, A.E., Oldridge, D.A., Greenplate, A.R., Wu, J.E., Alanio, C., Kuri-Cervantes, L., Pampena, M.B., D'Andrea, K., et al. (2020). Deep immune profiling of COVID-19 patients reveals distinct immunotypes with therapeutic implications. Science *369*, eabc8511.

McCarthy, K.R., Rennick, L.J., Nambulli, S., Robinson-McCarthy, L.R., Bain, W.G., Haidar, G., and Duprex, W.P. (2021). Recurrent deletions in the SARS-CoV-2 spike glycoprotein drive antibody escape. Science *371*, 1139–1142.

McMahan, K., Yu, J., Mercado, N.B., Loos, C., Tostanoski, L.H., Chandrashekar, A., Liu, J., Peter, L., Atyeo, C., Zhu, A., et al. (2020). Correlates of protection against SARS-CoV-2 in rhesus macaques. Nature.

McNab, F., Mayer-Barber, K., Sher, A., Wack, A., and O'Garra, A. (2015). Type I interferons in infectious disease. Nature Reviews Immunology *15*, 87–103.

Meng, B., Kemp, S.A., Papa, G., Datir, R., Ferreira, I.A.T.M., Marelli, S., Harvey, W.T., Lytras, S., Mohamed, A., Gallo, G., et al. (2021). Recurrent emergence of SARS-CoV-2 spike deletion H69/V70 and its role in the Alpha variant B.1.1.7. Cell Reports *35*, 109292.

Merad, M., and Vabret, N. (2021). Highlights from a year in a pandemic. Journal of Experimental Medicine *218*.

Metkar, S.S., Wang, B., Aguilar-Santelises, M., Raja, S.M., Uhlin-Hansen, L., Podack, E., Trapani, J.A., and Froelich, C.J. (2002). Cytotoxic Cell Granule-Mediated Apoptosis. Immunity *16*, 417–428.

Metkar, S.S., Menaa, C., Pardo, J., Wang, B., Wallich, R., Freudenberg, M., Kim, S., Raja, S.M., Shi, L., Simon, M.M., et al. (2008). Human and Mouse Granzyme A Induce a Proinflammatory Cytokine Response. Immunity *29*, 720–733.

Mogilenko, D.A., Shpynov, O., Andhey, P.S., Arthur, L., Swain, A., Esaulova, E., Brioschi, S., Shchukina, I., Kerndl, M., Bambouskova, M., et al. (2021). Comprehensive Profiling of an Aging Immune System Reveals Clonal GZMK+ CD8+ T Cells as Conserved Hallmark of Inflammaging. Immunity *54*, 99-115.e12.

Monks, C.R.F., Freiberg, B.A., Kupfer, H., Sciaky, N., and Kupfer, A. (1998). Three-dimensional segregation of supramolecular activation clusters in T cells. Nature *395*, 82–86.

Mosmann, T.R., Cherwinski, H., Bond, M.W., Giedlin, M.A., and Coffman, R.L. (1986). Two types of murine helper T cell clone. I. Definition according to profiles of lymphokine activities and secreted proteins. Journal of Immunology (Baltimore, Md. : 1950) *136*, 2348–2357.

Muik, A., Wallisch, A.-K., Sänger, B., Swanson, K.A., Mühl, J., Chen, W., Cai, H., Maurus, D., Sarkar, R., Türeci, Ö., et al. (2021). Neutralization of SARS-CoV-2 lineage B.1.1.7 pseudovirus by BNT162b2 vaccine–elicited human sera. Science *371*, 1152–1153.

Müller, M.A., Corman, V.M., Jores, J., Meyer, B., Younan, M., Liljander, A., Bosch, B.-J., Lattwein, E., Hilali, M., Musa, B.E., et al. (2014). MERS coronavirus neutralizing antibodies in camels, Eastern Africa, 1983-1997. Emerging Infectious Diseases *20*, 2093–2095.

Nalbandian, A., Sehgal, K., Gupta, A., Madhavan, M. V., McGroder, C., Stevens, J.S., Cook, J.R., Nordvig, A.S., Shalev, D., Sehrawat, T.S., et al. (2021). Post-acute COVID-19 syndrome. Nature Medicine *27*, 601–615.

Neefjes, J., Jongsma, M.L.M., Paul, P., and Bakke, O. (2011). Towards a systems understanding of MHC class i and MHC class II antigen presentation. Nature Reviews Immunology *11*, 823–836.

Nelde, A., Bilich, T., Heitmann, J.S., Maringer, Y., Salih, H.R., Roerden, M., Lübke, M., Bauer, J., Rieth, J., Wacker, M., et al. (2020). SARS-CoV-2-derived peptides define heterologous and COVID-19-induced T cell recognition. Nature Immunology.

Ng, D., Maître, B., Cummings, D., Lin, A., Ward, L.A., Rahbar, R., Mossman, K.L., Ohashi, P.S., and Gommerman, J.L. (2015). A Lymphotoxin/Type I IFN Axis Programs CD8 + T Cells To Infiltrate a Self-Tissue and Propagate Immunopathology. The Journal of Immunology *195*, 4650–4659.

Nikolich-Žugich, J., Slifka, M.K., and Messaoudi, I. (2004). The many important facets of T-cell repertoire diversity. Nature Reviews Immunology *4*, 123–132.

Peiris, J., Lai, S., Poon, L., Guan, Y., Yam, L., Lim, W., Nicholls, J., Yee, W., Yan, W., Cheung, M., et al. (2003). Coronavirus as a possible cause of severe acute respiratory syndrome. The Lancet *361*, 1319–1325.

Peiris, J.S.M., Guan, Y., and Yuen, K.Y. (2004). Severe acute respiratory syndrome. Nature Medicine *10*, S88–S97.

Peng, Y., Mentzer, A.J., Liu, G., Yao, X., Yin, Z., Dong, D., Dejnirattisai, W., Rostron, T., Supasa, P., Liu, C., et al. (2020). Broad and strong memory CD4+ and CD8+ T cells induced by SARS-CoV-2 in UK convalescent individuals following COVID-19. Nature Immunology *21*.

Perlman, S., and Netland, J. (2009). Coronaviruses post-SARS: Update on replication and pathogenesis. Nature Reviews Microbiology *7*, 439–450.

Piccoli, L., Park, Y.-J., Tortorici, M.A., Czudnochowski, N., Walls, A.C., Beltramello, M., Silacci-Fregni, C., Pinto, D., Rosen, L.E., Bowen, J.E., et al. (2020). Mapping Neutralizing and

Immunodominant Sites on the SARS-CoV-2 Spike Receptor-Binding Domain by Structure-Guided High-Resolution Serology. Cell *183*, 1024-1042.e21.

PichImair, A., Schulz, O., Tan, C.P., Näslund, T.I., Liljeström, P., Weber, F., and Reis e Sousa, C. (2006). RIG-I-mediated antiviral responses to single-stranded RNA bearing 5'-phosphates. Science (New York, N.Y.) *314*, 997–1001.

Pircher, H., Moskophidis, D., Rohrer, U., Burki, K., Hengartner, H., and Zinkernagel, R.M. (1990). Viral escape by selection of cytotoxic T cell-resistant virus variants in vivo. Nature *346*, 629–633.

Popa, A., Genger, J.-W., NIcholson, M., Penz, T., Schmid, D., Aberle, S.W., Agerer, B., Lercher, A., Endler, L., Colaço, H., et al. (2020). Genomic epidemiology of superspreading events reveals mutational dynamics and transmission properties of SARS-CoV-2. Science Translational Medicine.

Poran, A., Harjanto, D., Malloy, M., Arieta, C.M., Rothenberg, D.A., Lenkala, D., van Buuren, M.M., Addona, T.A., Rooney, M.S., Srinivasan, L., et al. (2020). Sequence-based prediction of SARS-CoV-2 vaccine targets using a mass spectrometry-based bioinformatics predictor identifies immunogenic T cell epitopes. Genome Medicine.

Pretti, M.A.M., Galvani, R.G., Farias, A.S., and Boroni, M. (2021). New SARS-CoV-2 lineages could evade CD8+ T-cells response. BioRxiv 2021.03.09.434584.

Price, D.A., Asher, T.E., Wilson, N.A., Nason, M.C., Brenchley, J.M., Metzler, I.S., Venturi, V., Gostick, E., Chattopadhyay, P.K., Roederer, M., et al. (2009). Public clonotype usage identifies protective Gag-specific CD8+ T cell responses in SIV infection. Journal of Experimental Medicine *206*, 923–936.

Qiu, C., Xiao, C., Wang, Z., Chen, X., Gao, L., Deng, J., Su, J., Su, H., Fang, E.F., Zhang, Z.-J., et al. (2021). CD8+ T cell epitope variations suggest a potential antigen presentation deficiency for spike protein of SARS-CoV-2. BioRxiv 2021.01.22.427863.

Quann, E.J., Merino, E., Furuta, T., and Huse, M. (2009). Localized diacylglycerol drives the polarization of the microtubule-organizing center in T cells. Nature Immunology *10*, 627–635.

Quann, E.J., Liu, X., Altan-Bonnet, G., and Huse, M. (2011). A cascade of protein kinase C isozymes promotes cytoskeletal polarization in T cells. Nature Immunology *12*, 647–654.

Radbruch, A., Muehlinghaus, G., Luger, E.O., Inamine, A., Smith, K.G.C., Dörner, T., and Hiepe, F. (2006). Competence and competition: the challenge of becoming a long-lived plasma cell. Nature Reviews Immunology *6*, 741–750.

Rammensee, H.-G., Falk, K., and Rötzschke, O. (1993). MHC molecules as peptide receptors. Current Opinion in Immunology *5*, 35–44.

Redd, A.D., Nardin, A., Kared, H., Bloch, E.M., Pekosz, A., Laeyendecker, O., Abel, B., Fehlings, M., Quinn, T.C., and Tobian, A.A.R. (2021). CD8+ T cell responses in COVID-19 convalescent individuals target conserved epitopes from multiple prominent SARS-CoV-2 circulating variants. Open Forum Infectious Diseases.

Rescigno, M., Granucci, F., and Ricciardi-Castagnoli, P. (2000). Molecular events of bacterial-induced maturation of dendritic cells. Journal of Clinical Immunology *20*, 161–166.

Reusken, C.B., Haagmans, B.L., Müller, M.A., Gutierrez, C., Godeke, G.-J., Meyer, B., Muth, D., Raj, V.S., Vries, L.S.-D., Corman, V.M., et al. (2013). Middle East respiratory syndrome coronavirus neutralising serum antibodies in dromedary camels: a comparative serological study. The Lancet Infectious Diseases *13*, 859–866.

Ribes, M., Chaccour, C., and Moncunill, G. (2021). Adapt or perish: SARS-CoV-2 antibody escape variants defined by deletions in the Spike N-terminal Domain. Signal Transduction and Targeted Therapy *6*, 164.

Riou, C., Keeton, R., Moyo-Gwete, T., Hermanus, T., Kgagudi, P., Baguma, R., Tegally, H., Doolabh, D., Iranzadeh, A., Tyers, L., et al. (2021). Loss of recognition of SARS-CoV-2 B.1.351 variant spike epitopes but overall preservation of T cell immunity. MedRxiv 2021.06.03.21258307.

Rock, K.L., Gramm, C., Rothstein, L., Clark, K., Stein, R., Dick, L., Hwang, D., and Goldberg, A.L. (1994). Inhibitors of the proteasome block the degradation of most cell proteins and the generation of peptides presented on MHC class I molecules. Cell *78*, 761–771.

Rydyznski Moderbacher, C., Ramirez, S.I., Dan, J.M., Grifoni, A., Hastie, K.M., Weiskopf, D., Belanger, S., Abbott, R.K., Kim, C., Choi, J., et al. (2020). Antigen-Specific Adaptive Immunity to SARS-CoV-2 in Acute COVID-19 and Associations with Age and Disease Severity. Cell 19–21.

Sallusto, F., and Lanzavecchia, A. (2000). Understanding dendritic cell and T-lymphocyte traffic through the analysis of chemokine receptor expression. Immunological Reviews *177*, 134–140.

Sawicki, S.G., and Sawicki, D.L. (1995). Coronaviruses use Discontinuous Extension for Synthesis of Subgenome-Length Negative Strands. pp. 499–506.

Schoggins, J.W., Wilson, S.J., Panis, M., Murphy, M.Y., Jones, C.T., Bieniasz, P., and Rice, C.M. (2011). A diverse range of gene products are effectors of the type i interferon antiviral response. Nature *472*, 481–485.

Schroder, K., and Tschopp, J. (2010). The Inflammasomes. Cell *140*, 821–832.

Schubert, K., Karousis, E.D., Jomaa, A., Scaiola, A., Echeverria, B., Gurzeler, L.-A., Leibundgut, M., Thiel, V., Mühlemann, O., and Ban, N. (2020). SARS-CoV-2 Nsp1 binds the ribosomal mRNA channel to inhibit translation. Nature Structural & Molecular Biology *27*, 959–966.

Schulien, I., Kemming, J., Oberhardt, V., Wild, K., Seidel, L.M., Killmer, S., Sagar, Daul, F., Salvat Lago, M., Decker, A., et al. (2020). Characterization of pre-existing and induced SARS-CoV-2-specific CD8+ T cells. Nature Medicine.

Sekine, T., Perez-Potti, A., Rivera-Ballesteros, O., Strålin, K., Gorin, J.-B., Olsson, A., Llewellyn-Lacey, S., Kamal, H., Bogdanovic, G., Muschiol, S., et al. (2020). Robust T cell immunity in convalescent individuals with asymptomatic or mild COVID-19. Cell.

Sette, A., and Crotty, S. (2021). Adaptive immunity to SARS-CoV-2 and COVID-19. Cell.

Shang, J., Wan, Y., Luo, C., Ye, G., Geng, Q., Auerbach, A., and Li, F. (2020). Cell entry mechanisms of SARS-CoV-2. Proceedings of the National Academy of Sciences of the United States of America *117*.

Shomuradova, A.S., Vagida, M.S., Sheetikov, S.A., Zornikova, K. v, Kiryukhin, D., Titov, A., Peshkova, I.O., Khmelevskaya, A., Dianov, D. v, Malasheva, M., et al. (2020). SARS-CoV-2 Epitopes Are Recognized by a Public and Diverse Repertoire of Human T Cell Receptors. Immunity *53*, 1245-1257.e5.

Shu, Y., and McCauley, J. (2017). GISAID: Global initiative on sharing all influenza data – from vision to reality. Eurosurveillance *22*.

de Silva, T.I., Liu, G., Lindsey, B.B., Dong, D., Shah, D., Mentzer, A.J., Angyal, A., Brown, R., Parker, M.D., Yin, Z., et al. (2021). The Impact of Viral Mutations on Recognition by SARS-CoV-2 Specific T-Cells. SSRN Electronic Journal.

Silvin, A., Chapuis, N., Dunsmore, G., Goubet, A.-G., Dubuisson, A., Derosa, L., Almire, C., Hénon, C., Kosmider, O., Droin, N., et al. (2020). Elevated Calprotectin and Abnormal Myeloid Cell Subsets Discriminate Severe from Mild COVID-19. Cell *182*, 1401-1418.e18.

Slifka, M.K., and Whitton, J.L. (2000). Antigen-Specific Regulation of T Cell–Mediated Cytokine Production. Immunity *12*, 451–457.

Smyth, M., Khamina, K., Popa, A., Gudipati, V., Agerer, B., Lercher, A., Kosack, L., Endler, L., Baazim, H., Viczenczova, C., et al. (2021). Characterization of CD8 T Cell-Mediated Mutations in the Immunodominant Epitope GP33-41 of Lymphocytic Choriomeningitis Virus. Frontiers in Immunology *12*, 1–11.

Snijder, E.J., Decroly, E., and Ziebuhr, J. (2016). The Nonstructural Proteins Directing Coronavirus RNA Synthesis and Processing. pp. 59–126.

Soiza, R.L., Scicluna, C., and Thomson, E.C. (2021). Efficacy and safety of COVID-19 vaccines in older people. Age and Ageing *50*, 279–283.

Sudre, C.H., Murray, B., Varsavsky, T., Graham, M.S., Penfold, R.S., Bowyer, R.C., Pujol, J.C., Klaser, K., Antonelli, M., Canas, L.S., et al. (2021). Attributes and predictors of long COVID. Nature Medicine *27*.

Summers deLuca, L., Ng, D., Gao, Y., Wortzman, M.E., Watts, T.H., and Gommerman, J.L. (2011). LTβR signaling in dendritic cells induces a type I IFN response that is required for optimal clonal expansion of CD8 + T cells. Proceedings of the National Academy of Sciences *108*, 2046–2051.

Sun, L., Wu, J., Du, F., Chen, X., and Chen, Z.J. (2013). Cyclic GMP-AMP Synthase Is a Cytosolic DNA Sensor That Activates the Type I Interferon Pathway. Science *339*, 786–791.

Sun, X., Shi, Y., Akahoshi, T., Fujiwara, M., Gatanaga, H., Schönbach, C., Kuse, N., Appay, V., Gao, G.F., Oka, S., et al. (2016). Effects of a Single Escape Mutation on T Cell and HIV-1 Co-adaptation. Cell Reports *15*, 2279–2291.

Suthar, M.S., Zimmerman, M.G., Kauffman, R.C., Mantus, G., Linderman, S.L., Hudson, W.H., Vanderheiden, A., Nyhoff, L., Davis, C.W., Adekunle, O., et al. (2020). Rapid Generation of Neutralizing Antibody Responses in COVID-19 Patients. Cell Reports Medicine *1*, 100040.

Sutton, V.R., and Trapani, J.A. (2010). Proteases in lymphocyte killer function: redundancy, polymorphism and questions remaining. Biological Chemistry *391*.

Takeuchi, O., and Akira, S. (2010). Pattern Recognition Receptors and Inflammation. Cell *140*, 805–820.

Tan, A.T., Linster, M., Tan, C.W., le Bert, N., Chia, W.N., Kunasegaran, K., Zhuang, Y., Tham, C.Y.L., Chia, A., Smith, G.J.D., et al. (2021). Early induction of functional SARS-CoV-2-specific T cells associates with rapid viral clearance and mild disease in COVID-19 patients. Cell Reports *34*, 108728.

Tarke, A., Sidney, J., Kidd, C.K., Dan, J.M., Ramirez, S.I., Yu, E.D., Mateus, J., da Silva Antunes, R., Moore, E., Rubiro, P., et al. (2021a). Comprehensive analysis of T cell immunodominance and immunoprevalence of SARS-CoV-2 epitopes in COVID-19 cases. Cell Reports Medicine 100204.

Tarke, A., Sidney, J., Methot, N., Zhang, Y., Dan, J.M., Goodwin, B., Rubiro, P., Sutherland, A., da Silva Antunes, R., Frazier, A., et al. (2021b). Negligible impact of SARS-CoV-2 variants on CD4+ and CD8+ T cell reactivity in COVID-19 exposed donors and vaccinees. BioRxiv 2021.02.27.433180.

Tegally, H., Wilkinson, E., Giovanetti, M., Iranzadeh, A., Fonseca, V., Giandhari, J., Doolabh, D., Pillay, S., San, E.J., Msomi, N., et al. (2021). Detection of a SARS-CoV-2 variant of concern in South Africa. Nature *592*, 438–443.

Thiery, J., Keefe, D., Saffarian, S., Martinvalet, D., Walch, M., Boucrot, E., Kirchhausen, T., and Lieberman, J. (2010). Perforin activates clathrin- and dynamin-dependent endocytosis, which is required for plasma membrane repair and delivery of granzyme B for granzyme-mediated apoptosis. Blood *115*, 1582–1593.

Thoms, M., Buschauer, R., Ameismeier, M., Koepke, L., Denk, T., Hirschenberger, M., Kratzat, H., Hayn, M., Mackens-Kiani, T., Cheng, J., et al. (2020). Structural basis for translational shutdown and immune evasion by the Nsp1 protein of SARS-CoV-2. Science *369*, 1249–1255.

Timm, J., and Walker, C.M. (2015). Mutational escape of CD8+ T cell epitopes: implications for prevention and therapy of persistent hepatitis virus infections. Medical Microbiology and Immunology *204*, 29–38.

Timm, J., Lauer, G.M., Kavanagh, D.G., Sheridan, I., Kim, A.Y., Lucas, M., Pillay, T., Ouchi, K., Reyor, L.L., zur Wiesch, J.S., et al. (2004). CD8 Epitope Escape and Reversion in Acute HCV Infection. Journal of Experimental Medicine *200*, 1593–1604.

To, K.K.-W., Tsang, O.T.-Y., Leung, W.-S., Tam, A.R., Wu, T.-C., Lung, D.C., Yip, C.C.-Y., Cai, J.-P., Chan, J.M.-C., Chik, T.S.-H., et al. (2020). Temporal profiles of viral load in posterior oropharyngeal saliva samples and serum antibody responses during infection by SARS-CoV-2: an observational cohort study. The Lancet Infectious Diseases *20*, 565–574.

Trowsdale, J. (2005). HLA genomics in the third millennium. Current Opinion in Immunology *17*, 498–504.

Vabret, N., Britton, G.J., Gruber, C., Hegde, S., Kim, J., Kuksin, M., Levantovsky, R., Malle, L., Moreira, A., Park, M.D., et al. (2020). Immunology of COVID-19: Current State of the Science. Immunity *52*, 910–941.

Del Valle, D.M., Kim-Schulze, S., Huang, H.-H., Beckmann, N.D., Nirenberg, S., Wang, B., Lavin, Y., Swartz, T.H., Madduri, D., Stock, A., et al. (2020). An inflammatory cytokine signature predicts COVID-19 severity and survival. Nature Medicine *26*, 1636–1643.

Villa, T.G., Abril, A.G., Sánchez, S., de Miguel, T., and Sánchez-Pérez, A. (2020). Animal and human RNA viruses: genetic variability and ability to overcome vaccines. Archives of Microbiology 443–464.

de Villartay, J.-P., Fischer, A., and Durandy, A. (2003). The mechanisms of immune diversification and their disorders. Nature Reviews Immunology *3*, 962–972.

V'kovski, P., Kratzel, A., Steiner, S., Stalder, H., and Thiel, V. (2020). Coronavirus biology and replication: implications for SARS-CoV-2. Nature Reviews Microbiology.

van Vliet, S.J., Dunnen, J. den, Gringhuis, S.I., Geijtenbeek, T.B., and van Kooyk, Y. (2007). Innate signaling and regulation of Dendritic cell immunity. Current Opinion in Immunology *19*, 435–440.

Voskoboinik, I., Whisstock, J.C., and Trapani, J.A. (2015). Perforin and granzymes: Function, dysfunction and human pathology. Nature Reviews Immunology *15*, 388–400.

Wajnberg, A., Amanat, F., Firpo, A., Altman, D.R., Bailey, M.J., Mansour, M., McMahon, M., Meade, P., Mendu, D.R., Muellers, K., et al. (2020). Robust neutralizing antibodies to SARS-CoV-2 infection persist for months. Science *370*, 1227–1230.

Wall, E.C., Wu, M., Harvey, R., Kelly, G., Warchal, S., Sawyer, C., Daniels, R., Hobson, P., Hatipoglu, E., Ngai, Y., et al. (2021a). Neutralising antibody activity against SARS-CoV-2 VOCs B.1.617.2 and B.1.351 by BNT162b2 vaccination. The Lancet *397*, 2331–2333.

Wall, E.C., Wu, M., Harvey, R., Kelly, G., Warchal, S., Sawyer, C., Daniels, R., Adams, L., Hobson, P., Hatipoglu, E., et al. (2021b). AZD1222-induced neutralising antibody activity against SARS-CoV-2 Delta VOC. The Lancet.

Wang, D., Hu, B., Hu, C., Zhu, F., Liu, X., Zhang, J., Wang, B., Xiang, H., Cheng, Z., Xiong, Y., et al. (2020). Clinical Characteristics of 138 Hospitalized Patients With 2019 Novel Coronavirus–Infected Pneumonia in Wuhan, China. JAMA *323*, 1061.

Wang, P., Nair, M.S., Liu, L., Iketani, S., Luo, Y., Guo, Y., Wang, M., Yu, J., Zhang, B., Kwong, P.D., et al. (2021a). Antibody resistance of SARS-CoV-2 variants B.1.351 and B.1.1.7. Nature *593*, 130–135.

Wang, W., Zhou, Z., Xiao, X., Tian, Z., Dong, X., Wang, C., Li, L., Ren, L., Lei, X., Xiang, Z., et al. (2021b). SARS-CoV-2 nsp12 attenuates type I interferon production by inhibiting IRF3 nuclear translocation. Cellular and Molecular Immunology 1–9.

Watts, C., Zaru, R., Prescott, A.R., Wallin, R.P., and West, M.A. (2007). Proximal effects of Toll-like receptor activation in dendritic cells. Current Opinion in Immunology *19*, 73–78.

Werling, D., and Jungi, T.W. (2003). TOLL-like receptors linking innate and adaptive immune response. Veterinary Immunology and Immunopathology *91*, 1–12.

De Wit, E., Van Doremalen, N., Falzarano, D., and Munster, V.J. (2016). SARS and MERS: Recent insights into emerging coronaviruses. Nature Reviews Microbiology *14*, 523–534.

Wölfel, R., Corman, V.M., Guggemos, W., Seilmaier, M., Zange, S., Müller, M.A., Niemeyer, D., Jones, T.C., Vollmar, P., Rothe, C., et al. (2020). Virological assessment of hospitalized patients with COVID-2019. Nature *581*, 465–469.

Woolhouse, M.E.J., Adair, K., and Brierley, L. (2013). RNA Viruses: A Case Study of the Biology of Emerging Infectious Diseases. Microbiology Spectrum *1*, 83–97.

World Health Organization (2019). MERS Situation Update.

World Health Organization (2020). Coronavirus disease 2019 (COVID-19). Situation report – 51.

Wu, F., Zhao, S., Yu, B., Chen, Y.-M., Wang, W., Song, Z.-G., Hu, Y., Tao, Z.-W., Tian, J.-H., Pei, Y.-Y., et al. (2020). A new coronavirus associated with human respiratory disease in China. Nature *579*, 265–269.

Wu, J., Sun, L., Chen, X., Du, F., Shi, H., Chen, C., and Chen, Z.J. (2013). Cyclic GMP-AMP Is an Endogenous Second Messenger in Innate Immune Signaling by Cytosolic DNA. Science *339*, 826–830.

Xia, H., Cao, Z., Xie, X., Zhang, X., Chen, J.Y.-C., Wang, H., Menachery, V.D., Rajsbaum, R., and Shi, P.-Y. (2020). Evasion of Type I Interferon by SARS-CoV-2. Cell Reports *33*, 108234.

Xie, X., Liu, Y., Liu, J., Zhang, X., Zou, J., Fontes-garfias, C.R., Xia, H., Swanson, K.A., Cutler, M., Cooper, D., et al. (2021). Neutralization of SARS-CoV-2 spike 69 / 70 deletion , E484K and N501Y variants by BNT162b2 vaccine-elicited sera. Nature Medicine.

Yamada, T., Sato, S., Sotoyama, Y., Orba, Y., Sawa, H., Yamauchi, H., Sasaki, M., and Takaoka, A. (2021). RIG-I triggers a signaling-abortive anti-SARS-CoV-2 defense in human lung cells. Nature Immunology.

Yan, N., and Chen, Z.J. (2012). Intrinsic antiviral immunity. Nature Immunology *13*, 214–222.

Yewdell, J.W. (2006). Confronting Complexity: Real-World Immunodominance in Antiviral CD8+ T Cell Responses. Immunity *25*, 533–543.

Yi, J., Wu, X.S., Crites, T., and Hammer, J.A. (2012). Actin retrograde flow and actomyosin II arc contraction drive receptor cluster dynamics at the immunological synapse in Jurkat T cells. Molecular Biology of the Cell *23*, 834–852.

Yoneyama, M., Kikuchi, M., Natsukawa, T., Shinobu, N., Imaizumi, T., Miyagishi, M., Taira, K., Akira, S., and Fujita, T. (2004). The RNA helicase RIG-I has an essential function in double-stranded RNA-induced innate antiviral responses. Nature Immunology *5*, 730–737.

Zaki, A.M., van Boheemen, S., Bestebroer, T.M., Osterhaus, A.D.M.E., and Fouchier, R.A.M. (2012). Isolation of a Novel Coronavirus from a Man with Pneumonia in Saudi Arabia. New England Journal of Medicine *367*, 1814–1820.

Zhang, Q., Liu, Z., Moncada-Velez, M., Chen, J., Ogishi, M., Bigio, B., Yang, R., Arias, A.A., Zhou, Q., Han, J.E., et al. (2020). Inborn errors of type I IFN immunity in patients with life-threatening COVID-19. Science *370*.

Zhang, Y., Chen, Y., Li, Y., Huang, F., Luo, B., Yuan, Y., Xia, B., Ma, X., Yang, T., Yu, F., et al. (2021). The ORF8 protein of SARS-CoV-2 mediates immune evasion through down-regulating MHC-I. Proceedings of the National Academy of Sciences *118*, e2024202118.

Zhong, N.S., Zheng, B.J., Li, Y.M., Poon, L.L.M., Xie, Z.H., Chan, K.H., Li, P.H., Tan, S.Y., Chang, Q., Xie, J.P., et al. (2003). Epidemiology and cause of severe acute respiratory syndrome (SARS) in Guangdong, People's Republic of China, in February, 2003. Lancet *362*, 1353–1358.

Zhou, D., Dejnirattisai, W., Supasa, P., Liu, C., Mentzer, A.J., Ginn, H.M., Zhao, Y., Duyvesteyn, H.M.E., Tuekprakhon, A., Nutalai, R., et al. (2021). Evidence of escape of SARS-CoV-2 variant B.1.351 from natural and vaccine-induced sera. Cell 1–14.

Zhou, Z., Ren, L., Zhang, L., Zhong, J., Xiao, Y., Jia, Z., Guo, L., Yang, J., Wang, C., Jiang, S., et al. (2020). Heightened Innate Immune Responses in the Respiratory Tract of COVID-19 Patients. Cell Host & Microbe *27*, 883-890.e2.

Zinkernagel, R.M., and Dooherty, P.C. (1974). Restriction of in vitro T cell-mediated cytotoxicity in lymphocytic choriomeningitis within a syngeneic or semiallogeneic system. Nature *248*, 701–702.

Zou, L., Ruan, F., Huang, M., Liang, L., Huang, H., Hong, Z., Yu, J., Kang, M., Song, Y., Xia, J., et al. (2020). SARS-CoV-2 Viral Load in Upper Respiratory Specimens of Infected Patients. New England Journal of Medicine *382*, 1177–1179.

7. Curriculum Vitae

Benedikt Agerer, MSc

26/05/1994, Vienna, Austria, bagerer@cemm.at

Career Summary

Project lead of multiple research projects focusing on immune responses and viral infections. Applying bioinformatic and experimental approaches to solve complex questions. Guiding and participating in several highly collaborative projects that resulted in multiple peer-reviewed publications. Experience in big data analyses and business consulting. I am looking to employ my skills to drive innovation.

Key Skills

- Adapting and learning quickly
- Scientific project management
- Data analysis and presentation
- Cultivating international collaborations
- Creative troubleshooting
- Software Skills (Office, R, Illustrator)
- Coordinating multiple projects at one time
- Scientific writing
- Molecular biology/immunology
- In vivo models

Professional Experience

Predoctoral Fellow/Project Lead, CeMM

09/2017 – present, Vienna, Austria

- Lead and managed collaborative research projects in a competitive research institute, resulting in >10 peer-reviewed publications in respected journals.
- Worked in large international and multicultural teams to do cutting edge research.
- Co-organized symposium with 150 attendees.
- Initiated and organized fundraiser for cancer research and raised ~2000€.
- Trained and supervised new team members.
- Together with team members established sequencing workflow for sequencing SARS-CoV-2 genomes, directly contributing to decision processes of authorities.

Consultant, 180 Degree Consulting

03/2020 – 09/2020, Vienna, Austria

- Market analysis of the client's target market, demographics and customer behavior, facilitating a tailored product portfolio to enter the market, thereby increased the number of potential clients by 200%
- Participated in workshops organized by consultancies (zeb, Simon-Kucher, Wonderwerk)

Master Student, University of Vienna

08/2016 – 08/2017, Vienna, Austria

- Worked on a research project together with a PhD student, resulting in two scientific publications.
- Supervised and trained a Bachelor student.

Students Representative, Medical University of Innsbruck

04/2013 – 05/2015, Innsbruck, Austria

- Developed and negotiated collaborations with other student representatives from Germany.
- Supported and consulted fellow and future students.

Diverse Summer Jobs, Various Employers

Summers 2009-2012 and 2014, Tirol, Austria

- Testing of anticancer compounds in cell culture, OncoTyrol, August 2014
- Delivery of kitchens and administrative tasks, Küchenprofis Schranz&Wolf GmbH July – August 2012
- Production of sledges, Kathrein Rodel GmbH, July – August 2010 and July 2011
- Quality control in a Carbide factory, Donau Chemie AG, July – August 2009

Education

PhD in Immunology, Medical University of Vienna
09/2017 – present, Vienna, Austria

MSc in Immunobiology, University of Vienna
10/2015 – 10/2017, Vienna, Austria

BSc in Molecular Medicine, Medical University of Innsbruck
10/2012 – 08/2015, Innsbruck, Austria

Awards and Qualifications

- LEAD_able Summer School, 2021
  - Training on leadership
- European Business Competence License (EBC*L), 2020-2021
  - Business Administration
  - Controlling
  - Project Management
  - Sales and Marketing
- Naturtalente Program, 2017
  - Soft-skill training on leadership, group-dynamics and solution design for students with high potential.
- Performance Scholarship, 2017 University of Vienna

Languages

- German (Native)
- English (Fluent)
- Italian (Basic)

Publications

2021/06 Klein K, Witalisz-Siepracka A, Gotthardt D, **Agerer B**, Locker F, Grausenburger R, Bergthaler A, Sexl V. T cell-intrinsic CDK6 is dispensable for anti-viral and anti-tumor responses in vivo. **Front Immunol. 2021.** 2021 Jun 24, 12. doi: 10.3389/fimmu.2021.650977.

2021/06 Smyth M, Khamina K, Popa A, Gudipati V, **Agerer B**, Lercher A, Kosack L, Endler L, Baazim H, Viczenczova C, Huppa JB, Bergthaler A. Characterization of CD8 T Cell-Mediated Mutations in the Immunodominant Epitope GP33-41 of Lymphocytic Choriomeningitis Virus. **Front Immunol**. 2021 Jun 14;12:638485. doi: 10.3389/fimmu.2021.638485. PMID: 34194424; PMCID: PMC8236698.

2021/05 **Agerer B**, Lercher A, Bergthaler A. The serine's call: Suppressing interferon responses. **Cell Metab**. 2021 May 4;33(5):849-850. doi: 10.1016/j.cmet.2021.04.012. PMID: 33951468.

2021/03 **Agerer B***, Koblischke M*, Gudipati V*, Montaño-Gutierrez LF, Smyth M, Popa A, Genger JW, Endler L, Florian DM, Mühlgrabner V, Graninger M, Aberle SW, Husa AM, Shaw LE, Lercher A, Gattinger P, Torralba-Gombau R, Trapin D, Penz T, Barreca D, Fae I, Wenda S, Traugott M, Walder G, Pickl WF, Thiel V, Allerberger F, Stockinger H, Puchhammer-Stöckl E, Weninger W, Fischer G, Hoepler W, Pawelka E, Zoufaly A, Valenta R, Bock C, Paster W, Geyeregger R, Farlik M, Halbritter F, Huppa JB, Aberle JH, Bergthaler A. SARS-CoV-2 mutations in MHC-I-restricted epitopes evade CD8+ T cell responses. **Sci Immunol**. 2021 Mar 4;6(57):eabg6461. doi: 10.1126/sciimmunol.abg6461. PMID: 33664060; PMCID: PMC8224398.

2020/12 Girardi E, Agrimi G, Goldmann U, Fiume G, Lindinger S, Sedlyarov V, Srndic I, Gürtl B, **Agerer B**, Kartnig F, Scarcia P, Di Noia MA, Li√±eiro E, Rebsamen M, Wiedmer T, Bergthaler A, Palmieri L, Superti-Furga G. Epistasis-driven identification of SLC25A51 as a regulator of human mitochondrial NAD import. **Nat Commun**. 2020 Dec 1;11(1):6145. doi: 10.1038/s41467-020-19871-x. PMID: 33262325; PMCID: PMC7708531.

2020/11 Popa A, Genger JW, Nicholson MD, Penz T, Schmid D, Aberle SW, **Agerer B** Lercher A, Endler L, Cola√ßo H, Smyth M, Schuster M, Grau ML, Martinez-Jiminez F, Pich O, Borena W, Pawelka E, Keszei Z, Senekowitsch M, Laine J, Aberle JH, Redlberger-Fritz M, Karolyi M, Zoufaly A, Maritschnik S, Borkovec M, Hufnagl P, Nairz M, Weiss G, Wolfinger MT, von Laer D, Superti-Furga G, Lopez-Bigas N, Puchhammer-Stöckl E, Allerberger F, Michor F, Bock C, Bergthaler A. Genomic epidemiology of superspreading events in Austria reveals mutational dynamics and transmission properties of SARS-CoV-2. **Sci Transl Med**. 2020 Dec 9;12(573):eabe2555. doi: 10.1126/scitranslmed.abe2555. Epub 2020 Nov 23. PMID: 33229462; PMCID: PMC7857414.

2020/11 Liu GJ, Jaritz M, Wöhner M, **Agerer B**, Bergthaler A, Malin SG, Busslinger M. Repression of the B cell identity factor Pax5 is not required for plasma cell development. **J Exp Med.** 2020 Nov 2;217(11):e20200147. doi: 10.1084/jem.20200147. PMID: 32780801; PMCID: PMC7596824.

2020/10 Lercher A, Popa AM, Viczenczova C, Kosack L, Klavins K, **Agerer B**, Opitz CA, Lanz TV, Platten M, Bergthaler A. Hepatocyte-intrinsic type I interferon signaling reprograms metabolism and reveals a novel compensatory mechanism of the tryptophan-kynurenine pathway in viral hepatitis. **PLoS Pathog**. 2020 Oct 12;16(10):e1008973. doi: 10.1371/journal.ppat.1008973. PMID: 33045014; PMCID: PMC7580883.

2020/08 Alm E, Broberg EK, Connor T, Hodcroft EB, Komissarov AB, Maurer-Stroh S, Melidou A, Neher RA, O'Toole Á, Pereyaslov D; WHO European Region sequencing laboratories and GISAID EpiCoV group; WHO European Region sequencing laboratories and GISAID EpiCoV group*. Geographical and temporal distribution of SARS-CoV-2 clades in the WHO European Region, January to June 2020. **Euro Surveill**. 2020 Aug;25(32):2001410. doi: 10.2807/1560-7917.ES.2020.25.32.2001410. Erratum in: Euro Surveill. 2020 Aug;25(33): PMID: 32794443; PMCID: PMC7427299.

2020/07 Jaeger MG, Schwalb B, Mackowiak SD, Velychko T, Hanzl A, Imrichova H, Brand M, **Agerer B**, Chorn S, Nabet B, Ferguson FM, Müller AC, Bergthaler A, Gray NS, Bradner JE, Bock C, Hnisz D, Cramer P, Winter GE. Selective Mediator dependence of cell-type-specifying transcription. **Nat Genet**. 2020 Jul;52(7):719-727. doi: 10.1038/s41588-020-0635-0. Epub 2020 Jun 1. PMID: 32483291; PMCID: PMC7610447.

2019/12 Lercher A, Bhattacharya A, Popa AM, Caldera M, Schlapansky MF, Baazim H, **Agerer B**, Gürtl B, Kosack L, Májek P, Brunner JS, Vitko D, Pinter T, Genger JW, Orlova A, Pikor N, Reil D, Ozsvár-Kozma M, Kalinke U, Ludewig B, Moriggl R, Bennett KL, Menche J, Cheng PN, Schabbauer G, Trauner M, Klavins K, Bergthaler A. Type I Interferon Signaling Disrupts the Hepatic Urea Cycle and Alters Systemic Metabolism to Suppress T Cell Function. **Immunity**. 2019 Dec 17;51(6):1074-1087.e9. doi: 10.1016/j.immuni.2019.10.014. Epub 2019 Nov 26. PMID: 31784108; PMCID: PMC6926485.

2019/05 Hacker K*, Benke S*, **Agerer B***, Scinicariello S, Budroni V, Versteeg GA. A repetitive acidic region contributes to the extremely rapid degradation of the cell-context essential protein TRIM52. **Sci Rep**. 2019 May 27;9(1):7901. doi: 10.1038/s41598-019-44359-0. PMID: 31133683; PMCID: PMC6536530.

2019/01 Kosack L, Wingelhofer B, Popa A, Orlova A, **Agerer B**, Vilagos B, Majek P, Parapatics K, Lercher A, Ringler A, Klughammer J, Smyth M, Khamina K, Baazim H, de Araujo ED, Rosa DA, Park J, Tin G, Ahmar S, Gunning PT, Bock C, Siddle HV, Woods GM, Kubicek S, Murchison EP, Bennett KL, Moriggl R, Bergthaler A. The ERBB-STAT3 Axis Drives Tasmanian Devil Facial Tumor Disease**. Cancer Cell**. 2019 Jan 14;35(1):125-139.e9. doi: 10.1016/j.ccell.2018.11.018. PMID: 30645971; PMCID: PMC6335503.

2018/02 Benke S, **Agerer B**, Haas L, Stöger M, Lercher A, Gabler L, Kiss I, Scinicariello S, Berger W, Bergthaler A, Obenauf AC, Versteeg GA. Human tripartite motif protein 52 is required for cell context-dependent proliferation. **Oncotarget**. 2018 Feb 5;9(17):13565-13581. doi: 10.18632/oncotarget.24422. PMID: 29568378; PMCID: PMC5862599.